The Lactococcus lactis Thioredoxin System

Efler, Petr; Hägglund, Per; Svensson, Birte

Publication date:
2013

Document Version
Publisher's PDF, also known as Version of record

The *Lactococcus lactis* Thioredoxin System

PhD thesis

2013

Petr Efler

Enzyme and Protein Chemistry (EPC)

Department of Systems Biology

Technical University of Denmark (DTU)

Supervisors:

Associate Professor Per Hägglund, EPC, Department of Systems Biology, DTU

Professor Birte Svensson, EPC, Department of Systems Biology, DTU

Preface

The presented PhD thesis is based on results of my study carried out in the Enzyme and Protein Chemistry Group at the Department of Systems Biology, Technical University of Denmark under supervision of Associate Professor Per Hägglund and Professor Birte Svensson. Part of the work has been carried out in the Centre for Systems Microbiology at the Department of Systems Biology, Technical University of Denmark, in a collaboration with Associate Professor Mogens Kilstrup.

The project was supported by the Danish Council for Technology and Production Sciences (FTP, grant nr 274-08-0413) and the PhD grant was in part financed by the Technical University of Denmark.

The work has resulted in following manuscripts:

Efler, P., Kilstrup, M., Johnsen, S., Svensson, B. and Hägglund, P. Two *Lactococcus lactis* thioredoxin paralogues play different roles in responses to arsenate and oxidative stress. *In preparation* (Chapter 2)

Efler, P., Björnberg, O., Ebong, E.D., Svensson, B. and Hägglund, P. Redox potential and catalytic properties of three thioredoxin superfamily disulfide reductases from *Lactococcus lactis*. *In preparation* (Chapter 3)

Acknowledgements

First of all, I would like to thank to my supervisors Prof. Birte Svensson and Associate Prof. Per Hägglund for allowing me to conduct my PhD study, for their careful leading my way through it and for their patience and being with me until the very final stage. I also appreciate very much their help with writing my thesis and manuscripts, especially Per made an incredible effort in making “order in chaos”, without which I would never finish.

I thank very much to DTU as well as the project 'A Quantitative Redox Proteomics and Protein Engineering Tool Box for Applications of Thioredoxin in Food Biotechnology' supported by Danish Council for Technology and Innovation (FTP) for financing my PhD.

I would like to acknowledge Associate Prof. Mogens Kilstrup who provided me material and work space at the Center for Systems Microbiology DTU, and introduced me into growth and radioactive labeling experiments. I would also like to thank him for fruitful discussions and help with writing of the related manuscript. At this point, I would like to thank Marzanna Pulka-Amin who constructed the *ΔtrxAΔtrxD* double mutant of *Lactococcus*. She showed me all remaining tricks in growing *Lactococcus* and was a great lab mate.

Prof. Anette Henriksen is thanked for providing me a chance to try to crystallize LlTrxD. Even though this experiment was not successful, it would not be possible to even try without her support.

I owe eternal gratitude to Olof Björnberg for all his contribution to the manuscript about the characterization of recombinant thioredoxins. He was also a very nice office, lab and faculty club mate. Stig Johnsen and is acknowledged for construction of the *ΔtrxA* and *ΔtrxD* single mutants of *Lactococcus* and Epie Denis Ebong is thanked for cloning *trxA*, *trxD* and *nrdH* genes into pET15b expression vectors, which made my life much easier. I would also like to thank Aida for producing and purifying most of the recombinant proteins used in this study and for running incredible amount of enzyme kinetics assays. Birgit Andersen is acknowledged for explaining me much about proteomics, also for running my LC/MS samples.

I very much appreciate help of Morten Ejby who introduced me gel-based proteomics and was very patient with me during the never-ending troubleshooting. I also thank very much to Joakim Andersen who was extremely helpful in whatever I asked him for, ranging from experiments, writing my Danish resume to fixing my bike. Both Joakim and Morten have always been very friendly and EPC would be just different without them. I would like to acknowledge all remaining members of EPC who provided me nice and friendly working atmosphere and who gave me many good advices at various stages of my study.

I also thank very much all my friends who I have not mentioned so far, especially Ofir, Pernille, Fen, Elena, Šárka and Hanne who always gave me good advices or, not less important, good laughs.

At the end I would like to thank to my family in the Czech Republic, Britain and Denmark for their support and faith in me, especially in moments when I lacked it totally. My very special thanks belong to my dearest fiancée Yvonne and her sons Frederik and Sebastian who accepted me as a part of their family and made me feel in Denmark like at home.

Summary

Thioredoxins (Trx) are small ubiquitous disulfide oxidoreductases involved in thiol redox control in all kingdoms of life and provides reducing equivalents to various enzymes (e.g. ribonucleotide reductase, methionine sulfoxide reductase and peroxiredoxins). Oxidized Trx is recycled by NADPH-dependent thioredoxin reductase (NTR) in order to complete its catalytic cycle. Glutathione-dependent glutaredoxin complements Trx in many organisms. This thesis focuses on disulfide reduction pathways in *Lactococcus lactis*, an important industrial microorganism used traditionally for cheese and buttermilk production. *L. lactis* lacks glutathione and glutaredoxin, but it a contains Trx system consisting of an NTR (LlTrxB), a classical Trx (LlTrxA) containing the conserved WCGPC active site motif, a Trx-like protein (LlTrxD) containing a WCGDC active site motif and a redoxin (LlNrdH) providing electrons to class Ib ribonucleotide reductase (NrdEF).

Physiological functions of LlTrxA and LlTrxD were studied using *ΔtrxA*, *ΔtrxD* and *ΔtrxAΔtrxD* mutant strains of *L. lactis* ssp. *cremoris* MG1363 exposed to various stress conditions and comparing them to the wild type (wt) strain. These experiments revealed that the *ΔtrxA* genotype caused about 30% growth inhibition at non-stressed conditions and significantly increased sensitivity to oxidants (e.g. H_2O_2, diamide), while deletion of *trxD* displayed an effect predominantly in the *ΔtrxAΔtrxD* mutant. The *ΔtrxD* mutant exhibited a significantly higher sensitivity only in case of exposure to sodium arsenate and potassium tellurite. Arsenate detoxicification involves arsenate reductase (ArsC), an established Trx target in *Bacillus subtilis*. The sensitivity of the *ΔtrxD* mutant may indicate that ArsC is reduced by TrxD in *L. lactis*. Comparison of protein profiles of the wt, *ΔtrxA* and *ΔtrxD* mutants by difference gel electrophoresis (DIGE) revealed significant changes between *ΔtrxA* and wt. Higher levels of several oxidative stress-related proteins (e.g. glutathione peroxidase) were observed in the *ΔtrxA* mutant. Proteomic analysis (pulse labeling by [^{35}S]-L-methionine) of the *ΔtrxD* mutant vs. wt upon exposure to sodium arsenate showed down-regulation of several ATPases (DnaK and GroEL) and GTPases (Ef-G, Ef-Ts) concomitantly with up-regulation of enzymes involved in aerobiosis and nucleotide metabolism in the *ΔtrxD* mutant. The *ΔtrxAΔtrxD* deletion mutant is viable, in agreement with a previous study showing that NTR in *L. lactis* is not essential. Therefore, the presence of an additional thiol redox system is hypothesized.

Biochemical studies demonstrated that recombinant LlTrxA, LlTrxD and LlNrdH are substrates for LlNTR, while only LlTrxA and LlNrdH are efficiently reduced by *E. coli* NTR. LlTrxA appears to have a higher redox potential (-259 mV) compared to *E. coli* EcTrx1 (-270 mV) but similar reactivity as EcTrx1 towards insulin disulfides and the alkylation reagent iodoacetamide (IAM). LlTrxD exhibited a high redox potential (-243 mV) and about 100-fold higher reactivity towards IAM than LlTrxA and EcTrx1, but no activity towards insulin was observed. LlNrdH showed a higher redox potential (-238 mV) compared to *E. coli* NrdH (-248 mV) and a lower reactivity towards insulin compared to LlTrxA.

Dansk resumé

Thioredoxiner (Trx) er allestedsnærværende små disulfid-oxidoreduktaser, som er involveret i thiol-redox kontrol og aktiviteten af en række enzymer (f.eks. ribonukleotidreduktaser og peroxiredoxiner) fra alle taksonomiske former af liv. Trx reducerer disulfider, og skal selv derefter reduceres, dette sker af en NADPH-afhængig thioredoxin reduktase (NTR), for at gennemføre sin katalytiske cyklus. Trx og NTR udgør således Trx systemet. Glutathion-afhængigt glutaredoxin systemet komplementerer Trx i mange organismer. I Dette projekt omhandler *Lactococcus lactis*, som er en vigtig industriel mikroorganisme, der bruges i produktionen af ost og kærnemælk. *L. lactis* mangler glutathion og glutaredoxin, men koder for et Trx system bestående af: NTR (TrxB), en Trx (TrxA) med et WCGPC active site motiv samt en ny type bakteriel Trx, der indeholder active site motivet WCGDC (TrxD) og endelig en specifik redoxin (NrdH), som bidrager med elektroner til en klasse Ib ribonukleotidreduktase (NrdEF).

De fysiologiske funktioner af LlTrxA og LlTrxD blev undersøgt med vækststudier af *ΔtrxA*, *ΔtrxD* og *ΔtrxAΔtrxD* mutanter af *L. lactis* ssp. *cremoris* MG1363 ved forskellige stress forhold og sammenlignet med vildtype (wt) stammen. Disse eksperimenter viste, at *ΔtrxA* genotypen bevirkede omkring 30% vækstinhibeæmning under ikke-stress vækstforhold og signifikant forøget følsomhed overfor oxidation (f.eks. H_2O_2, diamide), hvorimod gen-deletionen af *trxD* førte til en fenotype svarende til *ΔtrxAΔtrxD* mutanten. *ΔtrxD* mutanten udviste en signifikant højere følsomhed overfor tilstedeværelsen af natriumarsenat og telluritfosfat. Arsenat omdannes af et kendt Trx-afhængigt enzym, arsenatreduktase (ArsC). Derfor kan den øgede følsomhed af *ΔtrxD* mutanten betyde, at ArsC har specificitet for TrxD i *L. lactis*. Sammenligning af udtrykte proteinprofiler af wt, *ΔtrxA* and *ΔtrxD* mutanterne, ved hjælp af differentiel gel elektroforese (DIGE), viste signifikante forskelle imellem *ΔtrxA* og wt, hvorimod *ΔtrxD* var næsten identisk med wt. Navnlig opregulering af flere proteiner relateret til oxidativ stress (f.eks. glutahion peroxidase) blev observeret i *ΔtrxA* mutanten. Proteomanalyse (pulse labeling med [^{35}S]-L-methionin) af *ΔtrxD* mutanten og wt efter påvirkning med natriumarsenat viste en nedregulering af flere ATPaser (DnaK og GroEL) og GTPaser (Ef-G, Ef-Ts) samt en opregulering af få enzymer involveret i aerobiose og nukleotidmetabolisme i *ΔtrxD* mutanten. Ingen af gendeletionerne var dødelige for *L. lactis*, hvilket bekræfter en tidligere undersøgelse, der viste, at *L. lactis* NTR ikke er essentielt for overlevelse. På grundlag af resultaterne kan der opstilles hypotese om tilstedeværelse af andre redox systemer.

Biokemiske undersøgelse viste, at alle LlTrxA, LlTrxD og LlNrdH kan effektivt reduceres af LlNTR, men at kun LlTrxA og LlNrdH er mulige substrater for *Escherichia coli* NTR. LlTrxA udviste et tilsyneladende højere redoxpotentiale (-259 mV) sammenlignet med *E. coli* Trx1 (-270 mV), men havde lignende reaktivitet for insulin disulfider og alkyleringsreagenset jodacetamid (IAM). LlTrxD udviste et højt redoxpotentiale (-243 mV) og cirka 100 gange højere reaktivitet for IAM i forhold til LlTrxA og *E. coli* Trx1, men ingen aktivitet overfor insulin. LlNrdH udviste også et højere redoxpotentiale (-238 mV) sammenlignet med *E. coli* NrdH (-248 mV) og udviste kun lav reaktivitet overfor insulin.

Table of Contents

Abbreviations

ADH	Alcohol dehydrogenase
AhpC	Bacterial NADH peroxidase
AK	Acetate kinase
BSH	Bacillithiol
DTT	Dithiotreitol
DsbA	Periplasmic disulfide bond forming protein in Gram-negative bacteria
DsbD	Trans-membrane protein disulfide oxidoreductase facilitating reduction of periplasmic proteins in Gram-negative bacteria
ETC	Electron transport chain
FAD	Oxidized cofactor flavin adenine dinucleotide
$FADH_2$	Reduced cofactor flavin adenine dinucleotide
Flp	Bacterial redox sensor
FO	Flavin-oxidizing (conformation of NTR)
FR	Flavin-reducing (conformation of NTR)
GAPDH	Glyceraldehyde-3-phosphate dehydrogenase
GR	Glutathione reductase
Gpx	Glutathione peroxidase
Grx	Glutaredoxin
GSH	Reduced glutathione
IAM	iodoacetaimde
ICAT	Isotope-coded affinity tag
LAB	Lactic acid bacteria
LDH	Lactate dehydrogenase
LMW	Low molecular weight
MetSO	Methionine sulfoxide
MSH	Mycothiol
Msr	Methionine sulfoxide reductase
NAD^+	Oxidized nicotinamide adenine dinucleotide cofactor
NADH	Reduced nicotinamide adenine dinucleotide cofactor
NADPH	Reduced cofactor nicotinamide adenine dinucleotide phosphate cofactor
Nox-1 (AhpF)	Bacterial hydrogen peroxide forming NADH oxidase
NEM	N-ethylmaleimide
NrdEF	Class Ib ribonucleotide reductase
NrdH	Electron donor of class Ib ribonucleotide reductase
NrdI	Flavodoxin facilitating formation of tyrosyl radical in NrdF
OxyR	Bacterial hydrogen peroxide sensor
OsmC	Osmotically induced organic hydroperoxide reductase
PDI	Protein disulfide isomerase
PFL	Pyruvate-formate lyase
PMF	Proton motive force
Pyk	Pyruvate kinase
RNR	Ribonucleotide reductase
ROS	Reactive oxygen species
SOD	Superoxide dismutase
Spx	Bacterial redox sensor
Trx	Thioredoxin

1 Chapter 1 – Introduction

1.1 Oxidative stress

1.1.1 What is oxidative stress?

The story begins 4 billion years ago when life evolved in the anaerobic environment on planet Earth. The first organisms were fermenting heterotrophs living on abiotic sources of organic compounds or chemotrophs using hydrogen, hydrogen sulfide and methane as energy source. In the absence of oxygen there was no ozone layer shielding these organisms from harmful UV radiation and some organisms evolved protective light-absorbing pigments. These pigments were further developed and integrated in the photosynthetic machinery, a membrane-bound protein complex emerging among cyanobacteria-like organisms approximately 3.2 to 2.4 billion years ago. In this complex the energy of the light absorbed by photosynthetic pigments is captured into biosynthesis coupled to extraction of electrons from water (Eq. 1.1).[1]

$$2H_2O \rightarrow O_2 + 4H^+ + 4e^- \quad (1.1)$$

However, the byproduct of the reaction, oxygen, became a threat for the sensitive anaerobic organisms. Oxygen has a strong oxidative character and sequential one-electron reduction generates superoxide (O_2^-), hydrogen peroxide (H_2O_2) and hydroxyl radicals (HO·), respectively (Fig. 1). In addition, singlet oxygen ($^1O_2$; Fig. 1) is formed by excitation of standard triplet oxygen for example at photosynthetic reaction centers. These so-called reactive oxygen species (ROS) are very potent and often cause irreversible oxidative damage to DNA, proteins and lipids,[1, 2] as described more in detail below.

1.1.2 Reactive oxygen species (ROS)

The reactivity of oxygen and ROS is determined by redox potentials and structures of molecular orbitals. Molecular oxygen is a stable biradical with unpaired electrons in the π_x^* and π_y^* antibonding orbitals and does not oxidize amino acid side-chains or nucleic acids at a significant rate. However, oxygen can readily accept free electrons from transition metals or organic radicals (e.g. semiquinones).[2] ROS have higher redox potentials and are thus stronger oxidants compared to oxygen (Fig. 1B). However, the reactivity of ROS is also influenced by electrostatic forces, i.e. the negative charge of O_2^- causes repulsion from e^--rich oxidizable regions and makes it less reactive.[2]

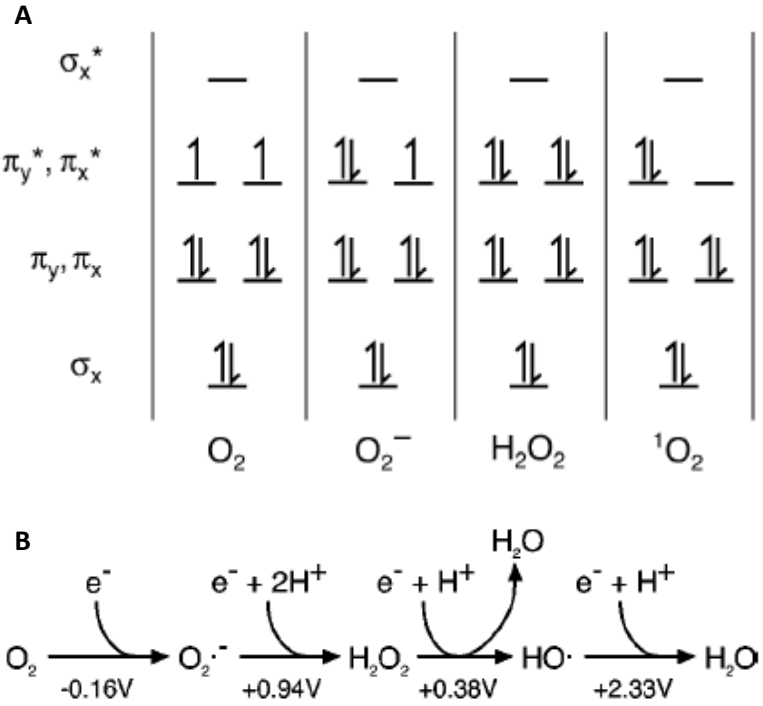

Fig. 1 Reactivity of ROS. (**A**) Molecular orbital structure of selected species. (**B**) Formation and redox potentials of ROS. 1 M oxygen was used as the standard state in the first step. Source: Imlay, 2003.[2]

1.1.2.1 Sources of ROS and general scavenging mechanisms

Organisms are exposed to exogenous ROS formed by abiotic chemical processes (e.g. reactions with UV light or ionizing radiation),[3] or endogenous ROS generated in various biological processes.[2] Typical examples of the latter ones are membrane-bound redox systems (e.g. the respiratory chain or photosystems). Molecular oxygen can diffuse through the cell membrane, and is converted to a mixture of O_2^- and H_2O_2 by autoxidation of various redox enzymes (Fig. 3A).[4–6] O_2^- is further reduced to H_2O_2 by transfer of e^- from redox centers or by the scavenging enzyme superoxide dismutase (SOD; Eq. 1.2).[7] The latter reaction takes place also non-enzymatically but it is about twice as slow as by SOD.[8] Therefore the function of SOD is to lower the steady state concentration of O_2^-.[8]

$$2O_2^- + 2e^- + 2H^+ \rightarrow H_2O_2 + O_2 \qquad (1.2)$$

H_2O_2 can undergo a reaction (1.5) to produce OH· in the presence of iron salts as discovered in 1890s by H.J.H. Fenton.[9] A reaction between O_2^- and H_2O_2 catalyzed by transition metals and generating HO· was proposed by Haber and Weiss in the 1930s (Eq. 1.3).[10] The intermediate steps based on *in vitro* experiments are described by equations (1.4) and (1.5).[10] However, it was shown later that reduction of Fe^{3+} by O_2^- does not occur in significant amounts *in vivo* due to a low reaction rate and a low O_2^- concentration.[11, 12] It was demonstrated that other compounds than O_2^- (e.g. $FADH_2$ cofactor and cysteine) are potent e^- donors in the reaction (Eq. 1.4).[13, 14] Therefore it is more correct to modify equation 1.4 to a generally applicable form

(Eq. 1.6). Evidence for gas-phase non-metal-catalyzed Haber-Weiss reaction (Eq. 1.3) has been presented and it was suggested that similar mechanism could occur in hydrophobic environment such as cell membranes or hydrophobic domains of proteins.[15]

$$O_2^- + H_2O_2 \rightarrow O_2 + HO\cdot + OH^- \quad (1.3)$$

$$O_2^- + Fe^{3+}\,(Cu^{2+}) \rightarrow O_2 + Fe^{2+}\,(Cu^{+}) \quad (1.4)$$

$$H_2O_2 + Fe^{2+}\,(Cu^{+}) \rightarrow Fe^{3+}(Cu^{2+}) + OH^- + HO\cdot \quad (1.5)$$

$$donor_{RED} + Fe^{3+} \rightarrow donor_{OX} + Fe^{2+} \quad (1.6)$$

HO· is the most reactive ROS, therefore H_2O_2 is effectively scavenged by peroxidases (Eq. 1.7) and catalases (Eq. 1.8) and Fe^{2+} is sequestered (see below).[2]

$$RH_2 + H_2O_2 \rightarrow R + 2H_2O \quad (1.7)$$

$$2H_2O_2 \rightarrow O_2 + 2H_2O \quad (1.8)$$

Formation of O_2^- and consequently other ROS is also increased by redox-cycling compounds like for example paraquat, menadione or phenazine methosulfate (Fig.2).[5, 16]

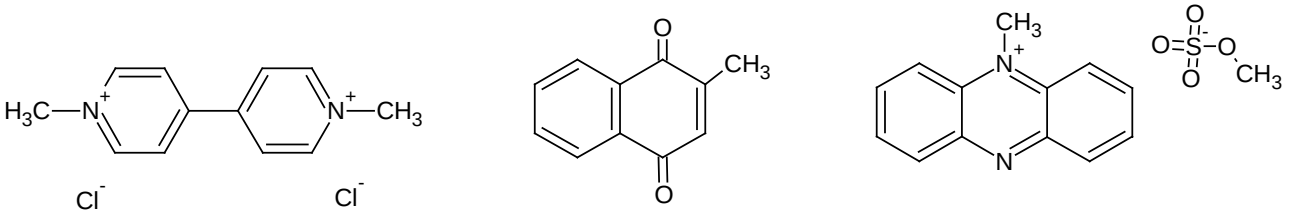

paraquat **menadione** **phenazine methosulfate**

Fig. 2 Examples of redox-cycling compounds.

The bacterium *Escherichia coli* has been used as a model system to study ROS metabolism. Intracellular O_2^- and H_2O_2 in this organism has been presumed to be generated mainly by the respiratory chain and high-abundant flavoenzymes (e.g. fumarate dehydrogenase or succinate dehydrogenase).[6, 17, 18] The respiratory chain was shown to be the major site of formation of periplasmic O_2^-, in particular due to e^- leakage through menaquinones.[19] However, not more than 10% of the total H_2O_2 was formed in this manner.[20] Recently, it was shown that autoxidation of NadB (L-aspartate oxidase, a desaturating dehydrogenase in the NAD biosynthesis pathway) contributes to the formation of H_2O_2 by 25 – 30% in a strain of *E. coli* lacking scavenging systems.[20] It was hypothesized that NadB as a low-abundant enzyme in a tightly controlled pathway can be allowed to produce H_2O_2. On the other hand, several enzymes performing an analogous reaction in pathways with a higher metabolic flux (dehydroorotate dehydrogenase, proline dehydrogenase, fumarate reductase) were shown to be connected to the

respiratory chain cytochrome d oxidase through the quinone pool thus avoiding high H_2O_2 formation upon aeration. The sources of about two thirds of H_2O_2 formed in *E. coli* remain to be discovered.[20]

1.1.2.2 Damage caused by ROS

ROS can effectively oxidize DNA, lipids and proteins.[2] HO· reacts with bases or sugar moieties in DNA resulting in formation of damaged nucleotides (e.g. 8-oxoguanine, thymine glycol). Sometimes the products are unstable, resulting in formation of *apurinic/apyrimidinic sites* or strand breaks.[21] These types of DNA damages have been associated with Fenton's reaction involving DNA bound Fe^{2+} (Eq.(1.5)) and often lead to mutations that eventually may have devastating effects on cellular metabolism. On the basis of H_2O_2 dose dependent kinetics of DNA damage, it was proposed that other products of Fenton's reaction are formed but they have not yet been identified.[21–23] Studies on sequence dependence of DNA oxidation revealed increased iron binding to specific repetitive sequences present for example at the ends of chromosomes, in telomeres. This finding may represent a connection between oxidative stress and aging.[23–25] Oxidized DNA is repaired by recombinational (e.g. recA) and base-excission systems (e.g. DNA glycosidases).[1, 5]

Peroxidation of lipids by ROS causes destabilization of membranes. This type of damage is prevalent in mammalian cells containing high amounts of membrane-associated polyunsaturated fatty acids that promote efficient propagation of the radical chain reaction.[2, 26] Polyunsaturated fatty acids are also found in thylakoid membranes in cyanobacteria and chloroplasts of higher plants.[2] Monounsaturated fatty acids, e.g. in bacterial cell membranes are less susceptible to ROS-induced oxidation. However, an *E. coli* strain with a lowered content of monounsaturated fatty acids exhibits an elevated resistance to ROS.[27]

Proteins are also targets for ROS-induced oxidation. Radicals associated with ROS may abstract a hydrogen from the Cα atom in the peptide backbone resulting in formation of a peroxyl radical in the presence of oxygen. The peroxyl radical may react further to generate fragmentation of the main chain.[28, 29] The chemical properties of amino acid side-chains and cofactors of enzymes also allow a broad range of modifications, most of which are irreversible. Aliphatic amino acids can undergo hydrogen atom abstraction and peroxyl radical formation in the side-chain and subsequent radical-radical termination reactions often lead to carbonyl and alcohol formation.[30] Amino groups present on side-chains of Lys, Arg, Asn and Gln can form halogenamine/halogenamide derivatives in the presence of HOX (X=Cl, Br).[29, 31, 32] These products are often unstable and form nitrogen-centred radicals and carbonyls.[32] Aromatic amino acids possess electron-rich side chains and are particularly susceptible to oxidation. For example a phenoxyl radical of tyrosine is formed either by deprotonation of the hydroxyl group or by addition-eliminaton reaction with HO·. Dimerization of the phenoxyl radical can result in protein cross-linking, or alternatively it can be repaired for example by reaction with suitable hydrogen donors (e.g. thiols, ascorbate). ROS react with His, Trp and Phe to form hydroxylated derivatives.[29, 30] O_2^- and H_2O_2 damage $[4Fe\text{-}4S]^{2+}$ clusters of dehydratases (e.g. aconitase[33]). The cluster is oxidized concomitantly with release of Fe^{2+} or Fe^{3+}, while $[3Fe\text{-}4S]^+$ remains attached to the enzyme (Eq. 1.7 and 1.8; Fig. 3BD).[34–36] In addition, Fe^{2+} or Fe^{3+} also contribute to further oxidative damage by Fenton's reaction (Fig. 3CE; see above).[2, 37] If only one iron atom is released, the cluster can be repaired by a so far unknown mechanism. Otherwise it has to be assembled *de novo.*[38]

$$\text{Enz-}[4Fe\text{-}4S]^{2+} + \cdot O_2^- + 2H^+ \rightarrow \text{Enz-}[3Fe\text{-}4S]^+ + H_2O_2 + Fe^{2+} \qquad (1.7)$$

$$Enz\text{-}[4Fe\text{-}4S]^{2+} + H_2O_2 \rightarrow Enz\text{-}[3Fe\text{-}4S]^{+} + 2OH^{-} + Fe^{3+} \quad (1.8)$$

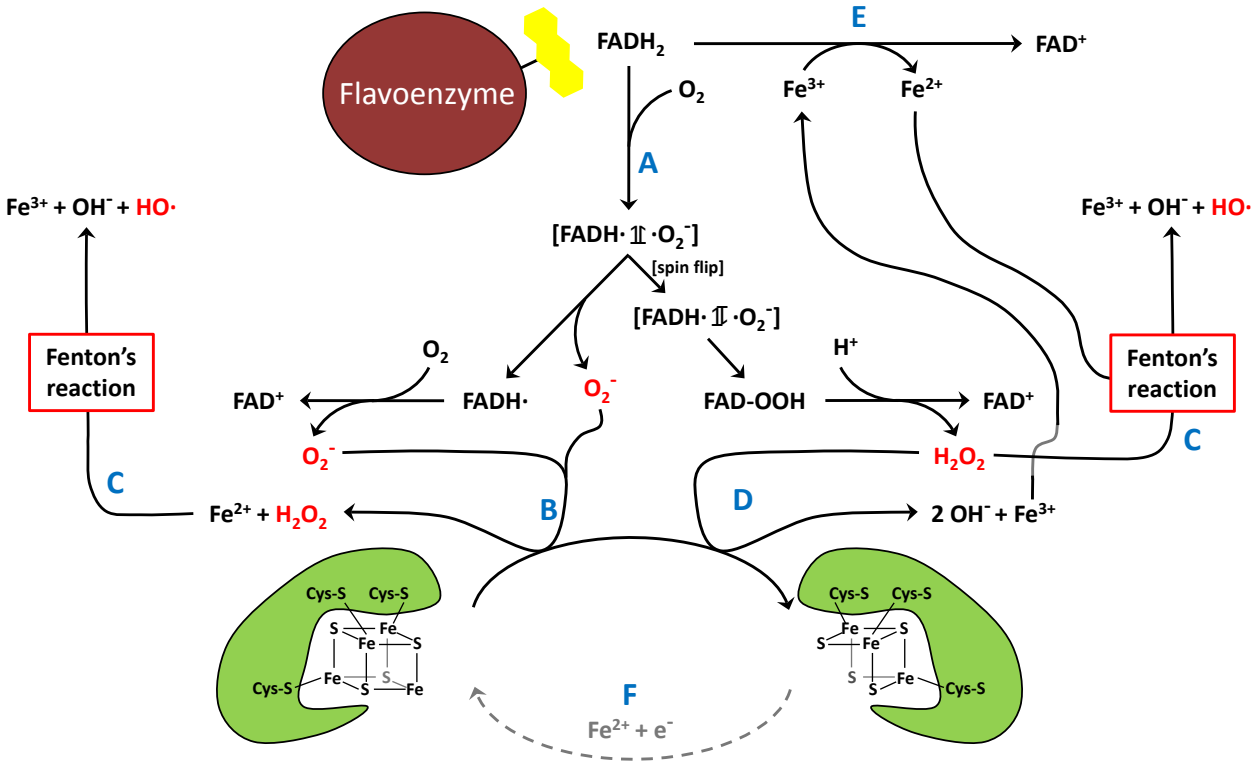

Fig. 3 Damage of [4Fe-4S] clusters by ROS. (**A**) Flavin cofactors can transfer e^- to oxygen, thus generating a mixture of O_2^- and H_2O_2. Both species can damage iron-sulfur clusters. O_2^- performs univalent oxidation (**B**) which can be followed by Fenton's reaction (**C**). H_2O_2 reacts divalently with [Fe-S] clusters (**D**). Fe^{3+} generated in this reaction can be reduced by available cellular reductants, e.g. $FADH_2$ (**E**). Dashed arrow represents the suggested repair mechanism of the iron-sulfur cluster (**F**). Based on Imlay (2003).[2]

Sulfur-containing amino acids (cysteine, methionine) are exceptionally reactive and susceptible to reversible and irreversible oxidative modifications.[29] The oxidation product of methionine is in most cases (R)- and (S)-methionine sulfoxide (MetSO). The ratio of the two stereoisomers depends both on the oxidant and the structure of the particular protein.[39] Further oxidation leads to the methionine sulfone (Fig. 4).[29] MetSO can be enzymatically repaired by methionine sulfoxide reductases but oxidation to methionine sulfone appears to be irreversible. Most organisms contain one isoform of MetSO reductase for each enantiomer (MsrA for (S)- and MsrB for (R)-).[5, 40, 41] MsrA can reduce both protein-bound and free Met-(S)-SO while MsrB is specific for protein-bound Met-(R)-SO. Enzymes specific for free MetSO have been discovered in *E. coli*.[42, 43]

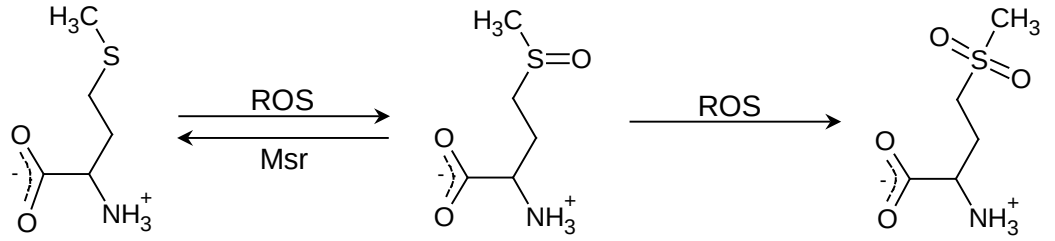

methionine **methionine sulfoxide** **methionine sulfone**

Fig. 4 Oxidation of methionine. Assymetric incorporation of oxygen leads to the mixture of (R)- and (S)- stereoisomers of methionine sulfoxide which can be reduced again by methionine sulfoxide reductases. Further oxidation to sulfone is irreversible. The figure demonstrates oxidation of free methinonine, but this occurs frequently on protein level. For more details see text.

By action of ROS, a cysteine thiol group can be oxidized to sulfenic, sulfinic and sulfonic acid, or react with a second thiol to form a disulfide (Fig. 5ABCDE). Based on binding partners, disulfides can be intramolecular or intermolecular. The latter ones are formed either between two proteins or between a protein and a low molecular weight (LMW) thiol (e.g. glutathione; GSH). Only sulfenic acid and disulfides are generally formed reversibly while sulfinic and sulfonic acids are usually irreversible.[2] However, in case of several eukaryotic peroxidases, active site over-oxidized cysteine as sulfinic acid can be reduced by sulfiredoxins.[44–46] Cysteine sulfonic acid can also be formed by hydrolysis of halogenated derivatives resulting from reactions with HOCl (Fig. 5F).[29, 32, 47] Apart from ROS, cysteine can react with reactive nitrogen species (RNS; Fig. 5GH) and reactive electrophilic species (RES; Fig. 5I).[48–51]

Oxidation of free thiols or [Fe-S] clusters of various cytoplasmic proteins by ROS may lead to inactivation. For instance, enzymes involved in glycolysis (e.g. glyceraldehyde-3-phosphate dehydrogenase, pyruvate kinase and enolase), pyruvate dehydrogenase complex, tricarboxylic acid cycle (e.g. citrate synthase, aconitase, α-ketoglutarate dehydrogenase) and also in translation (e.g. elongation factors) are inactivated by ROS.[52] On the other hand, proteins functioning as redox sensors (e.g. OxyR in *E. coli*) are activated upon oxidation, which leads to transcription of genes involved in ROS scavenging, thiol protection or repair processes (see 1.3.2 below).[49]

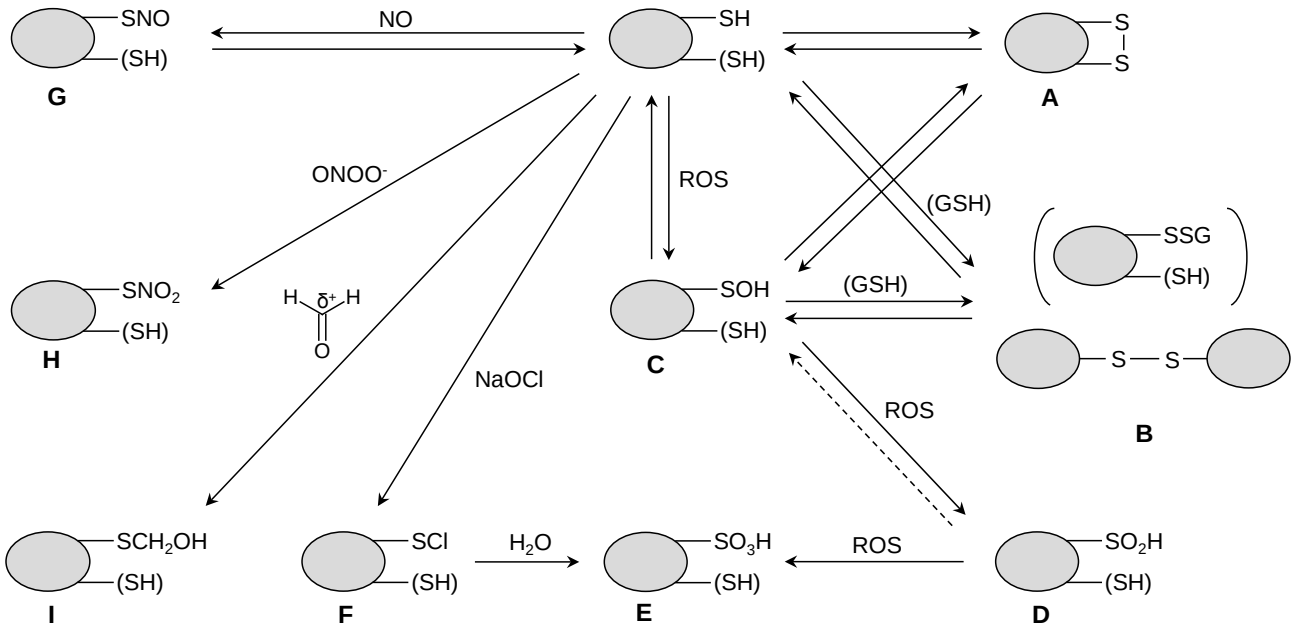

Fig. 5 Oxidative protein thiol modifications. Proteins containing free thiols can form intra- or intermolecular disulfides (**A**, **B**). Oxidation by ROS leads to sulfenic acid (**C**) and this intermediate can either form intra- or intermolecular disulfides (**A**, **B**), or undergo further oxidization to sulfinic acid (**D**) and sulfonic acid (**E**). Sulfenyl chloride (**F**) formed by a reaction with sodium hypochlorite, can be hydrolyzed to sulfonic acid. Oxidation by RNS (NO, $ONOO^-$) forms nitroso- or nitrothiols, respectively (**G**, **H**). RES (e.g. formaldehyde) also readily attack free thiols by their electrodeficient carbon centers, which results in a corresponding alkylthiol (e.g. hydroxymethylthiol; **I**).

1.2 Thiol-redox control

1.2.1 General overview

As outlined above, reduced protein thiol groups are highly reactive and susceptible to ROS-induced oxidation. The reactivity of protein thiol groups is also captured in a wide range of metabolic pathways where active site cysteine residues in enzymes undergo reversible redox reactions such as disulfide bond formation.[52–54] Regulation of thiol redox status is essential and catalysed by thiol-disulfide oxidoreductases of the thioredoxin superfamily which share structural features and a redox-active CXX[C/S] active site motif (see section 1.2.3.2). In the cytoplasm thiol groups are in general maintained in a reduced state by LMW thiols (e.g. the tripeptide glutathione) and/or small protein disulfide reductases such as thioredoxins (Trx) and glutaredoxins (Grx) at the expense of NADPH. On the other hand, structural disulfides are typically formed in secreted proteins and extracellular domains of membrane proteins by protein disulfide isomerase (PDI) in the oxidizing endoplasmic reticulum of eukaryotes (Fig. 6) or Dsb proteins in the periplasm of Gram-negative bacteria such as *E. coli* (see 1.3).[55–57] In addition, under certain conditions (e.g. oxidative stress), thiol groups in intracellular target proteins are glutathionylated by glutathione-S-transferase.

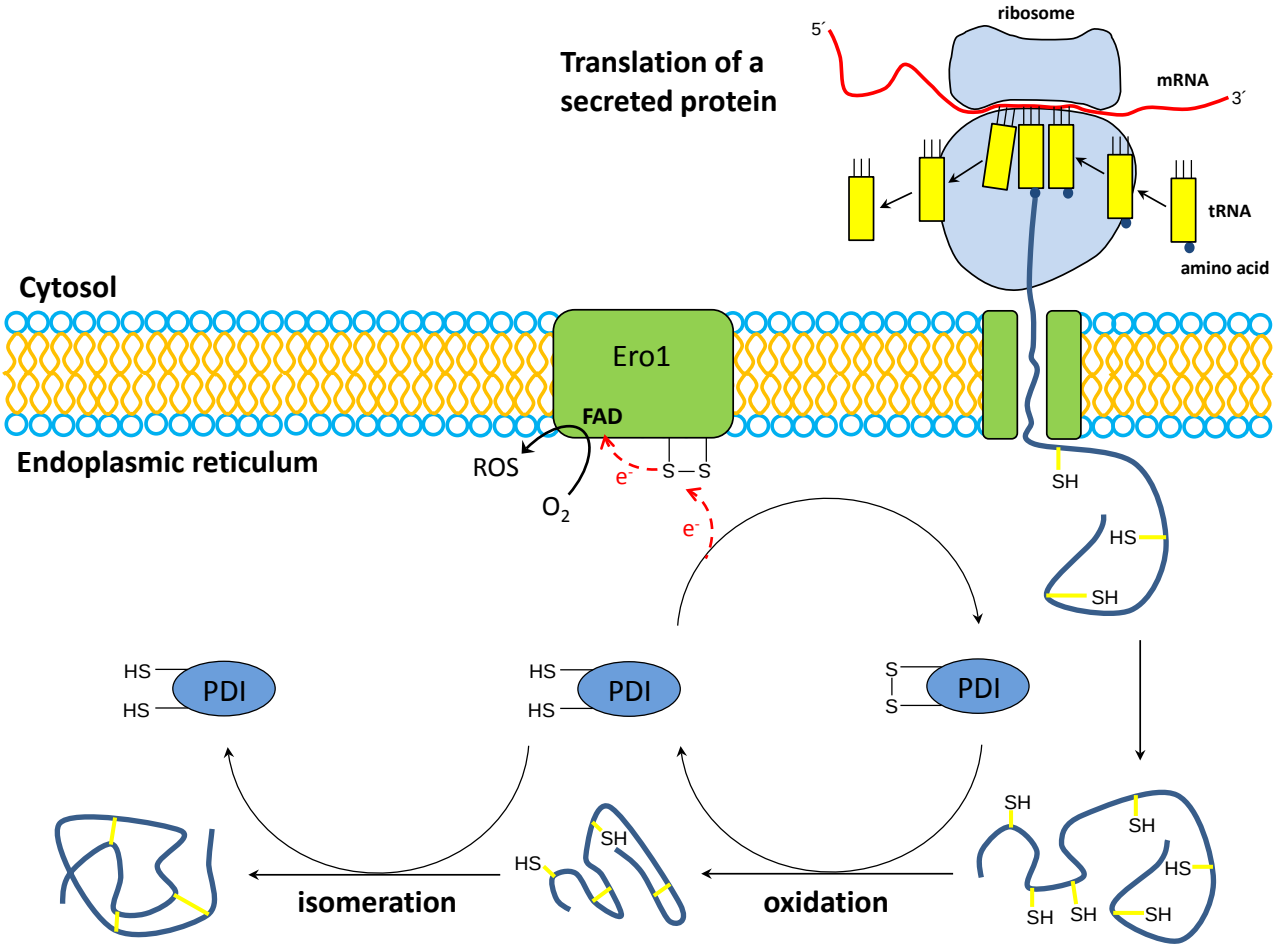

Fig. 6 Oxidative protein folding. Secreted proteins in eukaryotes are translocated into ER where they are folded into their native conformation. PDI catalyzes both formation and isomerisation of disulfide bonds. When reduced, PDI is re-oxidized by a trans-membrane flavoprotein Ero1 concomitantly reducing molecular oxygen. Based on Schwaller (2003) and Tu (2004).[56, 57]

1.2.2 Disulfide reduction pathways

Trx and Grx reduce inter- and intramolecular protein disulfides and mixed protein-GSH disulfides.[58, 59] Trx is in general reduced by NADPH-dependent thioredoxin reductase (NTR), but photosynthetic organisms also contain ferredoxin-dependent Trx reductase coupled to photosynthesis (FTR). Grx is reduced non-enzymatically by GSH, which in turn is reduced by NADPH-dependent glutathione reductase (GR). Physiological studies in yeast and bacteria lacking either Trx or Grx systems suggest significant cross-talk between these two thiol redox pathways.[60, 61] A schematic depiction of the Trx and Grx systems is shown in Fig. 7.

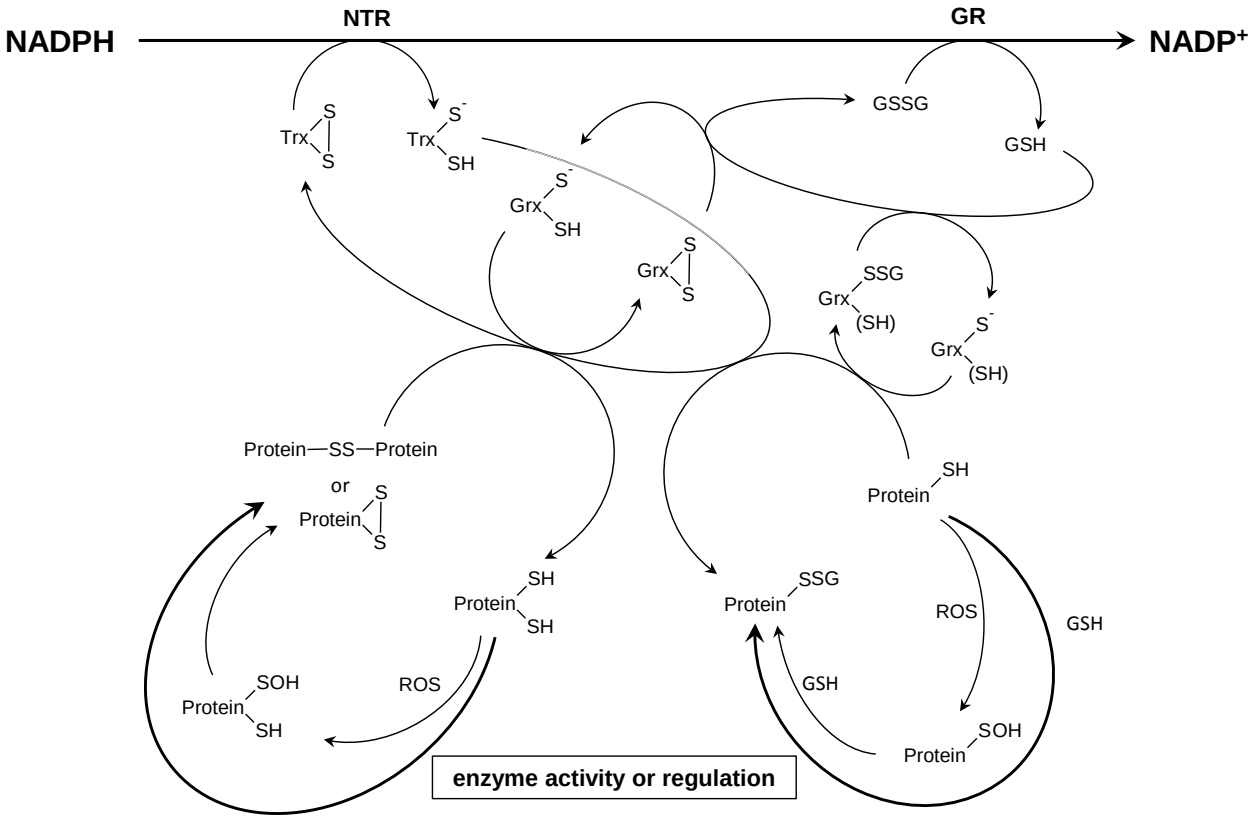

Fig. 7 General overview of Trx and Grx systems. Intramolecular-, intermolecular- and mixed protein disulfides are reduced by NADPH-NTR-Trx and NADPH-GR-GSH-Grx, although particular target proteins do not always overlap. (See text)

Trx is a ubiquitous protein-disulfide oxidoreductase of approximately 10–12 kDa. It was first discovered in the 1960s as a source of reducing power for aerobic (class I) ribonucleotide reductase (RNR) in *E. coli*.[62, 63] The GSH/Grx system was discovered shortly after as an alternative e^- source for class I RNR in a *trx* mutant.[64] Subsequently, many other functions of Trx and Grx have been reported in different biological systems. Validated target proteins (i.e. confirmed by biochemical studies) include for example antioxidant enzymes like glutathione peroxidases (Gpx) and peroxiredoxins,[65–68] sulfate assimilation enzyme 3'-phosphoadenosine-5'-phosphosulfate (PAPS) reductase,[69, 70] arsenate reductase,[71–73] and methionine sulfoxide reductase.[74, 75] Other target proteins regulated by Trx/Grx include e.g. barley α-amylase/subtilisin inhibitor (BASI)[76], limit dextrinase inhibitor,[77] transcription factors OxyR, NF-κB and Ref-1,[78–80] and elongation factor EF-G.[81] In addition to disulfide reductase activity, the reduced form of *E. coli* Trx1 is a component of the processive bacteriophage T7 DNA polymerase[82] and displays chaperone activity *in vitro*.[83] A scheme (Fig. 8) displays examples of known Trx and/or Grx targets with emphasis on bacterial systems.

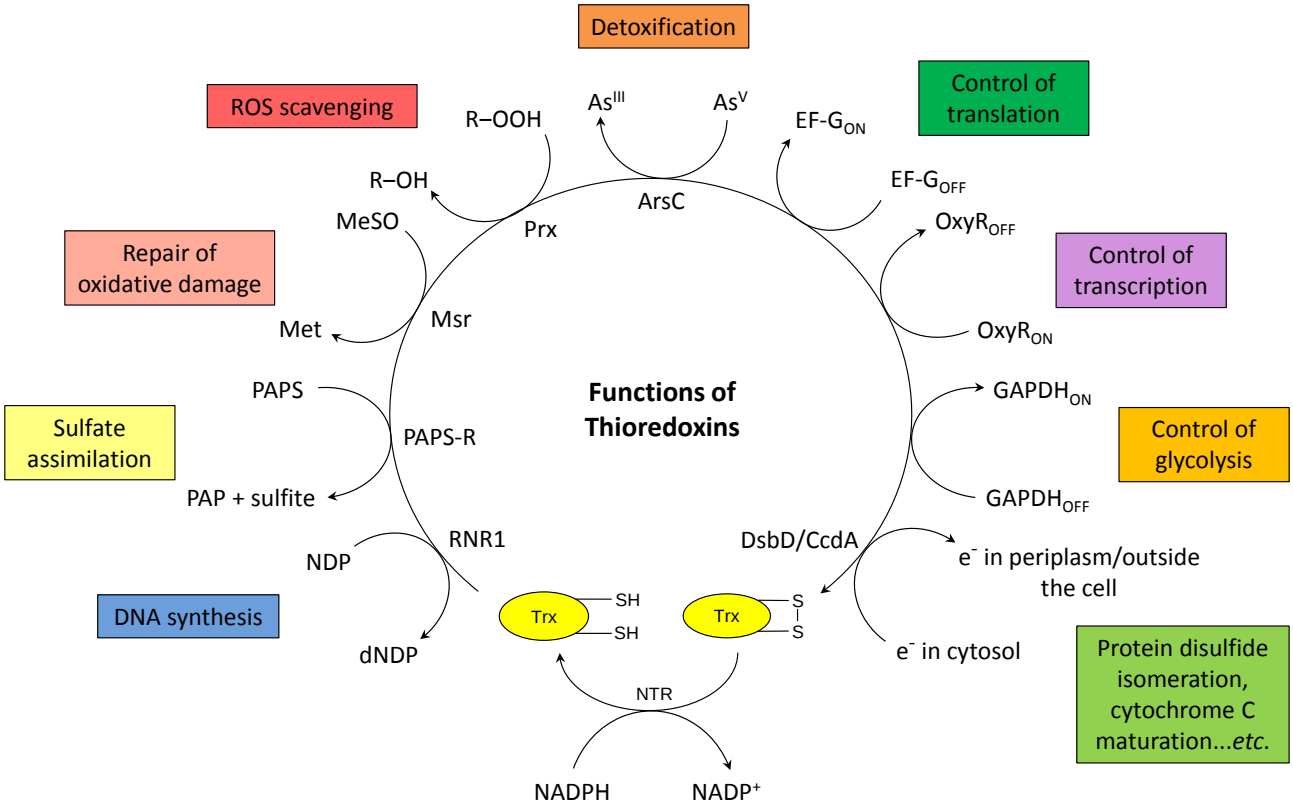

Fig. 8 Functions of Trx. This scheme shows a list of several "well-known" Trx target proteins with emphasis on bacteria; RNR1 – class I ribonucleotide reductase; PAPS-R – 3'-phosphoadenosine-5'-phosphosulfate reductase; Msr – methionine sulfoxide reductase; Prx – peroxiredoxin; ArsC – arsenate reductase; DsbD/CcdA – transmembrane disulfide reductases in Gram-negative (DsbD) or Gram-positive bacteria (CcdA), see Fig.16; PAP - adenosine 3',5'-bisphosphate; MetSO – methionine sulfoxide; R-OOH – alkyl peroxide (or H_2O_2); R-OH – alcohol (or H_2O); EF-G – translation elongation factor G; OxyR – H_2O_2 sensor in *E. coli* and other bacteria (see 1.3.2); GAPDH – glyceraldehyde-3-phosphate dehydrogenase.

Various potential Trx or Grx targets were identified by proteomics methods involving affinity chromatography and/or thiol-specific labeling.[52] Methods based on affinity chromatography involve the use of immobilized active site mutants to trap intermolecular disulfide complexes (Fig.9B; see section 1.2.3.1.) of target proteins from various protein extracts.[52] Many target proteins were identified using this approach, including some established targets (e.g. peroxiredoxins and elongation factors). Studies in plants showed that all enzymes associated with TCA cycle were found to be redox-regulated (see above) and most of them to be targets of Trx (aconitase, PDH E1, PDH E2, PDH E3, isocitrate dehydrogenase, malate dehydrogenase, succinate dehydrogenase, succinyl-CoA ligase) and/or Grx (acetyl-CoA ligase, succinate dehydrogenase, malate dehydrogenase, isocitrate dehydrogenase).[52, 84–86] The situation was similar in chloroplasts where almost all involved enzymes were found to be Trx and/or Grx targets.[52, 84, 85]

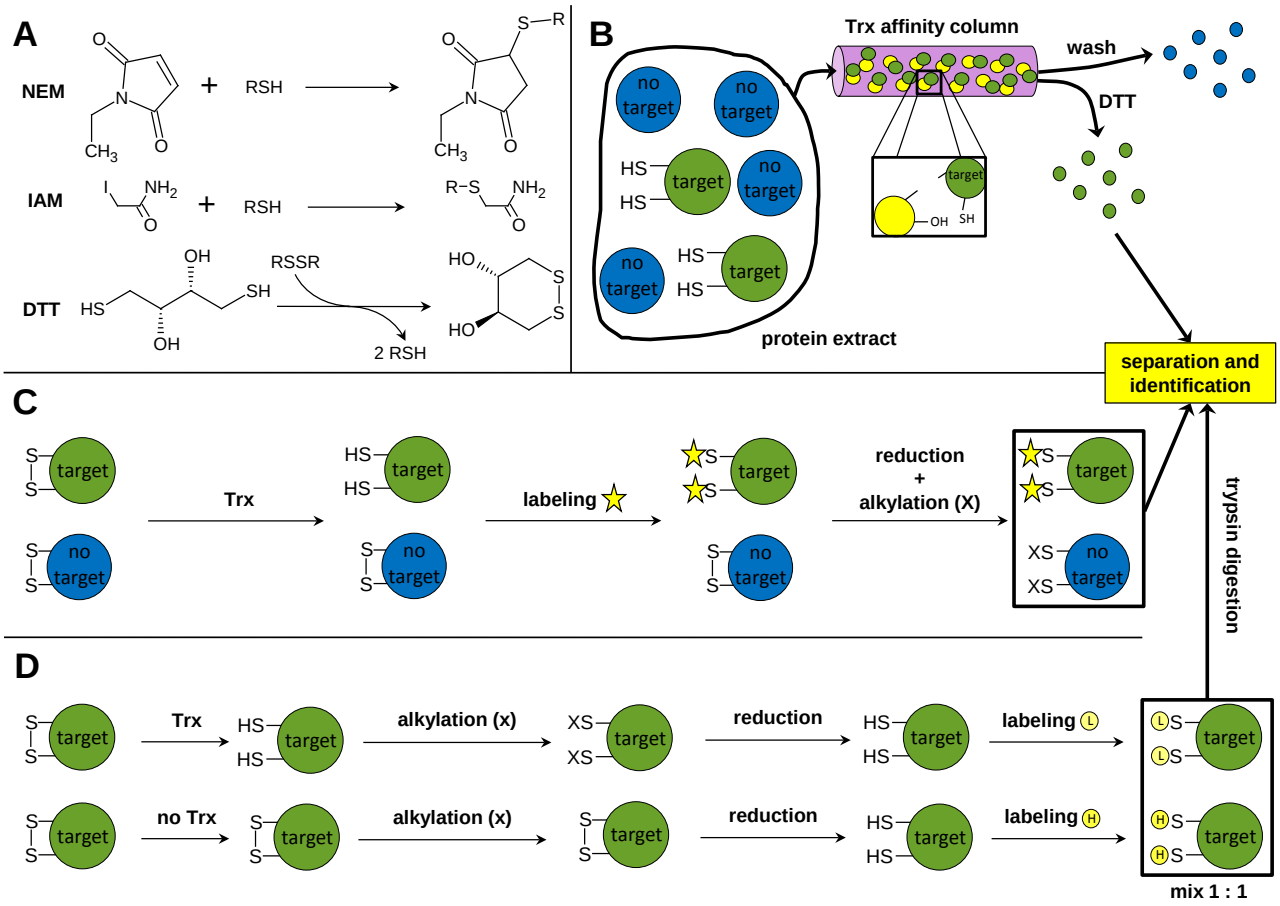

Fig. 9 Identification of Trx targets by proteomics. (**A**) Reactions of two common thiol-specific alkylating agents N-ethylmaleimide (NEM) and iodoacetamide (IAM) and the reducing agent dithiothreitol (DTT); (**B**) Trx affinity chromatography is based on trapping Trx-target complexes on a column with immobilized Trx. Reducing agent (e.g. DTT) elutes the target proteins, which can be separated and identified by mass spectrometry (MS). (**C**) A protein extract can be treated by Trx and released thiols labeled by a thiol-specific fluorescent dye. The remaining disulfides are reduced, alkylated and proteins are separated by e.g. 2D-gel electrophoresis followed by visualization of the fluorescence and further identification by MS. (**D**) Two identical protein samples are either treated by Trx or not and the thiols released by Trx are alkylated. Then reduction of remaining disulfides is performed, followed by differential labeling of the samples ± Trx by light (L) or heavy (H) ICAT reagent. Samples are then mixed 1:1, digested by trypsin and LC/MS follows. Then labeled peptides are identified, quantified and samples with ratio H/L > 1 are Trx targets. Based on Lindahl (2011)[52] and Hägglund (2010).[91]

Methods based on thiol-specific labeling include 2D-gel electrophoresis or LC-MS based proteomics. Gel-based approaches often involve thiol-specific fluorescent labels like e.g. monobromobimane, thiol-specific versions of Cy3 and Cy5 dyes, or BODIPY FL C_1-IA. Generally, protein thiols in extracts treated by Trx are labeled, separated by 2D PAGE, visualized and compared to a control without Trx (Fig.9C).[52, 87, 88] An example of an LC-MS based method involves labeling with thiol specific isotope-coded affinity tag (ICAT)

reagents containing nine isotopically labeled (^{13}C (heavy) or ^{12}C (light)) carbon atoms. Trx treated samples and controls (-Trx) are subjected to differential labeling with heavy and light ICAT followed by trypsin digestion and LC-MS analysis. Peptides containing cysteines from targets can thus be identified and the extent of disulfide reduction quantified by from ICAT heavy/light labeling ratios (Fig.9D).[52, 89] Studies conducted in barley and wheat seeds confirmed several previously identified glycolytic (e.g. GAPDH) and TCA cycle enzymes (e.g. malate dehydrogenase) and stress proteins (e.g. 1-Cys peroxiredoxins, dehydroascorbate reductase). Identified targets also include several storage proteins and proteinaceous inhibitors of enzymes responsible for nutrients mobilization (e.g. BASI).[52, 89–91] A proteomics approach based on so-called tandem affinity purification was applied to identify proteins interacting with *E. coli* Trx independent of the redox active site, including glycolytic proteins (e.g. glyceraldehyde-3-phosphate dehydrogenase and enolase) as well as some transcription factors not containing cysteine (e.g. RcsB and NusG).[52, 92]

1.2.3 Thioredoxin system

1.2.3.1 The catalytic mechanism of Trx

Trx is more thermodynamically stable in its oxidized form than its reduced form. For example the differences between the energies needed for unfolding ($\Delta\Delta G°_{H2O}$ = 15 kJ/mol) and between melting temperatures (ΔT_m = 13 °C) in favor of the oxidized protein were determined for EcTrx1.[93] This stability difference provides the necessary driving force for the disulfide reduction reaction and determines the strong redox potential of Trx (E'^0= -270 mV for *E. coli* Trx1).[94] Generally, Trx reduces target protein disulfides by a thiol-disulfide exchange reaction as depicted in Fig.10. In the first step the thiolate form of the more N-terminal active site Cys (C_N; CGPC) makes a nucleophilic attack on the target disulfide, which results in formation of an intermolecular disulfide intermediate. This intermediate is attacked by the more C-terminal Cys (C_C; CGPC) in Trx and the complex is resolved into reduced target protein and oxidized Trx. The pK_a of the surface-exposed C_N of Trx (approximately 7) is a key feature enabling the first step of the reaction at physiological conditions. The thiolate anion is stabilized by hydrogen bonds with the backone amide of the active site glycine and C_C, and probably also $K57_{EcTrx}$ and $D26_{EcTrx1}$.[95, 96] The pK_a of the buried C_C is around 9 and it is expected to be protonated in this first half of the thiol-disulfide exchange reaction.[97–100] The second, resolving step demands deprotonation of C_C in order to attack the intermolecular disulfide bond and dissociate the Trx-target complex. Mutation of the conserved $D26_{Ectrx1}$ to uncharged residues significantly slowed down the cleavage of the complex. Acid/base catalysis involving the β-carboxyl group of $D26_{EcTrx1}$ was proposed to facilitate deprotonation of C_c.[101] This hypothesis was challenged recently, and it was suggested that a transient interaction with the backbone amide of W preceding the active site (WCGPC) is responsible for this deprotonation.[72, 95, 102, 103]

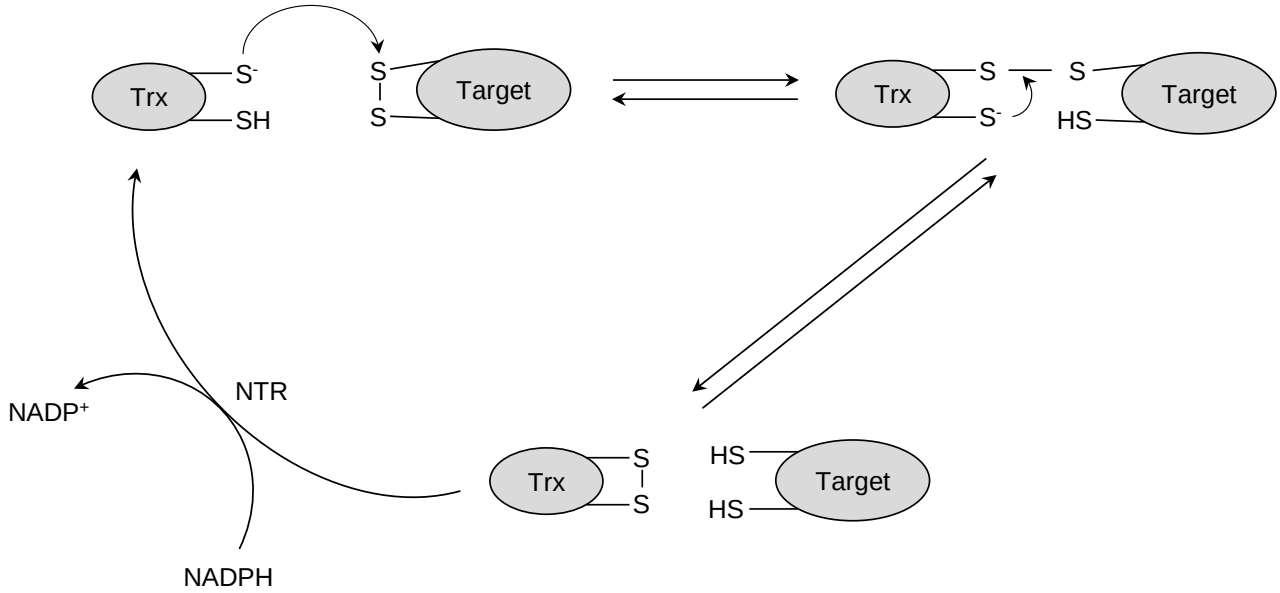

Fig.10 Trx mechanism. The thiolate anion of the C_N in the active site C_NGPC_C motif of the reduced Trx attacks the target protein disulfide and an intermolecular disulfide is formed. This disulfide is attacked by the thiolate of the C_C in the active site of Trx, which results in release of the reduced target protein and oxidized Trx. The latter is reduced by NTR in order to fulfill a catalytic cycle.

1.2.3.2 Structure of Trx

The structure of Trx consists of a five-stranded β-sheet surrounded by four α-helices (βαβαβαββα) and contains a conserved CXXC redox-active motif.[104] The central pattern of a four-stranded β-sheet and three α-helices (βαβαββα) thus lacking the N-terminal βα, represents the whole structure of Grx, and is conserved in many other thiol-disulfide oxidoreductases including for example DsbA (has also a homolog in Gram-positive bacteria called BdbD), PDI, and in various Trx-like proteins; e.g. human TRP14; bacterial proteins StoA; ResA; Ccmg; and many others. The fold was first observed in the Trx structure, therefore it is called the Trx fold, and the proteins sharing it constitute the Trx superfamily.[105–114]

The following section describes important residues in Trx with reference to the well-characterized Trx1 from *E. coli* (Fig. 11, Fig. 12). When starting from the N-terminus, $F12_{EcTrx1}$ is conserved and was suggested to be a part of a hydrophobic pocket together with $F27_{EcTrx1}$.[115] The latter residue is located right behind $D26_{EcTrx1}$, which was suggested to be involved in catalysis by stabilizing the thiolate anion of the C-terminal active-site cysteine residue (C_C) facilitating its attack on inter-molecular disulfide intermediates (see section 1.2.3.1.).[101, 116] $D26_{EcTrx1}$ together with $K57_{EcTrx1}$ forms a charged region between the β-sheet and α2-helix, which was also suggested to stabilize the low pK_a of the N-terminal active site cysteine (C_N; Fig. 11E).[96, 117] $W31_{EcTrx1}$, which is important for the thermodynamic stability of Trx, interacts with other conserved residues, namely $A29_{EcTrx1}$ and $D61_{EcTrx1}$ (Fig. 11E).[104, 115, 118, 119] $W31_{EcTrx1}$ is followed by the CGPC active site motif. In reduced Trx, C_N is solvent-exposed and more nucleophilic than C_C, which is buried. The disulfide

formation in Trx does not introduce major conformational changes. However, a few local changes in dihedral angles and hydrogen bonding occur around the active site.[120, 121] Mutations of G or P in the active site motif influence redox properties and stability of Trx.[95, 99, 122] The active site is followed by the conserved $P41_{EcTrx1}$, which forms a kink in the α2-helix and stabilizes Trx structure.[123, 124] $P76_{EcTrx1}$ is in a *cis*-conformation, and is conserved in all Trx-like proteins. It interacts with the active site and influences the redox potential.[95, 124, 125] Together with the two preceding residues, $P76_{EcTrx1}$ forms a loop contributing to recognition of target proteins.[76, 126] $P76_{EcTrx1}$ is followed by $T77_{EcTrx1}$ forming a hydrogen bond with its own and the following residue's main chain oxygens.[95, 115] Conserved $G84_{EcTrx1}$ and $G92_{EcTrx1}$ surround the β5-strand and are important for Trx activity. In particular $G92_{EcTrx1}$, which is a part of the VGA motif seems to be important for the interaction with target proteins.[76, 126] Some other positions containing hydrophobic residues ($I72_{EcTrx1}$, $I75_{EcTrx1}$, $L78_{EcTrx1}$) form a hydrophobic pocket next to the active site, which was suggested to be important for the interaction with NTR in bacteria.[106]

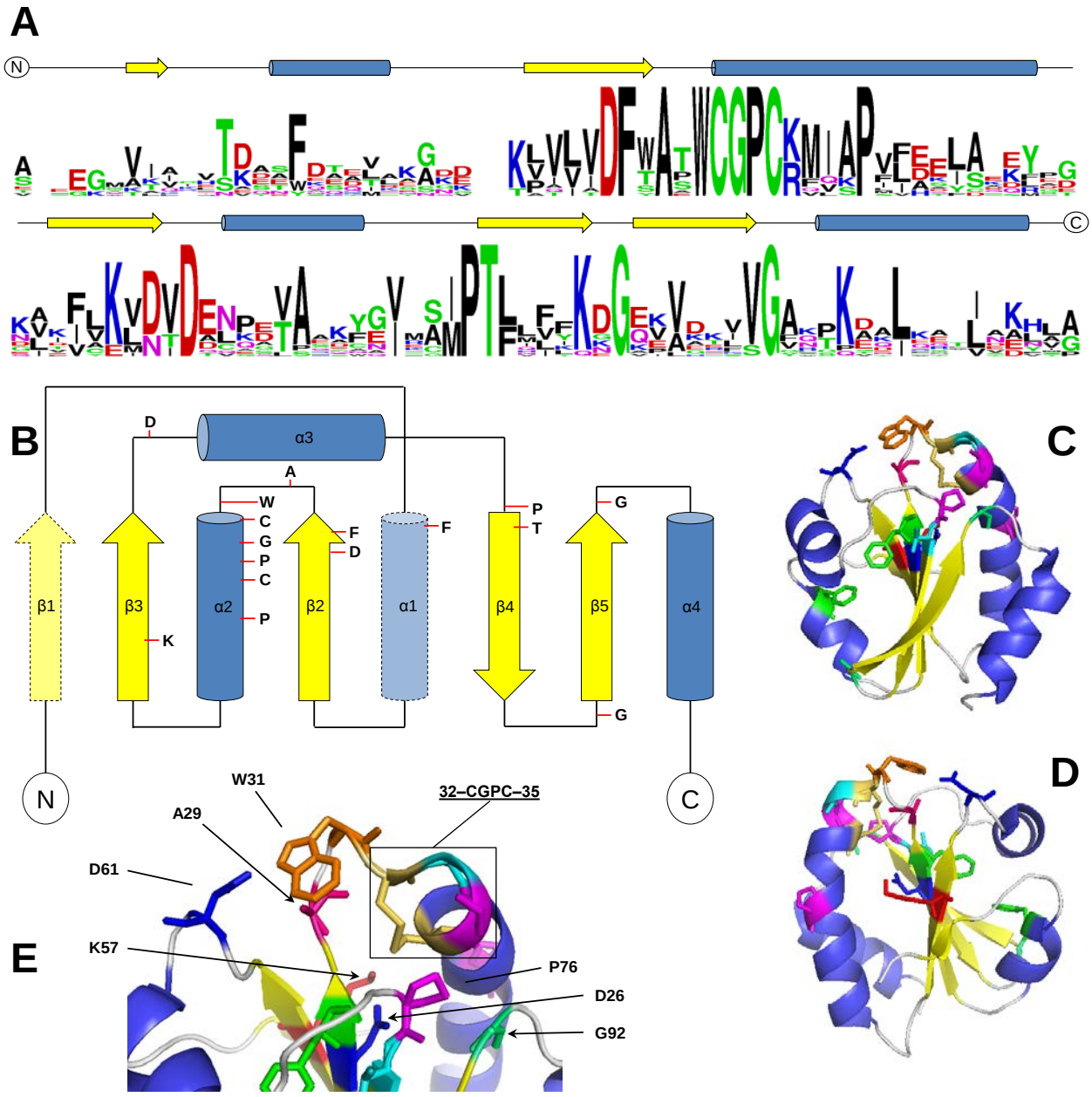

Fig.11 Structure of Trx. (**A**) Sequence logo based on ClustalW multiple alignment of classical thioredoxins (Fig. 12) with secondary structure marked above the sequence; (**B**) Scheme of the secondary structure of Trx showing positions of important residues and highlighting the parts belonging to Trx fold shared by other proteins (see the text); (**C, D**) Structure of oxidized Trx from two different angles showing the positions of the conserved residues marked as follows: active site disulfide (gold), hydrophobic residues (green), positively charged (red), negatively charged (dark blue), proline (purple), glycine (cyan), tryptophan (orange), alanine (pink); (**E**) Close-up look at the active site (EcTrx1 numbering); for more details see the text. 3D-structure images were made in PyMOL v1.3 (Schrödinger LLC) from PDB file 2O7K representing oxidized TrxA of *S. aureus*. The secondary structure scheme is based on the same data. The logo is made by use of Weblogo (http://weblogo.berkeley.edu/). Based on Collet & Messens, 2010.[95]

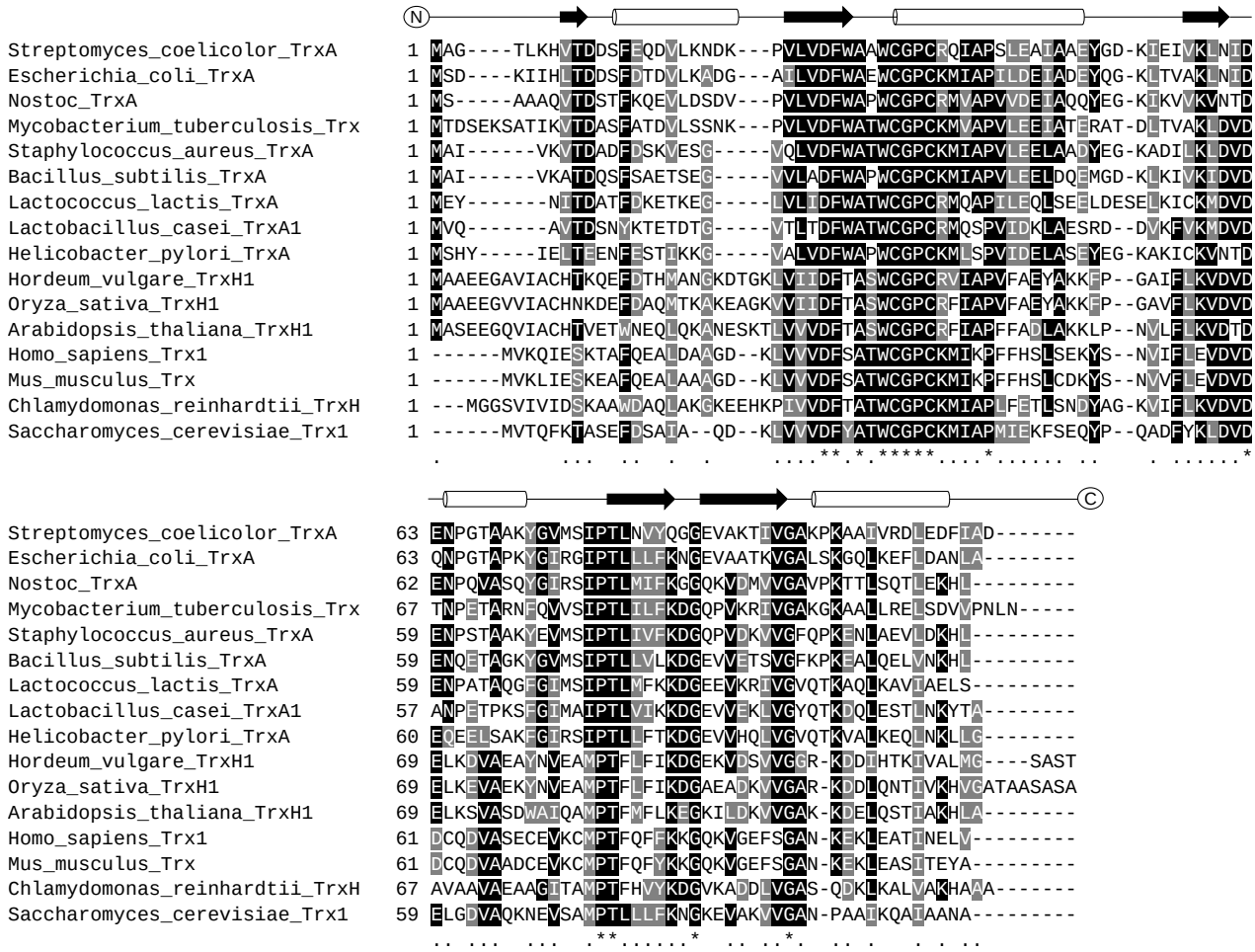

Fig.12 Multiple alignment of selected classical Trx homologs. UniProt accession numbers: *S. coelicolor* TrxA (P52230), *E. coli* TrxA (P0AA25), *Nostoc TrxA* (P0A4L1), *M. tuberculosis* Trx (P0A616), *S. aureus* TrxA (A6QG47), *B. subtilis* TrxA (P14949), *L. lactis* TrxA (A2RJC9), *L. casei* TrxA1 (G1U9U9), *H. pylori* TrxA (P66928), *H. vulgare* TrxH1 (Q7XZK3), *O. sativa* TrxH1 (Q0D840), *A. thaliana* TrxH1 (P29448), *H. sapiens* Trx1 (P10599), *M. musculus* Trx (P10639), *C. reinhardtii* TrxH (P80028), *S. cerevisiae* Trx1 (P22217); residues identical or similar to the consensus sequence based on present alignment are marked black or gray, respectively; the alignment was made by using ClustalW2 algorithm and BoxShade 3.21 online editing tool (http://www.ch.embnet.org/software/BOX_form.html); secondary structure was marked according to the Figure 11.

1.2.3.3 The Trx reductase

Oxidized Trx needs to be recycled and gain two electrons in order to complete a catalytic cycle. The electron source is in most cases a homodimeric flavoenzyme called NADPH-dependent thioredoxin reductase (NTR; see above). Bacteria, archea and some lower eukaryotes (e.g. plants, yeast) possess low-molecular-weight NTR (35 kDa per monomer) containing one CXXC redox center. Higher eukaryotes (e.g. mammals) possess high-molecular-weight NTR (55 kDa per monomer) containing an additional C-terminal redox center employing a nucleophilic selenocysteine. This difference is also reflected in functionality, as

mammalian NTRs exhibit a relatively wide substrate specificity.[127–130] There are also other forms of NTRs like e.g. NTR-C, which is a fusion protein in plants and cyanobacteria, containing NTR and Trx within the same polypeptide.[131, 132] A similar fusion protein was also observed in *Mycobacterium leprae*.[133]

A low-molecular-weight NTR polypeptide consists of an NADPH-binding domain harboring the CXXC active site motif and an FAD-binding domain. The catalytic mechanism of NTR includes a 67° rotation between two conformations called flavin-oxidizing (FO) and flaving-reducing (FR; Fig. 13). This event was suggested to be a rate-limiting step of the NTR reaction mechanism.[134–138] In the FO conformation, $FADH_2$ reduces the active site disulfide, which is buried in its vicinity. Then the NADPH-binding domain rotates 67° resulting in exposure of CXXC, making it available for interactions with Trx. Concomitantly, the bound NADPH molecule is displaced 17 Å and positioned in close vicinity of FAD. A recent study of barley NTR2 proposed a hypothesis that an initial surface interaction between Trx and NTR in the FO conformation can be a trigger for the conformational change to FR. Only at this stage, NADPH binding followed by FAD reduction can occur, concomitantly with reduction of Trx (Fig. 13).[139]

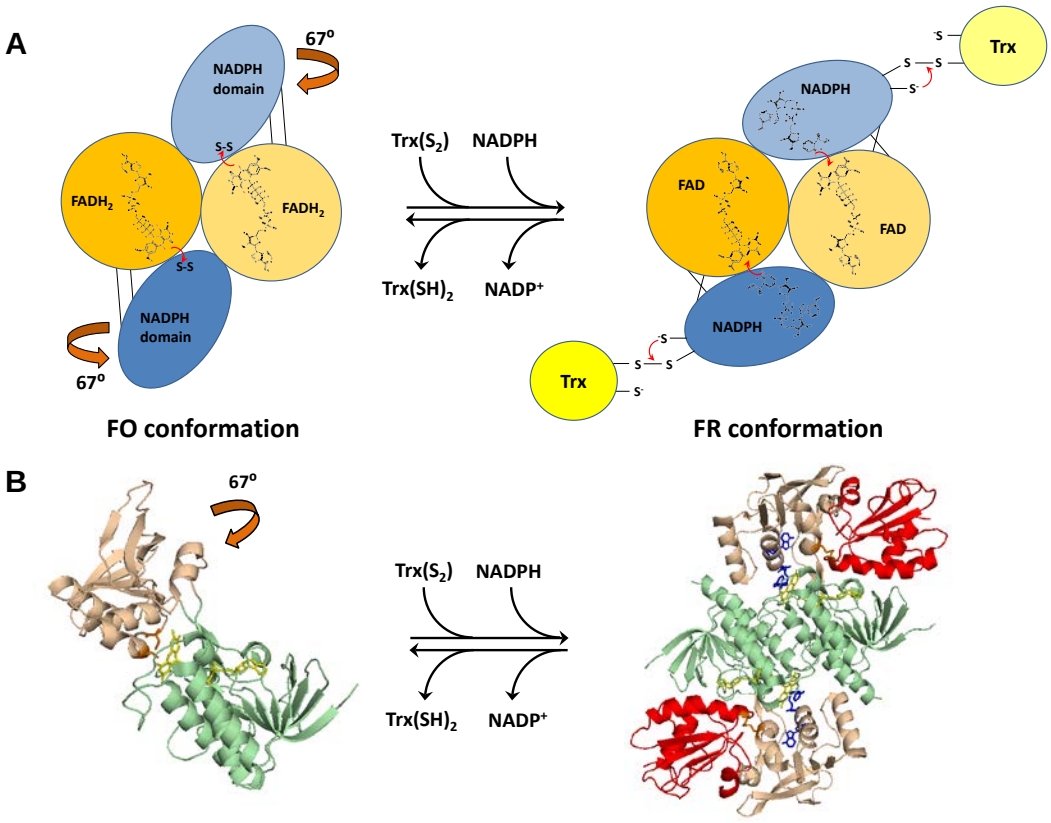

Fig.13 NTR mechanism. (**A**) Schematic representation: In the FO conformation $FADH_2$ reduces the buried disulfide in NTR. In the FR conformation the active site CXXC motif in NTR can react with Trx while NADPH regenerates the flavin cofactor. Red arrows mark the direction of the electron flow. Based on Kirkensgaard *et al.* (2009).[139] (**B**) Structure of an NTR monomer in the FO conformation showing FAD in vicinity of the active site dithiol. Structure of the stable complex of dimeric NTR with Trx demonstrates the FR conformation where the NADPH-domain is rotated and the active site is accessible to Trx and FAD is reduced by NADPH. NADPH-domain – pink, FAD-domain – green, Cys – orange, FAD – yellow, NADPH – blue, Trx – red; Images were made in PyMOL v1.3 (Schrödinger LLC) based on structures of *E. coli* enzymes; PDB files: 1CL0 (NTR monomer), 1F6M (NTR-Trx complex).

1.3 Bacterial thiol redox systems

1.3.1 General overview

Thiol oxidoreduction in bacteria is catalyzed by the ubiquitous types of thioredoxin family proteins described above. The Trx system of *E. coli*, *B. subtilis* and *S. aureus* has been thoroughly investigated.[140–144] *E. coli* is viable when either the Trx or Grx system is active. However, it demands an exogenously added disulfide reductant for growth when both disulfide reductants are impaired.[61, 145, 146] Deletion of *trxA* in *B. subtilis* introduced deoxyribonucleoside, Cys/Met auxothrophy and impaired extracellular redox processes like e.g. spore formation.[147] A transcriptomic study examining gene expression at different levels of TrxA showed overexpression of genes involved in oxidative stress and sulfur metabolism upon TrxA depletion.[148]

In addition several atypical Trx-like or Grx-like proteins have been identified among bacterial species. *E. coli* Trx2 is a Trx-like protein containing two additional N-terminal CXXC motives (CTHC, CGRC) complexing Zn^{2+} ions. Oxidation by H_2O_2 releases Zn^{2+} and induces conformational changes.[149] A similar concept of oxidation-related zinc release from a complex with thiols commonly exists in thiol-based redox sensors (e.g. Spx in *B. subtilis*, RsrA in *Streptomyces coelicolor* or human KEAP1/Nrf2).[49, 150–152] Such a function was suggested also for Zn^{2+}-binding in EcTrx2.[149] Bound Zn^{2+} was shown to increase thermodynamic stability and influence redox properties of EcTrx2. Particularly, disruption of Zn^{2+}-binding by C to S mutation decreased the redox potential from -221 mV to -254 mV and pK_a shifted from 5.1 to 7.1.[93] Unlike EcTrx1, which is under control of the stringent response factor ppGpp and is highly induced in stationary phase, EcTrx2 is under control of OxyR (see below), which suggests a role in oxidative stress response.[153, 154] EcTrx2 can reduce ribonucleotide reductase, PAPS reductase and DsbD, but not methionine sulfoxide reductase.[149, 155] Trx2 from *Deinococcus radiodurans* has been partially characterized and potential homologs were found in various other bacteria.[149, 156]

Several putative thioredoxins containing WC[G/P]DC sites have been reported, e.g. *H. pylori* Trx2 (WCPDC), *L. lactis* TrxD (chapter 2 and 3), *B. subtilis* YtpP and YdpP (WCPDC), *B. anthracis* Trx2 (WCPDC). HpTrx2 was shown to contribute in oxidative and nitrosative stresses, especially cumene hydroperoxide.[157] Protein disulfide reductase activity of HpTrx2 was confirmed by insulin assay.[158] However, it was shown not to interact with the ubiquitous bacterial NADH-peroxidase AhpC, which is dependent on a WCGPC-type Trx in this organism. The genes *ytpP* and *ydpP* in *B. subtilis* are non-essential and were observed to be induced by Spx in the presence of diamide.[148, 159–161] The latter one is also induced by the stress factor σ_B and its up-regulation in correlation with TrxA (WCGPC-type) depletion was observed.[148, 162] BaTrx2 was shown to be less abundant than BaTrx1 (WCGPC-type), did not exhibit disulfide reductase activity toward ribonucleotide reductase class Ib (see below), but was active on the model disulfide substrate 5,5'-dithiobis-(2-nitrobenzoic acid); DTNB; Ellman's reagent.

A glutaredoxin-like protein NrdH provides reducing equivalents to NrdEF, an aerobic RNR (class Ib).[163–167] RNR constitutes of two subunits: a large (NrdE) and a small (NrdF). The mechanism includes formation of a tyrosyl radical on the metalloprotein NrdF (Y105 in *E. coli* NrdF) by the action of oxygen.[168] A thiyl radical on a catalytic cysteine of NrdE (C439 in *E. coli* NrdE) is generated by the action of the mentioned tyrosine radical on NrdF.[169] Oxidized NrdF is regenerated by a flavodoxin NrdI.[168] The formed thiyl radical on NrdE attacks the sugar moiety of the ribonucleotide substrate, resulting in deoxyribonucleotide generation and formation of an intramolecular disulfide in the active site of NrdE (C225-C462 in *E. coli*). This disulfide is

reduced by a C-terminal CXXC motif, in turn reduced by NrdH.[167, 169] The mechanism is analogous in class Ia RNR (NrdAB) where Trx1 or Grx1 (in *E. coli*) are the corresponding disulfide reductases.[167, 170] NrdH displays sequence similarity to Grx but is reduced by NTR.[165] The structures of NrdH from *E. coli* and *C. ammoniagenes* revealed the minimalistic version of Trx-fold similar to Grx (see 1.2.3.2; Fig. 11). However, GSH binding site appeared to be replaced by a hydrophobic pocket, which was suggested to be important for the interaction with NTR.[106, 171] Generally, all NrdH contain an N-terminal CXXC motif, and most of the homologs contain a specific C-terminal motif stabilizing the structure. These were used in NrdH classification: class 1 (CVQC; WSGFRP[ED]; e.g. *E. coli*), class 2 (C[MVI]QC; FSGF[RQ]P; e.g. *L. lactis*), class 3 (C[MI]QC; GPXP; e.g. *Lb. plantarum*) and class 4 (CPPC; no C-terminal motif; e.g. *B. anthracis*).[171, 172] A partial correlation of this classification with *nrdH* and *nrdIEF* gene organization is also interesting, as classes 1-3 NrdH form either *nrdHIEF* or *nrdHEF* operons (*nrdI* is separate in the latter case). Only class 4 NrdH is encoded by a gene separated from *nrdIEF*.[171, 172] *E. coli* NrdH cannot be replaced by Trx1. Grx1 showed activity towards NrdEF *in vitro*, but only NrdH seems to be the electron donor *in vivo*. [165, 167] *B. anthracis* and *S. aureus* NrdH (both class 4) can be replaced by Trx1 both *in vitro* and *in vivo*.[172, 173]

Several bacterial species including *E. coli* produce GSH (Fig.14A) as a major cellular antioxidant. *S. agalactiae*, *L. monocytogenes*, and *Pasteurella multocida* possess a non-classical bifunctional GSH biosynthesis enzyme GshF fulfilling the action, which is commonly distributed between GshA and GshB.[174–176] Some lactic acid bacteria lack GSH synthesis genes but are able to import and utilize GSH.[177–179] Coenzyme A (CoA-SH; Fig.14B) is also a highly abundant LMW thiol in e.g. *Bacilli* and *Staphylococci* and it has been suggested to function in thiol redox control.[177, 180–182] Many other Gram-positive bacteria lacking GSH produce alternative LMW thiols. Mycothiol (MSH; Fig.14C) is a major disulfide reductant among actinomycetes and donates electrons to the Grx-like mycoredoxin.[47, 107, 177, 183–185] Bacillithiol (BSH; Fig.14D) was discovered recently as the major LMW thiol rather than CoA-SH in *Bacillus* sp., *S. aureus* and *Deinococcus radiodurans*, and putative bacilliredoxins (Brx) have been suggested as BSH substrates.[47, 144, 177, 184, 186] The mechanism of action of these LMW thiol redox pathways is not known in detail. However they were hypothesized to act as functional analogues of the GSH/Grx system (Fig. 7).[47, 107, 144]

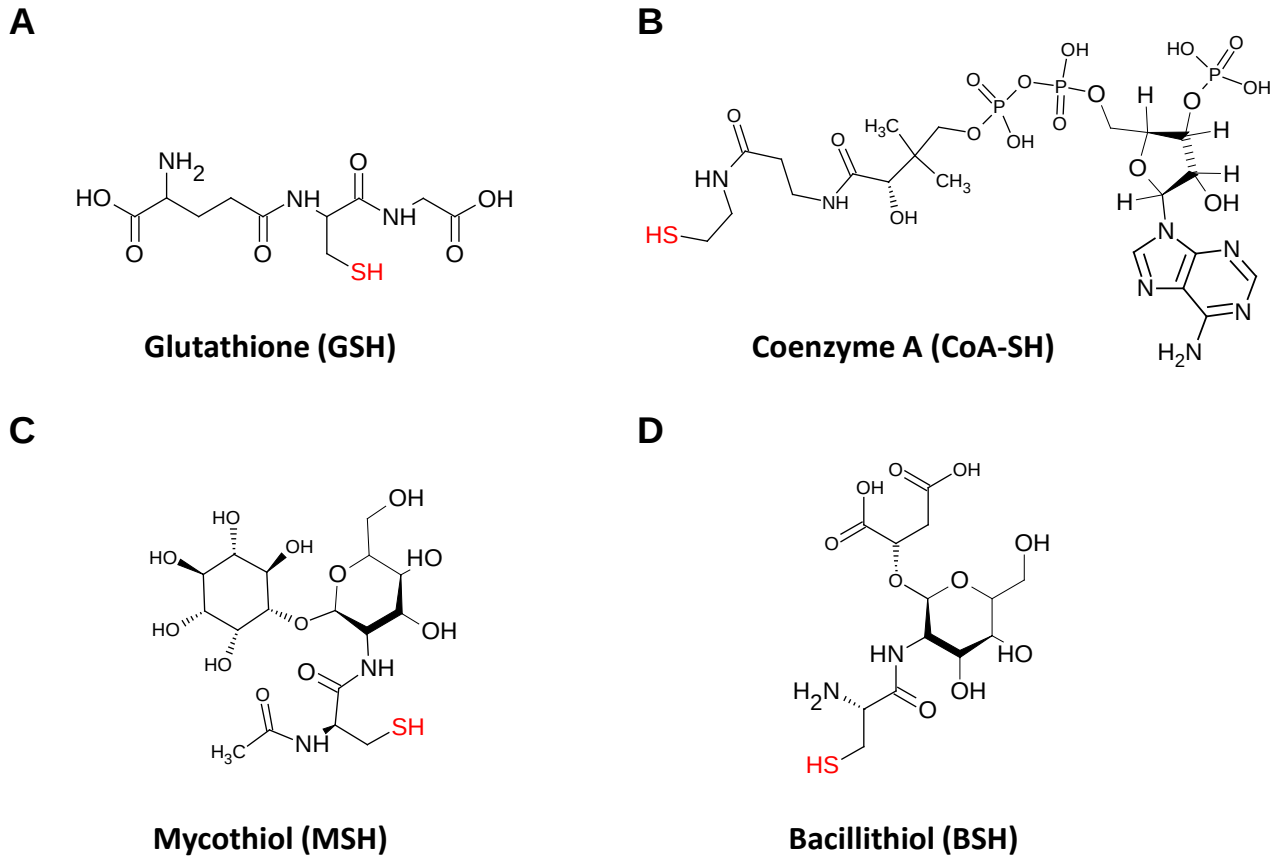

Fig.14 Examples of LMW thiols present in bacteria. (A) Apart from eukaryotes, GSH is often present in Gram-negative bacteria e.g. *E. coli*. (B) CoA-SH was suggested to function in thiol redox control in several Gram-positive bacteria e.g. *B. megaterium*. (C) MSH was found to be the major LMW thiol in actinomycetes e.g. *C. glutamicum*. (D) BSH was recently discovered in *Bacilli*.

Disulfide bond formation in *E. coli* is catalyzed by the so-called Dsb (Dsb comes from "disulfide bond") system.[187] Oxidized DsbA (E'_0 = -122 mV and pK_a around 3.5) accepts electrons from disulfide bonds in target proteins.[188] Electrons are then transferred from the reduced DsbA to the respiratory chain via a transmembrane protein DsbB and the quinone pool (Fig.15).[189]

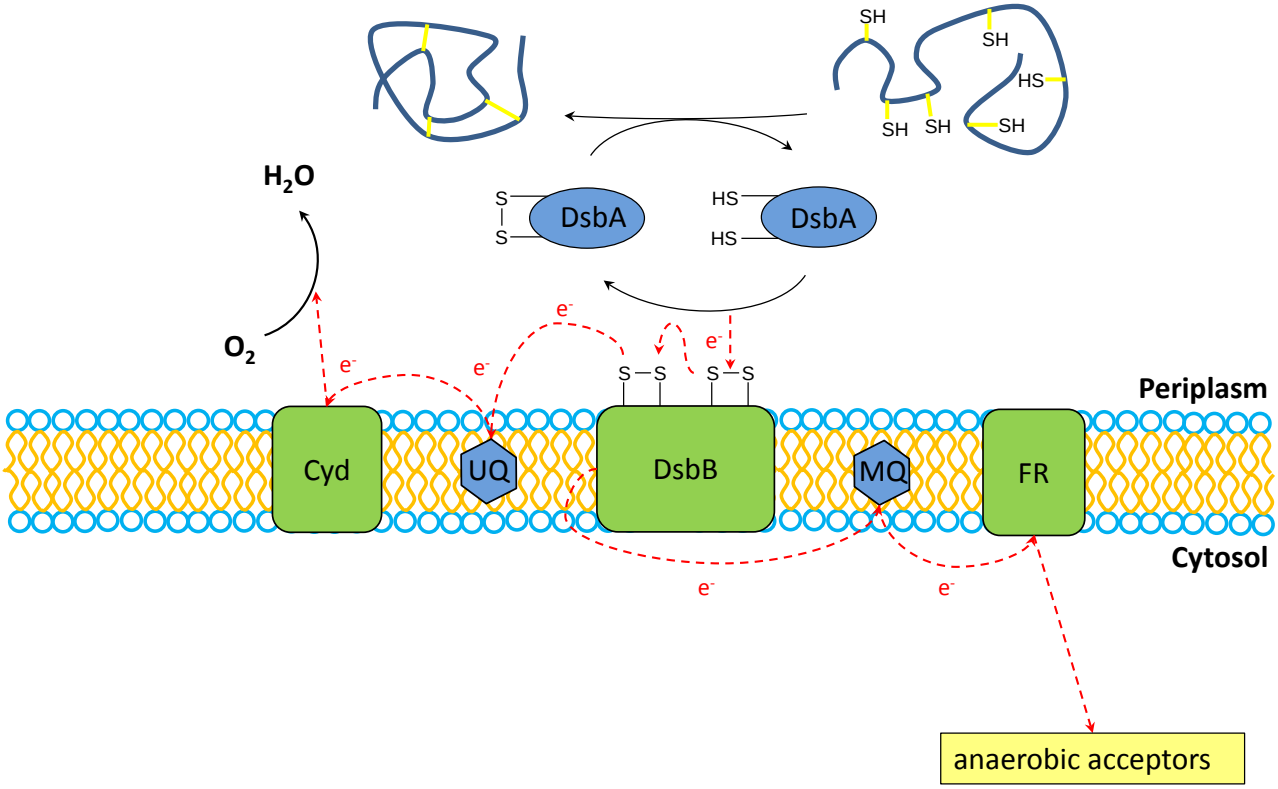

Fig.15 DsbA and DsbB periplasmic redox system in *E. coli*. Oxidized DsbA forms disulfide bonds in target proteins by accepting electrons from reduced thiol groups. The reducing equivalents are transferred to either aerobic (Cyd) or anaerobic (FR) respiration chain through the quinone pool via DsbB. The electron flow is indicated by red dashed arrows. MQ – menaquinone; UQ – ubiquinone; FR – fumarate reductase; Cyd – cytochrome C oxidase. Based on Messens & Collet (2006).[187]

Disulfide bond isomerization is catalyzed by two isomerases DsbC and DsbG. These proteins gain electrons from the cytosol via a transmembrane protein DsbD.[190, 191] DsbD is a target of Trx and electrons are transferred over the membrane through a single target disulfide buried in its transmembrane subunit. DsbD provides reducing equivalents to various periplasmic proteins involved in e.g. cytochrome maturation and oxidative stress defense (Fig. 16).[112, 190, 192, 193] In *B. subtilis* CcdA, a protein homologous to the β subunit of DsbD, transfers electrons to Trx-like proteins ResA and StoA in a Trx-dependent manner (Fig. 16). ResA reduces cytochrome C (similar function has CcmG in *E. coli*),[113] and StoA is involved in spore formation. Impaired spore formation in a *trxA* deletion strain was suppressed by deficiency of BdbC and BdbD, which are a homologs of DsbA and DsbB.[194, 195]

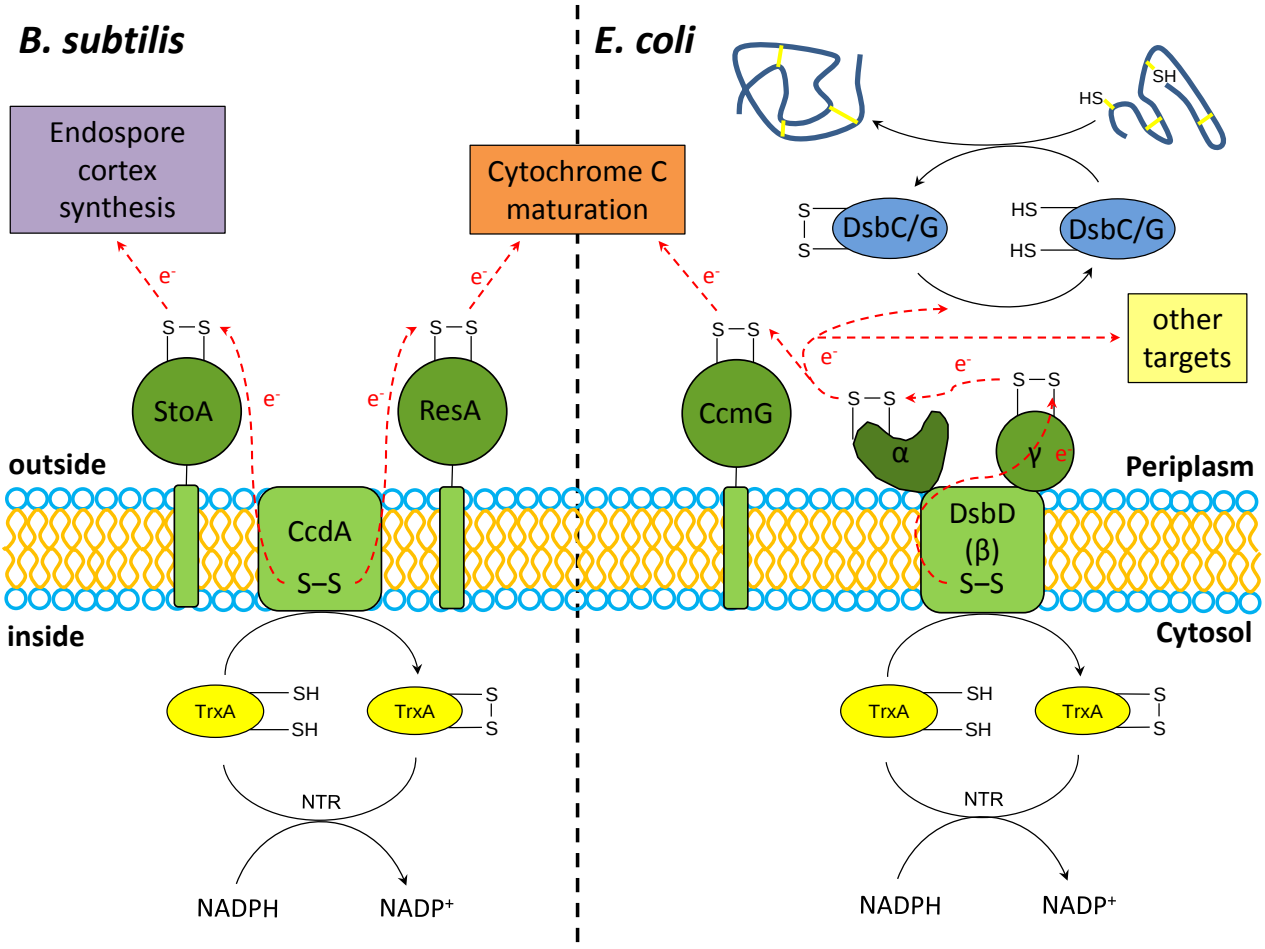

Fig.16 DsbD and CcdA systems. (*right*) Some Gram-negative bacteria like *E. coli* contain the transmembrane protein DsbD. Electrons originating from the cytosolic Trx system are transferred by a sequence of thiol-disulfide exchanges. First, Trx reduces a disulfide in the transmembrane β-subunit and then a Trx-like γ-subunit transfers the electrons to an immunoglobulin-like α-subunit. Finally, the latter reduces target proteins, e.g. CcmG and the periplasmic protein-disulfide isomerases DsbC or DsbG. CcmG keeps apo-cytochrome C in a reduced form in order to be correctly processed. (*left*) CcdA is a single-subunit DsbD-like transmembrane protein in *B. subtilis*. CcdA donates electrons to cytochrome C *via* ResA. In addition CcdA reduces StoA, one of the key enzymes of endospore cortex synthesis. Red dashed arrows mark the flow of e^-. Based on Messens & Collet (2006) [187], Möller & Hederstedt (2008)[147] and Stirnimann *et al.* (2005).[113]

1.3.2 Thiol-redox sensors and transcriptional control of stress resistance

Various pathways of oxidative stress responses involving redox sensors, which upon oxidation directly or indirectly modulate transcription of involved genes have been described in bacteria.[1, 2] Such pathways often involve thiol-disulfide exchange reactions which provide high sensitivity towards oxidants and reversibility. A well characterized example of a bacterial thiol-based redox sensor is OxyR, which mediates response to H_2O_2 in e.g. *E. coli*, *Salmonella typhimurium*, *Deinococcus radiodurans*, *Shigella flexneri*.[5, 196–202]

OxyR in *E. coli* is a tetrameric protein with two cysteines (Cys199 and Cys208) per monomer. In the presence of H_2O_2, Cys199 is oxidized to sulfenic acid (Fig. 5C) followed by formation of an intramolecular disulfide with Cys208 (Fig. 5A), which leads to a conformational change enabling DNA-binding and interaction with RNA polymerase.[203] The OxyR-mediated response in *E. coli* includes induction of *e.g.* catalase (*katG*), peroxiredoxin (*AhpCF*), glutaredoxin (*grxA*), glutathione reductase (*gorA*), thioredoxin 2 (*trxC*), ferritin involved in DNA protection (*dps*), iron homeostasis regulator (*fur*), manganese importer (*mntH*), and iron-sulfur clusters assembly (*sufABC*).[5, 204–208]

FLP, which stands for FNR-like protein, represents a sensor involved in oxidative stress resistance in Gram-positive bacteria.[209, 210] FLP forms a homodimer containing non-stoichiometric amounts of Cu and Zn. FLP has two cysteines forming an intramolecular disulfide which is necessary for DNA binding. [210] Two FLP homologs (FlpA, FlpB) were found in *L. lactis* ssp. *cremoris* MG1363 and a strain lacking both *flpA* and *flpB* exhibited hypersensitivity to H_2O_2 and depleted the intracellular Zn pool.[211] Two paralogous operons ($orfX_A orfY_A flp_A$ and $orfX_B orfY_B flp_B$) controlled by FlpA anf FlpB in *L. lactis* encode the sensors themselves as well as putative metallochaperones ($orfX_{A/B}$) and Dps proteins ($orfY_{A/B}$).[211, 212]

A different thiol-based strategy is employed by the pleiotropic disulfide sensor Spx, which was first discovered in *B. subtilis*.[213] This protein contains an N-terminal $C_{10}XXC_{13}$ motif and is structurally similar to the Grx-dependent arsenate reductase (ArsC) in *E. coli*.[214, 215] Reduced Spx is inactivated by formation of a complex with the protein YjbH and degraded by ClpXP protease. Upon oxidation, Spx forms an intramolecular disulfide between Cys10-Cys13, is released from YjbH and thus avoids proteolytic degradation.[150] Oxidized Spx binds to the α-C-terminal domain of RNA polymerase and thus regulates transcription.[161, 213, 214, 216] In *B. subtilis* transcription of 275 genes were induced by Spx/RNAP upon oxidative stress induced by diamide including e.g. Trx (*trxA*), NTR (*trxB*), ferritin (*mrgA*), PerR (*perR*) and catalase (*katA*).[160, 161, 216, 217] *L. lactis* ssp. *cremoris* MG1363 possesses seven putative Spx homologs.[218] One of these (TrmA) was connected with heat and oxidative stress and another one (SpxB) was suggested to play a role in response to cell envelope stress induced by lysozyme.[219–222]

Genes *trxA* and *trxB* (NTR) in *B. subtilis* are under control of a vegetative σ_A factor as well as under control by the general stress factor σ_B.[140, 159, 161, 223] Oppositely, *trxB* in *S. aureus* was shown to be unaffected in the σ_B^- strain, while being severely decreased in the growth impaired *spx*$^-$ strain.[224] The *trxB* gene in this organism is also negatively regulated by transcription factor SarA, which controls various genes connected with pathogenesis.[225, 226] *Corynebacterium glutamicum*, showed downregulation of NTR in strains with inactivated potential redox sensors, but the strains were significantly more viable than *B. subtilis* or *S. aureus trx* mutants.

1.4 Lactic acid bacteria (LAB)

1.4.1 General features

Various foods and beverages based on lactic acid fermentation have been accompanying our civilization for thousands of years. These processes involve lactic acid bacteria (LAB), a relatively wide group of (facultative) anaerobic Gram-positive bacteria converting sugars in raw materials (e.g. fruits, vegetables, cereals, milk or meat) predominantly into lactic acid.[227] Production of lactic acid prolongs shelf-life of food and beverages as the increased acidity inhibits microbial growth. The shelf-life is also increased by various

compounds e.g. H_2O_2, acetic acid and antimicrobial peptides (bacteriocins) produced by LAB.[228, 229] Acidification leads to protein precipitation, which is essential for cheese production. Furthermore, acidification influence flavor and texture development together with proteolysis and lipolysis.[230, 231]

The group of LAB comprises mainly genera belonging to *Firmicutes* (order *Lactobacillales*), e.g. *Lactococcus*, *Lactobacillus*, *Pediococcus*, *Leuconostoc*, *Oenococcus*, *Streptococcus* and *Enterococcus*.[232] However, some LAB e.g. *Bifidobacterium* spp. belong to the *Actinobacteria*.[233] Genera like for example *Streptococcus* and *Enterococcus* include known pathogens e.g. *S. pneumoniae* and *E. faecalis*, while the non-pathogenic strains are often "generally recognized as safe" (GRAS). Many LAB colonize mucosal surfaces of animals, and some strains of *Bifidobacteria* and *Lactobacilli* exhibit probiotic effects.[234–237] *Lactococcus lactis* is one of the most important industrial LAB, since it forms the main component of starter cultures for various cheeses and buttermilk.[230, 231, 238] Moreover, its relatively small genome (2.5 Mb) and simple metabolism makes it an optimal model organism for studying LAB.[218, 239, 240] Development of tools for heterologous protein expression in *L. lactis* along with its GRAS status allow it to be used as an efficient delivery system for therapeutic proteins.[241–243] The fermentative metabolism of *L. lactis* is depicted (Fig. 17). When grown exponentially under anaerobic conditions with no nutrient limitations conversion of one glucose equivalent to pyruvate in the glycolysis pathway results in production of two molecules of NADH by glyceraldehyde-3-phosphate dehydrogenase (GAPDH) and two ATP by pyruvate kinase (Pyk). In so-called homolactic fermentation pyruvate is converted to lactate by lactate dehydrogenase (LDH), which results in NAD^+ regeneration.[227, 244] Alternatively pyruvate is metabolized to acetyl-CoA and formate by pyruvate-formate lyase (PFL). Acetyl-CoA is then transformed to acetate and ethanol by acetate kinase (AK) and alcohol dehydrogenase (ADH), respectively. AK produces ATP while ADH contributes to NAD^+ regeneration (Fig. 17).[245] However, PFL is inhibited by triosephosphates, which are present at high levels during high glycolytic flux. Therefore most (up to 90%) of the pyruvate is readily converted to lactate by LDH (Fig. 17). Large-scale industrial productions can expose LAB to different stress conditions such as nutrient starvation, low pH, high temperature and, last but not least, oxidative stress. For example carbon-source starvation decreases the glycolytic flux, therefore the $NADH/NAD^+$ ratio decreases, which inhibits LDH. This results in a shift from lactate formation towards formate, acetate and ethanol production. This metabolic phenotype is called mixed-acid fermentation.[246, 247] A slightly different shift occurs in presence of oxygen, which will be described in the following section.

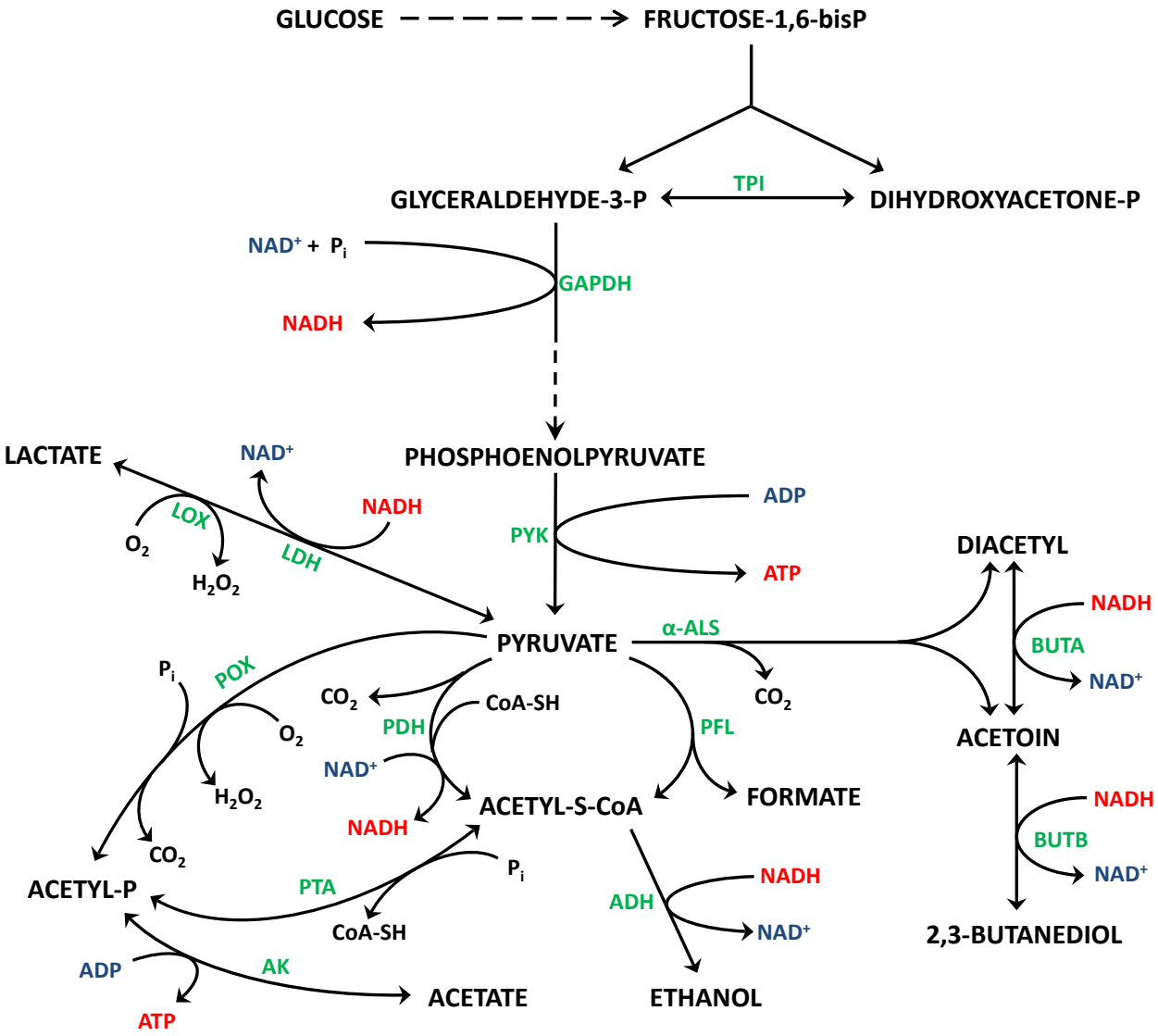

Fig.17 Fermentation in *L. lactis*. Under anaerobic conditions, pyruvate is almost completely converted to lactate by LDH. The rest goes to formate, acetate and ethanol. Adding oxygen into the system shifts the metabolism more towards acetate, acetoin and CO_2. LOX and POX can both utilize lactate and drive the flux towards acetate in aerobic conditions. Only LOX activity was observed in *L. lactis* ssp. *lactis*, but both enzymes are known in other LAB. See details in the text. TPI – triosephosphate isomerase; GADPH – glyceraldehyde-3-phosphate dehydrogenase; PYK – pyruvate kinase; LDH – lactate dehydrogenase; PDH – pyruvate dehydronegase complex; PFL – pyruvate-formate lyase; ADH – alcohol dehydrogenase; PTA – phosphotransacetylase; AK – acetate kinase; POX – pyruvate oxidase; LOX – lactate oxidase; α-ALS – α-acetolactate synthase; BUTA – acetoin reductase; BUTB – 2,3-butanediol dehydrogenase; color code: green – enzymes; red and blue mark the high- or low-energetic compound, respectively in the pairs of ATP/ADP and NADH/NAD^+.

1.4.2 NADH oxidase and metabolism under aerobic conditions

LAB are sensitive to oxidative damage of various cellular components and under aerobic conditions oxygen is removed by NADH oxidases. The flavoprotein AhpF (Nox-1) exhibits H_2O_2-forming NADH oxidase activity coupled to the peroxidase AhpC. When AhpC is in excess NADH consumption doubles and practically all oxygen is converted to H_2O without H_2O_2 leakage.[248] This excess had to be at least 200-fold in order to avoid H_2O_2 formation in *L. lactis* while 50-fold was sufficient in *B. cereus*.[249, 250] Even though transcriptomic studies of aerated cultures of *L. lactis* showed both AhpC and AhpF induced to similar extent by the presence of oxygen, LAB often exhibit low AhpC activity and therefore H_2O_2-formation by AhpF is predominant. [249, 251, 252] LAB also contain an H_2O-forming NADH-oxidase (Nox-2; sometimes referred to as NoxE in *L. lactis*). This enzyme not only converts oxygen predominantly to water (about 1% H_2O_2 leakage was observed *in vitro*), it also has more than six times higher activity than AhpCF in *L. lactis*, while AhpCF is about 17% more active than Nox-2 in *B. cereus*. [249, 250] Physiological studies in *S. mutans* and *L. lactis* showed that AhpCF contributes very little to the total NADH-oxidase activity while Nox-2 seems to be the key enzyme in this respect.[253, 254] On the other hand, *S. mutans ahpCF* was able to complement *E. coli ΔahpCF* strain, showing clearly that it is functional. Even *ahpC* alone could complement probably because AhpF can be substituted by the Trx system when it is absent.[158, 253, 255] The function of Nox-2 is not primarily in oxygen removal but in NAD^+ regeneration since *nox-2* knockout strains of neither *S. mutans* nor *L. lactis* ssp. *cremoris* were significantly more sensitive to oxidative stress. Moreover they exhibited a shift towards production of lactate compared to wild type. Strains overexpressing Nox-2 showed a shift towards mixed acid fermentation.[253, 256] A recent study in *S. mutans* showed an increased oxidative stress resistance of *Δnox-2* strain. This was probably caused by a general induction of defense mechanisms by elevated intracellular concentration of oxygen.[257]

Aerobic growth introduces important changes in the carbon metabolism of LAB. In the presence of a small amount of oxygen PFL is inhibited and ADH is down-regulated at the protein level. Concomitantly, NADH oxidases, PDH and α-acetolactate synthase (α-ALS) are induced. NADH oxidases take over NAD^+ regeneration instead of ADH, therefore the flux shift from PFL-ADH towards PDH-AK results in less ethanol but more acetate and ATP (Fig. 17). At these "micro-aerophilic" conditions, biomass increases by 10% while activities of GAPDH and LDH are still unaffected.[245] When the amount of oxygen is high, the activity of NADH oxidases increases. Consequently the NADH/NAD^+ ratio falls, which leads to inhibition of LDH.[247] Therefore acetate, acetoin, diacetyl and ethanol are the major metabolites under these conditions.[252]

The effects of aerobic non-respirative growth were also studied in *Streptococci* and *Lactobacilli*. These bacteria can use oxygen for conversion of pyruvate to acetylphosphate by an H_2O_2-producing enzyme pyruvate oxidase (POX), followed by formation of acetate and ATP (Fig. 17).[244, 258] Another H_2O_2-producing enzyme lactate oxidase (LOX) converts lactate to pyruvate in LAB (Fig. 17). Genes homologous to POX were found in several common strains of *L. lactis*, but POX activity was not detected. [218, 244, 259–261] LOX was up-regulated in *L. lactis* ssp. *lactis* upon exposure to copper and its activity was confirmed.[260, 262, 263]

1.4.3 LAB and respiration

Some LAB (e.g. *L. lactis*) are capable of aerobic respiration when exogenous heme is supplemented.[264–266] Other species (e.g. *S. agalactiae*) need heme and menaquinone.[266–268] The minimum requirement for respiration is a functional electron transport chain (ETC): (1) a membrane NADH dehydrogenase as an

electron donor, (2) a quinone carrier (menaquinone in Gram-positive bacteria) delivering electrons from the dehydrogenase to (3) cytochrome oxidase, which reduces O_2 to H_2O and requires heme as a cofactor. *Lb. plantarum* and *E. faecalis* also possess anaerobic ETC with terminal electron acceptors nitrate or fumarate, respectively.[269, 270] The proton motive force (PMF) generated by the ETC is utilized for ATP synthesis by F_oF_1 H^+-ATP-synthase.[271]

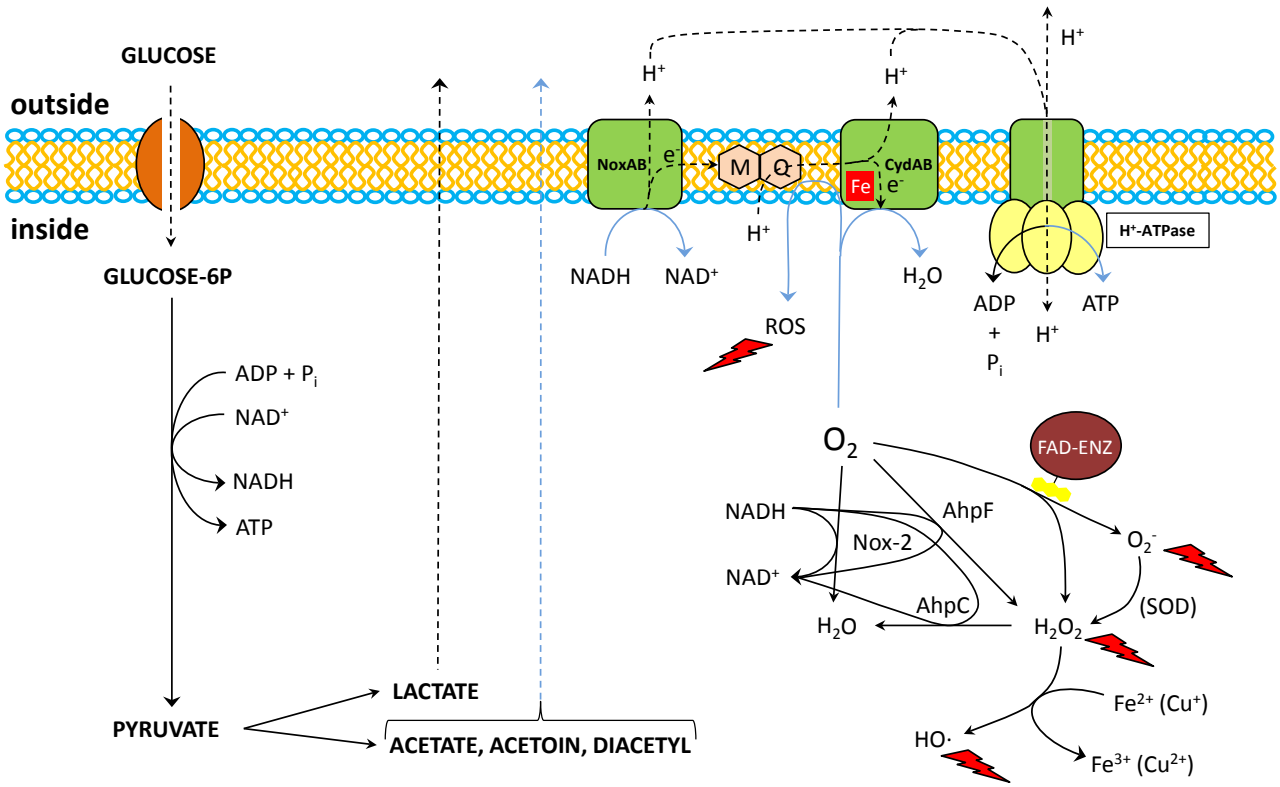

Fig.18 Oxidative stress in *L. lactis*. Fermentation (black) vs. respiration (blue); During respiration, ETC effectively removes oxygen, produces the proton gradient and consequently ATP. ETC can also produce ROS. Fermentation in the presence of oxygen increases risk of ROS formation, since Nox-2 is probably not as effective as respiration (decrease in intracellular oxidative damage was observed upon respiration vs. aerobic fermentation),[277] and AhpF can contribute to ROS by H_2O_2 formation which is removed by AhpC with only a low efficiency. ROS can be also produced by e.g. autoxidation of flavoenzymes and Fenton's reaction (1.1.2.1; Fig. 3).

The ETC in *L. lactis* contains membrane-bound NADH dehydrogenases NoxA and NoxB,[254, 272] and a menaquinone biosynthesis pathway encoded by *men* genes.[273, 274] Cytochrome bd oxidase CydAB is common to all respiring LAB studied so far.[266] Interestingly, the genes involved in respiration are constitutively expressed in *L. lactis* and *S. agalactiae*.[251, 265, 268] Therefore, respiration can start rapidly once the nutritional requirements are met. The ETC also provides PMF for maintaining membrane transport. This process saves ATP, which would be used for pumping protons over the membrane in order to achieve PMF at non-respiring conditions. It was suggested that H^+-ATPase fulfilling this function synthesizes ATP during respiration.[266, 275] Changes in metabolite profiles are similar to what was described above for non-

respiratory aerobic growth. Briefly, NADH is rapidly oxidized by ETC, therefore the NADH/NAD^+ ratio falls. This leads to a significant decrease of lactate in favor of acetate and acetoin and up-regulation of PDH and α-ALS.[265, 276]

The major advantages of respiration are: (1) long-term survival due to an effective oxygen removal by ETC combined with decreased acidification,[277] (2) a higher biomass yield achieved by increased ATP synthesis and more efficient ATP consumption,[275] and (3) improved survival of co-cultured non-respiring strains.[277] These features make respiratory growth attractive in industrial applications and have been applied for preparation of starter cultures.[266]

1.4.4 Redox regulation and oxidative stress resistance in LAB

As described above, Gram-positive bacteria in general do not contain GSH/Grx disulfide reductase systems while Trx appears to be ubiquitous. Alternative LMW thiols such as BSH and MSH (see 1.3.1) have not been identified in any LAB so far. The Trx system was hypothesized to play a key role in redox regulations in LAB. However, a strain of *L. lactis* lacking *trxB1* (NTR) is viable, and survives mild oxidative conditions.[278] Proteomic analysis of this mutant revealed induction of proteins involved in aerobic carbon metabolism (see previous sections) and several stress proteins.[275, 278] Surprisingly, a pI-shift of glyceraldehyde-3-phosphate dehydrogenase (GapB) in the alkaline direction occurred in the oxygen-sensitive *trxB1* mutant. The difference was caused by a higher level of the protein containing the active site cysteine in a reduced form, which was an unexpectable effect in the NTR-deficient strain.[278] A study of various *trx* mutants of *Lactobacillus casei* including an NTR deficient strain showed the Trx system to be non-essential, although the mutant missing NTR was unable to grow aerobically in a chemically defined medium. Addition of chemical reductants restored the growth of all these mutants almost to wild type level.[279]

Most LAB contain superoxide dismutase (SOD).[252] Mn-SOD (*sodA*) was identified in *L. lactis* where it was up-regulated during acid stress.[280, 281] It was also observed highly up-regulated during aerobic growth or in a strain lacking Trx reductase (*trxB1*), which exhibited an increased sensitivity towards oxygen.[251, 278] The H_2O_2 scavenging enzyme catalase which is present in most organisms is absent in most LAB. Some LAB (e.g. *E. faecalis* and some *Lactobacilli*) express the apo-enzyme, which is activated in the presence of heme.[282–285] Moreover, some *Lactobacilli* and *Pediococci* possess a non-heme Mn-catalase.[286–288] Nitroreductase (CinD) with non-heme catalase activity was found in *L. lactis*. However, expression of *cinD* is not induced by the presence of H_2O_2 and it seems to respond only to copper, silver and cadmium.[289, 290] In addition to AhpC LAB contain several thiol-based peroxidases including Gpx, Tpx, and OsmC. These enzymes have not been thoroughly studied in LAB but their homologs in e.g. *E. coli* exhibited peroxidatic activity *in vitro* (Tpx) and *in vivo* (OsmC and Gpx). Tpx was induced upon hydrogen peroxide stress in *Bacillus licheniformis* and was suggested to be under control of Spx in *B. subtilis*.[159, 291] Up-regulation of Tpx along with e.g. AhpCF, Trx and NTR in presence of oxygen was observed in *Porphyromonas gingivalis*, a Gram-negative pathogen living in the oral cavity.[292] OsmC was also shown to contribute significantly to peroxidatic activity in *Mycobacteria*.[293]

Gene disruption studies revealed that mutations in e.g. purine metabolism (*deoB*, *guaA*, *tktA*),[219, 294] high-affinity phosphate uptake (*pstABCDEF*, *pstS*),[219, 221, 294] Fe^{2+} uptake (*mntH*)[221] and an Spx homolog (*trmA*; see 1.3.2)[219–221] increased stress resistance. On the other hand, mutations impairing DNA repair and

homologous recombination (*recA*)[295] and a universal stress protein (*uspA*)[296] induced a decrease in stress resistance. Mutations in the *pst* locus was suggested to have an influence on metal homeostasis, particularly the amounts of bound vs. unbound Cu and Zn, therefore increasing resistance towards oxygen. This hypothesis was based on different effects of Cu and Zn in wild type vs. *pst* mutants without any changes in total Cu and Zn pools.[297] Disruption of Fe^{2+} uptake decreased tellurite and oxygen sensitivity by lowering the possibility of ROS generation through Fenton's reaction (see 1.1.2.1; Eq 1.5).[221] Apart from the redox sensors FlpA/B and Spx (see 1.3.2), six putative two-component systems each consisting of a histidine protein kinase receptor and a response regulator are present in *L. lactis*, and one of these was involved in H_2O_2 response.[298] Guanine and phosphate starvation was suggested to trigger the stringent response through the alarmone guanosine pentaphosphate ((p)ppGpp).[294] Transcriptomic and proteomic studies of aerobically grown *L. lactis* revealed increased levels of e.g. NADH oxidases (AhpF, AhpC, NoxE) and SodA, as well as methionine sulfoxide reductases (MsrA, MsrB), two homologs of organic hydroperoxide reductase OsmC and a putative glutathione reductase (GshR).[251, 276]

1.5 Objectives of the present investigation

Reversible thiol redox control is an extremely versatile biochemical mechanism, and is employed in many important aspects of cellular metabolism (e.g. DNA synthesis, central carbon metabolism, oxidative stress defense) in all forms of life. Thioredoxin is an important component of thiol redox control systems and regulates a variety of enzymes and transcription factors (Section 1.2). *L. lactis* is a very important industrial microorganism in food production. This model organism for lactic acid bacteria also has a strong potential as host for production of high-value recombinant proteins and as a carrier for delivery of therapeutic proteins. The physiology of *L. lactis* has been studied for decades, however, the knowledge of the thiol redox control system in this organism is limited (Section 1.4). The hypothesis of the present investigation is that the thioredoxin system is important for stress resistance in *L. lactis* and the main goal is to gain insight the physiological roles and biochemical mechanism of the two *L. lactis* thioredoxins TrxA and TrxD. This was accomplished by two approaches: (1) construction of *L. lactis* strains lacking the genes encoding *trxA* and *trxD* and studying their phenotypes in various stress conditions followed by proteomic analysis to identify proteins that are up- or down-regulated (Chapter 2), and (2) cloning, production and biochemical characterization of the proteins constituting the *L. lactis* Trx system (LlTrxA, LlTrxD, LlNrdH and LlNTR; Chapter 3).

1.6 References

1. Banerjee, R. (2008). Redox metabolism and life, p. 1–10. In *Redox Biochemistry*. A John Wiley & Sons, INC., Publication.

2. Imlay, J.A. (2003). Pathways of oxidative damage. *Annu Rev Microbiol* **57**:395–18.

3. Schröder, P., Krutmann, J. (2005). Environmental oxidative stress–environmental sources of ROS, p. 19–31. In Grune, T (ed.), *Reactions, Processes*. Springer Berlin Heidelberg.

4. Ligeza, A., Tikhonov, A.N., Hyde, J.S., Subczynski, W.K. (1998). Oxygen permeability of thylakoid membranes: electron paramagnetic resonance spin labeling study. *Biochim Biophys Acta* **1365**:453–63.

5. Imlay, J.A. (2008). Cellular defenses against superoxide and hydrogen peroxide. *Annu Rev Biochem* **77**:755–76.

6. Messner, K.R., Imlay, J.A. (1999). The identification of primary sites of superoxide and hydrogen peroxide formation in the aerobic respiratory chain and sulfite reductase complex of *Escherichia coli*. *J Biol Chem* **274**:10119–28.

7. McCord, J.M., Fridovich, I. (1969). Superoxide dismutase. An enzymic function for erythrocuprein (hemocuprein). *J Biol Chem* **244**:6049–55.

8. Liochev, S.I., Fridovich, I. (2007). The effects of superoxide dismutase on H_2O_2 formation. *Free Radic Biol Med* **42**:1465–69.

9. Fenton, H.J.H. (1894). LXXIII.–Oxidation of tartaric acid in presence of iron. *J Chem Soc, Trans* **65**:899.

10. Haber, F., Weiss, J. (1934). The catalytic decomposition of hydrogen peroxide by iron salts. *P Roy Soc Lond A Mat* **147**:332–51.

11. Imlay, J.A., Fridovich, I. (1991). Assay of metabolic superoxide production in *Escherichia coli*. *J Biol Chem* **266**:6957–65.

12. Bielski, B.H., Cabelli, D.E. (1991). Highlights of current research involving superoxide and perhydroxyl radicals in aqueous solutions. *Int J Radiat Biol* **59**:291–319.

13. Woodmansee, A.N., Imlay, J.A. (2002). Reduced flavins promote oxidative DNA damage in non-respiring *Escherichia coli* by delivering electrons to intracellular free iron. *J Biol Chem* **277**:34055–66.

14. Park, S., Imlay, J.A. (2003). High levels of intracellular cysteine promote oxidative DNA damage by driving the Fenton reaction. *J Bacteriol* **185**:1942–50.

15. Blanksby, S.J., Bierbaum, V.M., Ellison, G.B., Kato, S. (2007). Superoxide does react with peroxides: direct observation of the Haber-Weiss reaction in the gas phase. *Angew Chem Int Ed Engl* **46**:4948–50.

16. Hassan, H.M., Fridovich, I. (1978). Superoxide radical and the oxygen enhancement of the toxicity of paraquat in Escherichia coli. *J Biol Chem* **253**:8143–48.

17. Massey, V., Strickland, S., Mayhew, S.G., Howell, L.G., Engel, P.C., Matthews, R.G., Schuman, M., Sullivan, P.A. (1969). The production of superoxide anion radicals in the reaction of reduced flavins and flavoproteins with molecular oxygen. *Biochem Biophys Res Commun* **36**:891–97.

18. Seaver, L.C., Imlay, J.A. (2004). Are respiratory enzymes the primary sources of intracellular hydrogen peroxide? *J Biol Chem* **279**:48742–50.

19. Korshunov, S., Imlay, J.A. (2006). Detection and quantification of superoxide formed within the periplasm of *Escherichia coli*. *J Bacteriol* **188**:6326–34.

20. Korshunov, S., Imlay, J.A. (2010). Two sources of endogenous hydrogen peroxide in *Escherichia coli. Mol Microbiol* **1**:1389–401.

21. Linn, S. (1998). DNA damage by iron and hydrogen peroxide in vitro and in vivo. *Drug Metab Rev* **30**:313–26.

22. Luo, Y., Han, Z., Chin, S.M., Linn, S. (1994). Three chemically distinct types of oxidants formed by iron-mediated Fenton reactions in the presence of DNA. *Proc Natl Acad Sci U S A* **91**:12438–42.

23. Rai, P., Wemmer, D.E., Linn, S. (2005). Preferential binding and structural distortion by Fe2+ at RGGG-containing DNA sequences correlates with enhanced oxidative cleavage at such sequences. *Nucleic Acids Res* **33**:497–510.

24. Henle, E.S., Han, Z., Tang, N., Rai, P., Luo, Y., Linn, S. (1999). Sequence-specific DNA cleavage by Fe^{2+}-mediated fenton reactions has possible biological implications. *J Biol Chem* **274**:962–71.

25. Rai, P., Cole, T.D., Wemmer, D.E., Linn, S. (2001). Localization of Fe^{2+} at an RTGR sequence within a DNA duplex explains preferential cleavage by Fe^{2+} and H_2O_2. *J Mol Biol* **312**:1089–101.

26. Bielski, B.H., Arudi, R.L., Sutherland, M.W. (1983). A study of the reactivity of HO_2/O_2^- with unsaturated fatty acids. *J Biol Chem* **258**:4759–61.

27. Pradenas, G.A., Paillavil, B.A., Reyes-Cerpa, S., Pérez-Donoso, J.M., Vásquez, C.C. (2012). Reduction of the monounsaturated fatty acid content of *Escherichia coli* results in increased resistance to oxidative damage. *Microbiology* **158**:1279–83.

28. Davies, M.J. (1996). Protein and peptide alkoxyl radicals can give rise to C-terminal decarboxylation and backbone cleavage. *Arch Biochem Biophys* **336**:163–72.

29. Davies, M.J. (2005). The oxidative environment and protein damage. *Biochim Biophys Acta* **1703**:93–109.

30. Hawkins, C.L., Davies, M.J. (2001). Generation and propagation of radical reactions on proteins. *Biochim Biophys Acta* **1504**:196–219.

31. Pattison, D.I., Davies, M.J. (2001). Absolute rate constants for the reaction of hypochlorous acid with protein side chains and peptide bonds. *Chem Res Toxicol* **14**:1453–64.

32. Hawkins, C.L., Pattison, D.I., Davies, M.J. (2003). Hypochlorite-induced oxidation of amino acids, peptides and proteins. *Amino Acids* **25**:259–74.

33. Gardner, P.R., Fridovich, I. (1991). Superoxide sensitivity of the *Escherichia coli* aconitase. *J Biol Chem* **266**:19328–33.

34. Flint, D.H., Smyk-Randall, E., Tuminello, J.F., Draczynska-Lusiak, B., Brown, O.R. (1993). The inactivation of dihydroxy-acid dehydratase in Escherichia coli treated with hyperbaric oxygen occurs because of the destruction of its Fe-S cluster, but the enzyme remains in the cell in a form that can be reactivated. *J Biol Chem* **268**:25547–52.

35. Jang, S., Imlay, J.A. (2007). Micromolar intracellular hydrogen peroxide disrupts metabolism by damaging iron-sulfur enzymes. *J Biol Chem* **282**:929–37.

36. Djaman, O., Outten, F.W., Imlay, J.A. (2004). Repair of oxidized iron-sulfur clusters in *Escherichia coli*. *J Biol Chem* **279**:44590–99.

37. Liochev, S.I., Fridovich, I. (1994). The role of $O_2^{\cdot-}$ in the production of $HO^{\cdot}$: *in vitro* and *in vivo*. *Free Radic Biol Med* **16**:29–33.

38. Jang, S., Imlay, J.A. (2010). Hydrogen peroxide inactivates the *Escherichia coli* Isc iron-sulphur assembly system, and OxyR induces the Suf system to compensate. *Mol Microbiol* **78**:1448–67.

39. Sharov, V.S., Schöneich, C. (2000). Diastereoselective protein methionine oxidation by reactive oxygen species and diastereoselective repair by methionine sulfoxide reductase. *Free Radic Biol Med* **29**:986–94.

40. Arnér, E.S., Holmgren, A. (2000). Physiological functions of thioredoxin and thioredoxin reductase. *Eur J Biochem* **267**:6102–9.

41. Rouhier, N., Vieira Dos Santos, C., Tarrago, L., Rey, P. (2006). Plant methionine sulfoxide reductase A and B multigenic families. *Photosynth Res* **89**:247–62.

42. Lin, Z., Johnson, L.C., Weissbach, H., Brot, N., Lively, M.O., Lowther, W.T. (2007). Free methionine-(R)-sulfoxide reductase from *Escherichia coli* reveals a new GAF domain function. *Proc Natl Acad Sci U S A* **104**:9597–602.

43. Ezraty, B., Bos, J., Barras, F., Aussel, L. (2005). Methionine sulfoxide reduction and assimilation in *Escherichia coli*: new role for the biotin sulfoxide reductase BisC. *J Bacteriol* **187**:231–37.

44. Woo, H.A., Chae, H.Z., Hwang, S.C., Yang, K.-S., Kang, S.W., Kim, K., Rhee, S.G. (2003). Reversing the inactivation of peroxiredoxins caused by cysteine sulfinic acid formation. *Science* **300**:653–6.

45. Biteau, B., Labarre, J. (2003). ATP-dependent reduction of cysteine – sulphinic acid by *S . cerevisiae* sulphiredoxin. *Nature* **425**:980–84.

46. Baek, J.Y., Han, S.H., Sung, S.H., Lee, H.E., Kim, Y., Noh, Y.H., Bae, S.H., Rhee, S.G., Chang, T.-S. (2012). Sulfiredoxin protein is critical for redox balance and survival of cells exposed to low steady-state levels of H_2O_2. *J Biol Chem* **287**:81–89.

47. Antelmann, H., Hamilton, C.J. (2012). Bacterial mechanisms of reversible protein S-thiolation: structural and mechanistic insights into mycoredoxins. *Mol Microbiol*.

48. Nguyen, T.T.H., Eiamphungporn, W., Mäder, U., Liebeke, M., Lalk, M., Hecker, M., Helmann, J.D., Antelmann, H. (2009). Genome-wide responses to carbonyl electrophiles in *Bacillus subtilis*: control of the thiol-dependent formaldehyde dehydrogenase AdhA and cysteine proteinase YraA by the MerR-family regulator YraB (AdhR). *Mol Microbiol* **71**:876–94.

49. Antelmann, H., Helmann, J.D. (2011). Thiol-based redox switches and gene regulation. *Antioxid Redox Signal* **14**:1049–63.

50. Marshall, H.E., Merchant, K., Stamler, J.S. (2000). Nitrosation and oxidation in the regulation of gene expression. *FASEB J* **14**:1889–900.

51. Gupta, K.J. (2011). Protein S-nitrosylation in plants: photorespiratory metabolism and NO signaling. *Sci Signal* **4**:jc1.

52. Lindahl, M., Mata-Cabana, A., Kieselbach, T. (2011). The disulfide proteome and other reactive cysteine proteomes: analysis and functional significance. *Antioxid Redox Signal* **14**:2581–642.

53. Talfournier, F., Colloc'h, N., Mornon, J.P., Branlant, G. (1998). Comparative study of the catalytic domain of phosphorylating glyceraldehyde-3-phosphate dehydrogenases from bacteria and archaea via essential cysteine probes and site-directed mutagenesis. *Eur J Biochem* **252**:447–57.

54. Grant, C.M., Quinn, K.A., Dawes, I.W. (1999). Differential protein S-thiolation of glyceraldehyde-3-phosphate dehydrogenase isoenzymes influences sensitivity to oxidative stress. *Mol Cell Biol* **19**:2650–56.

55. Hwang, C., Sinskey, A.J., Lodish, H.F. (1992). Oxidized redox state of glutathione in the endoplasmic reticulum. *Science* **257**:1496–502.

56. Schwaller, M., Wilkinson, B., Gilbert, H.F. (2003). Reduction-reoxidation cycles contribute to catalysis of disulfide isomerization by protein-disulfide isomerase. *J Biol Chem* **278**:7154–59.

57. Tu, B.P., Weissman, J.S. (2004). Oxidative protein folding in eukaryotes: mechanisms and consequences. *J Cell Biol* **164**:341–46.

58. Greetham, D., Vickerstaff, J., Shenton, D., Perrone, G.G., Dawes, I.W., Grant, C.M. (2010). Thioredoxins function as deglutathionylase enzymes in the yeast *Saccharomyces cerevisiae*. *BMC Biochem* **11**:3.

59. Nielsen, J.W., Jensen, K.S., Hansen, R.E., Gotfredsen, C.H., Winther, J.R. (2012). A fluorescent probe which allows highly specific thiol labeling at low pH. *Anal Biochem* **421**:115–20.

60. Muller, E.G. (1996). A glutathione reductase mutant of yeast accumulates high levels of oxidized glutathione and requires thioredoxin for growth. *Mol Biol Cell* **7**:1805–13.

61. Prinz, W.A., Åslund, F., Holmgren, A., Beckwith, J. (1997). The role of the thioredoxin and glutaredoxin pathways in reducing protein disulfide bonds in the *Escherichia coli* cytoplasm. *J Biol Chem* **272**:15661–67.

62. Moore, E.C., Reichard, P., Thelander, L. (1964). Enzymatic synthesis of deoxyribonucleotides. V. Purification and properties of thioredoxin reductase from *Escherichia coli* B. *J Biol Chem* **239**:3445–52.

63. Laurent, T.C., Moore, E.C., Reichard, P. (1964). Enzymatic synthesis of deoxyribonucleotides. IV. Isolation and characterization of thioredoxin, the hydrogen donor from *Escherichia coli* B. *J Biol Chem* **239**:3436–44.

64. Holmgren, A. (1976). Hydrogen donor system for *Escherichia coli* ribonucleoside-diphosphate reductase dependent upon glutathione. *Proc Natl Acad Sci U S A* **73**:2275–79.

65. Rouhier, N., Gelhaye, E., Sautiere, P.E., Brun, A., Laurent, P., Tagu, D., Gerard, J., De Faÿ, E., Meyer, Y., Jacquot, J.P. (2001). Isolation and characterization of a new peroxiredoxin from poplar sieve tubes that uses either glutaredoxin or thioredoxin as a proton donor. *Plant Physiol* **127**:1299–309.

66. Herbette, S., Lenne, C., Leblanc, N., Julien, J.-L., Drevet, J.R., Roeckel-Drevet, P. (2002). Two GPX-like proteins from *Lycopersicon esculentum* and *Helianthus annuus* are antioxidant enzymes with phospholipid hydroperoxide glutathione peroxidase and thioredoxin peroxidase activities. *Eur J Biochem* **269**:2414–20.

67. Navrot, N., Collin, V., Gualberto, J., Gelhaye, E., Hirasawa, M., Rey, P., Knaff, D.B., Issakidis, E., Jacquot, J.-P., Rouhier, N. (2006). Plant glutathione peroxidases are functional peroxiredoxins distributed in several subcellular compartments and regulated during biotic and abiotic stresses. *Plant Physiol* **142**:1364–79.

68. Chae, H.Z., Chung, S.J., Rhee, S.G. (1994). Thioredoxin-dependent peroxide reductase from yeast. *J Biol Chem* **269**:27670–78.

69. Russel, M., Model, P., Holmgren, A. (1990). Thioredoxin or glutaredoxin in *Escherichia coli* is essential for sulfate reduction but not for deoxyribonucleotide synthesis. *J Bacteriol* **172**:1923–29.

70. Chartron, J., Shiau, C., Stout, C.D., Carroll, K.S. (2007). 3’-Phosphoadenosine-5'-phosphosulfate reductase in complex with thioredoxin: a structural snapshot in the catalytic cycle. *Biochemistry* **46**:3942–51.

71. Messens, J., Hayburn, G., Desmyter, A., Laus, G., Wyns, L. (1999). The essential catalytic redox couple in arsenate reductase from *Staphylococcus aureus*. *Biochemistry* **38**:16857–65.

72. Li, Y., Hu, Y., Zhang, X., Xu, H., Lescop, E., Xia, B., Jin, C. (2007). Conformational fluctuations coupled to the thiol-disulfide transfer between thioredoxin and arsenate reductase in *Bacillus subtilis*. *J Biol Chem* **282**:11078–83.

73. Villadangos, A.F., Van Belle, K., Wahni, K., Tamu Dufe, V., Freitas, S., Nur, H., De Galan, S., Gil, J. a, Collet, J.-F., Mateos, L.M., Messens, J. (2011). *Corynebacterium glutamicum* survives arsenic stress with arsenate reductases coupled to two distinct redox mechanisms. *Mol Microbiol* **82**:998–1014.

74. Brot, N., Weissbach, L., Werth, J., Weissbach, H. (1981). Enzymatic reduction of protein-bound methionine sulfoxide. *Proc Natl Acad Sci U S A* **78**:2155–58.

75. Ma, X.-X., Guo, P.-C., Shi, W.-W., Luo, M., Tan, X.-F., Chen, Y., Zhou, C.-Z. (2011). Structural plasticity of the thioredoxin recognition site of yeast methionine S-sulfoxide reductase Mxr1. *J Biol Chem* **286**:13430–37.

76. Maeda, K., Hägglund, P., Finnie, C., Svensson, B., Henriksen, A. (2006). Structural basis for target protein recognition by the protein disulfide reductase thioredoxin. *Structure* **14**:1701–10.

77. Jensen, J.M., Hägglund, P., Christensen, H.E.M., Svensson, B. (2012). Inactivation of barley limit dextrinase inhibitor by thioredoxin-catalysed disulfide reduction. *FEBS Lett* **586**:2479–82.

78. Qin, J., Clore, G.M., Kennedy, W.M., Huth, J.R., Gronenborn, a M. (1995). Solution structure of human thioredoxin in a mixed disulfide intermediate complex with its target peptide from the transcription factor NF kappa B. *Structure* **3**:289–97.

79. Qin, J., Clore, G.M., Kennedy, W.P., Kuszewski, J., Gronenborn, A.M. (1996). The solution structure of human thioredoxin complexed with its target from Ref-1 reveals peptide chain reversal. *Structure* **4**:613–20.

80. Åslund, F., Zheng, M., Beckwith, J., Storz, G. (1999). Regulation of the OxyR transcription factor by hydrogen peroxide and the cellular thiol-disulfide status. *Proc Natl Acad Sci U S A* **96**:6161–65.

81. Nagano, T., Kojima, K., Hisabori, T., Hayashi, H., Morita, E.H., Kanamori, T., Miyagi, T., Ueda, T., Nishiyama, Y. (2012). Elongation factor G is a critical target during oxidative damage to the translation system of *Escherichia coli*. *J Biol Chem* **287**:28697–704.

82. Holmgren, A., Kallis, G.B., Nordström, B. (1981). A mutant thioredoxin from *Escherichia coli tsnC* 7007 that is nonfunctional as subunit of phage T7 DNA polymerase. *J Biol Chem* **256**:3118–24.

83. Kern, R., Malki, A., Holmgren, A., Richarme, G. (2003). Chaperone properties of *Escherichia coli* thioredoxin and thioredoxin reductase. *Biochem J* **371**:965–72.

84. Rouhier, N., Villarejo, A., Srivastava, M., Gelhaye, E., Keech, O., Droux, M., Finkemeier, I., Samuelsson, G., Dietz, K.J., Jacquot, J., Wingsle, G. (2005). Identification of plant glutaredoxin targets. *Antioxid Redox Signal* **7**:919–29.

85. Balmer, Y., Koller, A., Del Val, G., Manieri, W., Schürmann, P., Buchanan, B.B. (2003). Proteomics gives insight into the regulatory function of chloroplast thioredoxins. *Proc Natl Acad Sci U S A* **100**:370–75.

86. Balmer, Y., Vensel, W.H., Tanaka, C.K., Hurkman, W.J., Gelhaye, E., Rouhier, N., Jacquot, J.-P., Manieri, W., Schürmann, P., Droux, M., Buchanan, B.B. (2004). Thioredoxin links redox to the regulation of fundamental processes of plant mitochondria. *Proc Natl Acad Sci U S A* **101**:2642–47.

87. Maeda, K., Finnie, C., Svensson, B. (2004). Cy5 maleimide labelling for sensitive detection of free thiols in native protein extracts: identification of seed proteins targeted by barley thioredoxin h isoforms. *Biochem J* **378**:497–507.

88. Hochgräfe, F., Mostertz, J., Albrecht, D., Hecker, M. (2005). Fluorescence thiol modification assay: oxidatively modified proteins in *Bacillus subtilis*. *Mol Microbiol* **58**:409–25.

89. Hägglund, P., Bunkenborg, J., Maeda, K., Svensson, B. (2008). Identification of thioredoxin disulfide targets using a quantitative proteomics approach based on isotope-coded affinity tags. *J Proteome Res* **7**:5270–76.

90. Wong, J.H., Balmer, Y., Cai, N., Tanaka, C.K., Vensel, W.H., Hurkman, W.J., Buchanan, B.B. (2003). Unraveling thioredoxin-linked metabolic processes of cereal starchy endosperm using proteomics. *FEBS Lett* **547**:151–56.

91. Hägglund, P., Bunkenborg, J., Yang, F., Harder, L.M., Finnie, C., Svensson, B. (2010). Identification of thioredoxin target disulfides in proteins released from barley aleurone layers. *J Proteomics* **73**:1133–36.

92. Kumar, J.K., Tabor, S., Richardson, C.C. (2004). Proteomic analysis of thioredoxin-targeted proteins in *Escherichia coli*. *Proc Natl Acad Sci U S A* **101**:3759–64.

93. El Hajjaji, H., Dumoulin, M., Matagne, A., Colau, D., Roos, G., Messens, J., Collet, J.-F. (2009). The zinc center influences the redox and thermodynamic properties of *Escherichia coli* thioredoxin 2. *J Mol Biol* **386**:60–71.

94. Krause, G., Lundström, J., Barea, J., De la Cuesta, C., Holmgren, A. (1991). Mimicking the active site of protein disulfide-isomerase by substitution of proline 34 in *Escherichia coli* thioredoxin. *J Biol Chem* **266**:9494–500.

95. Collet, J.-F., Messens, J. (2010). Structure, function, and mechanism of thioredoxin proteins. *Antioxid Redox Signal* **13**:1205–16.

96. Dyson, H.J., Jeng, M.F., Tennant, L.L., Slaby, I., Lindell, M., Cui, D.S., Kuprin, S., Holmgren, A. (1997). Effects of buried charged groups on cysteine thiol ionization and reactivity in *Escherichia coli* thioredoxin: structural and functional characterization of mutants of Asp 26 and Lys 57. *Biochemistry* **36**:2622–36.

97. Dillet, V., Dyson, H.J., Bashford, D. (1998). Calculations of electrostatic interactions and pK_as in the active site of *Escherichia coli* thioredoxin. *Biochemistry* **37**:10298–306.

98. Maeda, K., Hägglund, P., Björnberg, O., Winther, J.R., Svensson, B. (2010). Kinetic and thermodynamic properties of two barley thioredoxin h isozymes, HvTrxh1 and HvTrxh2. *FEBS Lett* **584**:3376–80.

99. Chivers, P.T., Prehoda, K.E., Raines, R.T. (1997). The CXXC motif: a rheostat in the active site. *Biochemistry* **36**:4061–66.

100. Kallis, G.B., Holmgren, A. (1980). Differential reactivity of the functional sulfhydryl groups of cysteine-32 and cysteine-35 present in the reduced form of thioredoxin from *Escherichia coli*. *J Biol Chem* **255**:10261–65.

101. Chivers, P.T., Raines, R.T. (1997). General acid/base catalysis in the active site of *Escherichia coli* thioredoxin. *Biochemistry* **36**:15810–16.

102. Roos, G., Foloppe, N., Van Laer, K., Wyns, L., Nilsson, L., Geerlings, P., Messens, J. (2009). How thioredoxin dissociates its mixed disulfide. *PLoS Comput Biol* **5**:e1000461.

103. Roos, G., Foloppe, N., Messens, J. (2013). Understanding the pK(a) of redox cysteines: the key role of hydrogen bonding. *Antioxid Redox Signal* **18**:94–127.

104. Katti, S.K., LeMaster, D.M., Eklund, H. (1990). Crystal structure of thioredoxin from *Escherichia* coli at 1.68 Å resolution. *J Mol Biol* **212**:167–84.

105. Martin, J.L. (1995). Thioredoxin--a fold for all reasons. *Structure* **3**:245–50.

106. Stehr, M., Schneider, G., Åslund, F., Holmgren, A., Lindqvist, Y. (2001). Structural basis for the thioredoxin-like activity profile of the glutaredoxin-like NrdH-redoxin from *Escherichia coli*. *J Biol Chem* **276**:35836–41.

107. Van Laer, K., Buts, L., Foloppe, N., Vertommen, D., Van Belle, K., Wahni, K., Roos, G., Nilsson, L., Mateos, L.M., Rawat, M., Van Nuland, N. a J., Messens, J. (2012). Mycoredoxin-1 is one of the missing links in the oxidative stress defence mechanism of Mycobacteria. *Mol Microbiol* **86**:787–804.

108. Woo, J.R., Kim, S.J., Jeong, W., Cho, Y.H., Lee, S.C., Chung, Y.J., Rhee, S.G., Ryu, S.E. (2004). Structural basis of cellular redox regulation by human TRP14. *J Biol Chem* **279**:48120–25.

109. Crow, A., Liu, Y., Möller, M.C., Le Brun, N.E., Hederstedt, L. (2009). Structure and functional properties of *Bacillus subtilis* endospore biogenesis factor StoA. *J Biol Chem* **284**:10056–66.

110. Crow, A., Lewin, A., Hecht, O., Carlsson Möller, M., Moore, G.R., Hederstedt, L., Le Brun, N.E. (2009). Crystal structure and biophysical properties of *Bacillus subtilis* BdbD. An oxidizing thiol:disulfide oxidoreductase containing a novel metal site. *J Biol Chem* **284**:23719–33.

111. Kadokura, H., Katzen, F., Beckwith, J. (2003). Protein disulfide bond formation in prokaryotes. *Annu Rev Biochem* **72**:111–35.

112. Brot, N., Collet, J.-F., Johnson, L.C., Jönsson, T.J., Weissbach, H., Lowther, W.T. (2006). The thioredoxin domain of *Neisseria gonorrhoeae* PilB can use electrons from DsbD to reduce downstream methionine sulfoxide reductases. *J Biol Chem* **281**:32668–75.

113. Stirnimann, C.U., Rozhkova, A., Grauschopf, U., Grütter, M.G., Glockshuber, R., Capitani, G. (2005). Structural basis and kinetics of DsbD-dependent cytochrome c maturation. *Structure* **13**:985–93.

114. Atkinson, H.J., Babbitt, P.C. (2009). An atlas of the thioredoxin fold class reveals the complexity of function-enabling adaptations. *PLoS Comput Biol* **5**:e1000541.

115. Eklund, H., Gleason, F.K., Holmgren, A. (1991). Structural and functional relations among thioredoxins of different species. *Proteins* **11**:13–28.

116. Menchise, V., Corbier, C., Didierjean, C., Saviano, M., Benedetti, E., Jacquot, J.P., Aubry, A. (2001). Crystal structure of the wild-type and D30A mutant thioredoxin h of *Chlamydomonas reinhardtii* and implications for the catalytic mechanism. *Biochem J* **359**:65–75.

117. Eklund, H., Cambillau, C., Sjöberg, B.M., Holmgren, A., Jörnvall, H., Höög, J.O., Brändén, C.I. (1984). Conformational and functional similarities between glutaredoxin and thioredoxins. *EMBO J* **3**:1443–49.

118. Krause, G., Holmgren, A. (1991). Substitution of the conserved tryptophan 31 in *Escherichia coli* thioredoxin by site-directed mutagenesis and structure-function analysis. *J Biol Chem* **266**:4056–66.

119. Roos, G., Geerlings, P., Messens, J. (2010). The conserved active site tryptophan of thioredoxin has no effect on its redox properties. *Protein Sci* **19**:190–94.

120. Jeng, M.F., Campbell, A.P., Begley, T., Holmgren, A., Case, D.A., Wright, P.E., Dyson, H.J. (1994). High-resolution solution structures of oxidized and reduced *Escherichia coli* thioredoxin. *Structure* **2**:853–68.

121. Maeda, K., Hägglund, P., Finnie, C., Svensson, B., Henriksen, A. (2008). Crystal structures of barley thioredoxin h isoforms HvTrxh1 and HvTrxh2 reveal features involved in protein recognition and possibly in discriminating the isoform specificity. *Protein Sci* **17**:1015–24.

122. Roos, G., Garcia-Pino, A., Van Belle, K., Brosens, E., Wahni, K., Vandenbussche, G., Wyns, L., Loris, R., Messens, J. (2007). The conserved active site proline determines the reducing power of *Staphylococcus aureus* thioredoxin. *J Mol Biol* **368**:800–11.

123. De Lamotte-Guéry, F., Pruvost, C., Minard, P., Delsuc, M.A., Miginiac-Maslow, M., Schmitter, J.M., Stein, M., Decottignies, P. (1997). Structural and functional roles of a conserved proline residue in the alpha2 helix of *Escherichia coli* thioredoxin. *Protein Eng* **10**:1425–32.

124. Chakrabarti, A., Srivastava, S., Swaminathan, C.P., Surolia, A., Varadarajan, R. (1999). Thermodynamics of replacing an alpha-helical Pro residue in the P40S mutant of *Escherichia coli* thioredoxin. *Protein Sci* **8**:2455–59.

125. Gleason, F.K. (1992). Mutation of conserved residues in *Escherichia coli* thioredoxin: effects on stability and function. *Protein Sci* **1**:609–16.

126. Björnberg, O., Maeda, K., Svensson, B., Hägglund, P. (2012). Dissecting Molecular interactions involved in recognition of target disulfides by the barley thioredoxin system. *Biochemistry* **51**:9930–9939.

127. Arscott, L.D., Gromer, S., Schirmer, R.H., Becker, K., Williams, C.H. (1997). The mechanism of thioredoxin reductase from human placenta is similar to the mechanisms of lipoamide dehydrogenase and glutathione reductase and is distinct from the mechanism of thioredoxin reductase from *Escherichia coli*. *Proc Natl Acad Sci U S A* **94**:3621–26.

128. Gasdaska, P.Y., Gasdaska, J.R., Cochran, S., Powis, G. (1995). Cloning and sequencing of a human thioredoxin reductase. *FEBS Lett* **373**:5–9.

129. Arnér, E.S.J. (2009). Focus on mammalian thioredoxin reductases--important selenoproteins with versatile functions. *Biochim Biophys Acta* **1790**:495–526.

130. Fritz-Wolf, K., Kehr, S., Stumpf, M., Rahlfs, S., Becker, K. (2011). Crystal structure of the human thioredoxin reductase-thioredoxin complex. *Nat Commun* **2**:383.

131. Serrato, A.J., Pérez-Ruiz, J.M., Spínola, M.C., Cejudo, F.J. (2004). A novel NADPH thioredoxin reductase, localized in the chloroplast, which deficiency causes hypersensitivity to abiotic stress in *Arabidopsis thaliana*. *J Biol Chem* **279**:43821–7.

132. Florencio, F.J., Pérez-Pérez, M.E., López-Maury, L., Mata-Cabana, A., Lindahl, M. (2006). The diversity and complexity of the cyanobacterial thioredoxin systems. *Photosynth Res* **89**:157–71.

133. Wieles, B., Van Soolingen, D., Holmgren, A., Offringa, R., Ottenhoff, T., Thole, J. (1995). Unique gene organization of thioredoxin and thioredoxin reductase in *Mycobacterium leprae*. *Mol Microbiol* **16**:921–29.

134. Waksman, G., Krishna, T.S., Williams, C.H., Kuriyan, J. (1994). Crystal structure of *Escherichia coli* thioredoxin reductase refined at 2 Å resolution. Implications for a large conformational change during catalysis. *J Mol Biol* **236**:800–16.

135. Lennon, B.W., Williams, C.H. (1997). Reductive half-reaction of thioredoxin reductase from *Escherichia coli*. *Biochemistry* **36**:9464–77.

136. Veine, D.M., Mulrooney, S.B., Wang, P.F., Williams, C.H. (1998). Formation and properties of mixed disulfides between thioredoxin reductase from *Escherichia coli* and thioredoxin: evidence that cysteine-138 functions to initiate dithiol-disulfide interchange and to accept the reducing equivalent from reduced flav*. Protein Sci* **7**:1441–50.

137. Lennon, B.W., Williams, C.H., Ludwig, M.L. (1999). Crystal structure of reduced thioredoxin reductase from *Escherichia coli*: structural flexibility in the isoalloxazine ring of the flavin adenine dinucleotide cofactor. *Protein Sci* **8**:2366–79.

138. Lennon, B.W. (2000). Twists in catalysis: Alternating conformations of *Escherichia coli* thioredoxin reductase*. Science (80-)* **289**:1190–94.

139. Kirkensgaard, K.G., Hägglund, P., Finnie, C., Svensson, B., Henriksen, A. (2009). Structure of *Hordeum vulgare* NADPH-dependent thioredoxin reductase 2. Unwinding the reaction mechanism. *Acta Crystallogr D Biol Crystallogr* **65**:932–41.

140. Scharf, C., Riethdorf, S., Ernst, H., Engelmann, S., Völker, U., Hecker, M. (1998). Thioredoxin is an essential protein induced by multiple stresses in *Bacillus subtilis*. *J Bacteriol* **180**:1869–77.

141. Uziel, O., Borovok, I., Schreiber, R., Cohen, G., Aharonowitz, Y. (2003). Transcriptional regulation of the *Staphylococcus aureus* thioredoxin and thioredoxin reductase genes in response to oxygen and disulfide stress*. J Bacteriol* **186**:326–34.

142. Newton, G.L., Rawat, M., La Clair, J.J., Jothivasan, V.K., Budiarto, T., Hamilton, C.J., Claiborne, A., Helmann, J.D., Fahey, R.C. (2009). Bacillithiol is an antioxidant thiol produced in *Bacilli*. *Nat Chem Biol* **5**:625–27.

143. Newton, G.L., Fahey, R.C., Rawat, M. (2012). Detoxification of toxins by bacillithiol in *Staphylococcus aureus*. *Microbiology* **158**:1117–26.

144. Chi, B.K., Roberts, A.A.A., Huyen, T.T.T.T., Bäsell, K., Becher, D., Albrecht, D., Hamilton, C.J., Antelmann, H. (2012). S-bacillithiolation protects conserved and essential proteins against hypochlorite stress in *Firmicutes* bacteria. *Antioxid Redox Signal* (in press).

145. Vlamis-Gardikas, A., Potamitou, A., Zarivach, R., Hochman, A., Holmgren, A. (2002). Characterization of *Escherichia coli* null mutants for glutaredoxin 2. *J Biol Chem* **277**:10861–68.

146. Potamitou, A., Holmgren, A., Vlamis-Gardikas, A. (2002). Protein levels of *Escherichia coli* thioredoxins and glutaredoxins and their relation to null mutants, growth phase, and function. *J Biol Chem* **277**:18561–67.

147. Möller, M.C., Hederstedt, L. (2008). Extracytoplasmic processes impaired by inactivation of *trxA* (thioredoxin gene) in *Bacillus subtilis*. *J Bacteriol* **190**:4660–65.

148. Smits, W.K., Dubois, J.F., Bron, S., Van Dijl, J.M., Kuipers, O.P. (2005). Tricksy business: transcriptome analysis reveals the involvement of thioredoxin A in redox homeostasis, oxidative stress, sulfur metabolism, and cellular differentiation in *Bacillus subtilis*. *J Bacteriol* **187**:3921–30.

149. Collet, J.-F., D'Souza, J.C., Jakob, U., Bardwell, J.C.A. (2003). Thioredoxin 2, an oxidative stress-induced protein, contains a high affinity zinc binding site. *J Biol Chem* **278**:45325–32.

150. Garg, S.K., Kommineni, S., Henslee, L., Zhang, Y., Zuber, P. (2009). The YjbH protein of *Bacillus subtilis* enhances ClpXP-catalyzed proteolysis of Spx. *J Bacteriol* **191**:1268–77.

151. Bae, J.-B., Park, J.-H., Hahn, M.-Y., Kim, M.-S., Roe, J.-H. (2004). Redox-dependent changes in RsrA, an anti-sigma factor in Streptomyces coelicolor: Zinc release and disulfide bond formation. *J Mol Biol* **335**:425–35.

152. Dinkova-Kostova, A.T., Holtzclaw, W.D., Wakabayashi, N. (2005). Keap1, the sensor for electrophiles and oxidants that regulates the phase 2 response, is a zinc metalloprotein. *Biochemistry* **44**:6889–99.

153. Lim, C.J., Daws, T., Gerami-Nejad, M., Fuchs, J. a (2000). Growth-phase regulation of the *Escherichia coli* thioredoxin gene. *Biochim Biophys Acta* **1491**:1–6.

154. Ritz, D., Patel, H., Doan, B., Zheng, M., Åslund, F., Storz, G., Beckwith, J. (2000). Thioredoxin 2 is involved in the oxidative stress response in *Escherichia coli*. *J Biol Chem* **275**:2505–12.

155. Jacob, C., Kriznik, A., Boschi-Muller, S., Branlant, G. (2011). Thioredoxin 2 from *Escherichia coli* is not involved in vivo in the recycling process of methionine sulfoxide reductase activities. *FEBS Lett* **585**:1905–9.

156. Obiero, J., Pittet, V., Bonderoff, S. a, Sanders, D. a R. (2010). Thioredoxin system from *Deinococcus radiodurans*. *J Bacteriol* **192**:494–501.

157. Comtois, S.L., Gidley, M.D., Kelly, D.J. (2003). Role of the thioredoxin system and the thiol-peroxidases Tpx and Bcp in mediating resistance to oxidative and nitrosative stress in *Helicobacter pylori*. *Microbiology* **149**:121–29.

158. Baker, L.M., Raudonikiene, A., Hoffman, P.S., Poole, L.B. (2001). Essential thioredoxin-dependent peroxiredoxin system from *Helicobacter pylori*: Genetic and kinetic characterization. *J Bacteriol* **183**:1961–73.

159. Nakano, S., Küster-Schöck, E., Grossman, A.D., Zuber, P. (2003). Spx-dependent global transcriptional control is induced by thiol-specific oxidative stress in *Bacillus subtilis*. *Proc Natl Acad Sci U S A* **100**:13603–8.

160. Leichert, L.I.O., Scharf, C., Hecker, M. (2003). Global characterization of disulfide stress in *Bacillus subtilis. J Bacteriol* **185**:1967–75.

161. Rochat, T., Nicolas, P., Delumeau, O., Rabatinová, A., Korelusová, J., Leduc, A., Bessières, P., Dervyn, E., Krásny, L., Noirot, P. (2012). Genome-wide identification of genes directly regulated by the pleiotropic transcription factor Spx in Bacillus subtilis. *Nucleic Acids Res* **40**:9571–83.

162. Petersohn, A., Bernhardt, J., Gerth, U., Höper, D., Koburger, T., Völker, U., Hecker, M. (1999). Identification of sigma(B)-dependent genes in *Bacillus subtilis* using a promoter consensus-directed search and oligonucleotide hybridization. *J Bacteriol* **181**:5718–24.

163. Jordan, A., Pontis, E., Atta, M., Krook, M., Gibert, I., Barbé, J., Reichard, P. (1994). A second class I ribonucleotide reductase in *Enterobacteriaceae*: characterization of the *Salmonella typhimurium* enzyme. *Proc Natl Acad Sci U S A* **91**:12892–96.

164. Jordan, A., Aragall, E., Gibert, I., Barbe, J. (1996). Promoter identification and expression analysis of *Salmonella typhimurium* and *Escherichia coli nrdEF* operons encoding one of two class I ribonucleotide reductases present in both bacteria. *Mol Microbiol* **19**:777–90.

165. Jordan, A., Åslund, F., Pontis, E., Reichard, P., Holmgren, A. (1997). Characterization of *Escherichia coli* NrdH. A glutaredoxin-like protein with a thioredoxin-like activity profile. *J Biol Chem* **272**:18044–50.

166. Jordan, A., Pontis, E., Åslund, F., Hellman, U., Gibert, I., Reichard, P. (1996). The ribonucleotide reductase system of *Lactococcus lactis*. Characterization of an NrdEF enzyme and a new electron transport protein. *J Biol Chem* **271**:8779–85.

167. Gon, S., Faulkner, M.J., Beckwith, J. (2006). In vivo requirement for glutaredoxins and thioredoxins in the reduction of the ribonucleotide reductases of *Escherichia coli*. *Antioxid Redox Signal* **8**:735–42.

168. Cotruvo, J. a, Stubbe, J. (2008). NrdI, a flavodoxin involved in maintenance of the diferric-tyrosyl radical cofactor in *Escherichia coli* class Ib ribonucleotide reductase. *Proc Natl Acad Sci U S A* **105**:14383–8.

169. Holmgren, A., Sengupta, R. (2010). The use of thiols by ribonucleotide reductase. *Free Radic Biol Med* **49**:1617–28.

170. Holmgren, A., Lu, J. (2010). Thioredoxin and thioredoxin reductase: current research with special reference to human disease. *Biochem Biophys Res Commun* **396**:120–24.

171. Stehr, M., Lindqvist, Y. (2004). NrdH-redoxin of *Corynebacterium ammoniagenes* forms a domain-swapped dimer. *Proteins* **55**:613–19.

172. Rabinovitch, I., Yanku, M., Yeheskel, A., Cohen, G., Borovok, I., Aharonowitz, Y. (2010). *Staphylococcus aureus* NrdH redoxin is a reductant of the class Ib ribonucleotide reductase. *J Bacteriol* **192**:4963–72.

173. Gustafsson, T.N., Sahlin, M., Lu, J., Sjöberg, B.-M., Holmgren, A. (2012). *Bacillus anthracis* thioredoxin systems, characterization and role as electron donors for ribonucleotide reductase. *J Biol Chem* **287**:39686–97.

174. Gopal, S., Borovok, I., Ofer, A., Yanku, M., Cohen, G., Goebel, W., Kreft, J., Aharonowitz, Y. (2005). A multidomain fusion protein in *Listeria monocytogenes* catalyzes the two primary activities for glutathione biosynthesis. *J Bacteriol* **187**:3839–47.

175. Janowiak, B.E., Hayward, M.A., Peterson, F.C., Volkman, B.F., Griffith, O.W. (2006). Gamma-glutamylcysteine synthetase-glutathione synthetase: domain structure and identification of residues important in substrate and glutathione binding. *Biochemistry* **45**:10461–73.

176. Stout, J., De Vos, D., Vergauwen, B., Savvides, S.N. (2012). Glutathione biosynthesis in bacteria by bifunctional GshF is driven by a modular structure featuring a novel hybrid ATP-grasp fold. *J Mol Biol* **416**:486–94.

177. Newton, G.L., Arnold, K., Price, M.S., Sherrill, C., Delcardayre, S.B., Aharonowitz, Y., Cohen, G., Davies, J., Fahey, R.C., Davis, C. (1996). Distribution of thiols in microorganisms: mycothiol is a major thiol in most actinomycetes. *J Bacteriol* **178**:1990–95.

178. Fernándes, L., Steele, J.L. (1993). Glutathione content of lactic acid bacteria. *J Dairy Sci* **76**:1233–42.

179. Li, Y., Hugenholtz, J., Abee, T., Molenaar, D. (2003). Glutathione protects *Lactococcus lactis* against oxidative stress. *Appl Environ Microbiol* **69**:5739–45.

180. Setlow, B., Setlow, P. (1977). Levels of acetyl coenzyme A, reduced and oxidized coenzyme A, and coenzyme A in disulfide linkage to protein in dormant and germinated spores and growing and sporulating cells of *Bacillus megaterium*. *J Bacteriol* **132**:444–52.

181. Nicely, N.I., Parsonage, D., Paige, C., Newton, G.L., Fahey, R.C., Leonardi, R., Jackowski, S., Mallett, T.C., Claiborne, A. (2007). Structure of the type III pantothenate kinase from *Bacillus anthracis* at 2.0 A resolution: implications for coenzyme A-dependent redox biology. *Biochemistry* **46**:3234–45.

182. Wallace, B.D., Edwards, J.S., Wallen, J.R., Moolman, W.J. a, Van der Westhuyzen, R., Strauss, E., Redinbo, M.R., Claiborne, A. (2012). Turnover-dependent covalent inactivation of *Staphylococcus aureus* coenzyme A-disulfide reductase by coenzyme A-mimetics: mechanistic and structural insights. *Biochemistry* **51**:7699–711.

183. Buchmeier, N. a, Newton, G.L., Koledin, T., Fahey, R.C. (2003). Association of mycothiol with protection of *Mycobacterium tuberculosis* from toxic oxidants and antibiotics. *Mol Microbiol* **47**:1723–32.

184. Rawat, M., Av-Gay, Y. (2007). Mycothiol-dependent proteins in actinomycetes. *FEMS Microbiol Rev* **31**:278–92.

185. Ordóñez, E., Van Belle, K., Roos, G., De Galan, S., Letek, M., Gil, J. a, Wyns, L., Mateos, L.M., Messens, J. (2009). Arsenate reductase, mycothiol, and mycoredoxin concert thiol/disulfide exchange. *J Biol Chem* **284**:15107–16.

186. Gaballa, A., Newton, G.L., Antelmann, H., Parsonage, D., Upton, H., Rawat, M., Claiborne, A., Fahey, R.C., Helmann, J.D. (2010). Biosynthesis and functions of bacillithiol, a major low-molecular-weight thiol in *Bacilli*. *Proc Natl Acad Sci U S A* **107**:6482–86.

187. Messens, J., Collet, J.-F. (2006). Pathways of disulfide bond formation in *Escherichia coli*. *Int J Biochem Cell Biol* **38**:1050–62.

188. Zapun, A., Bardwell, J.C., Creighton, T.E. (1993). The reactive and destabilizing disulfide bond of DsbA, a protein required for protein disulfide bond formation *in vivo*. *Biochemistry* **32**:5083–92.

189. Bader, M., Muse, W., Ballou, D.P., Gassner, C., Bardwell, J.C. (1999). Oxidative protein folding is driven by the electron transport system. *Cell* **98**:217–27.

190. Rietsch, A., Bessette, P., Georgiou, G., Beckwith, J. (1997). Reduction of the periplasmic disulfide bond isomerase, DsbC, occurs by passage of electrons from cytoplasmic thioredoxin. *J Bacteriol* **179**:6602–8.

191. Bessette, P.H., Cotto, J.J., Gilbert, H.F., Georgiou, G. (1999). In vivo and in vitro function of the *Escherichia coli* periplasmic cysteine oxidoreductase DsbG. *J Biol Chem* **274**:7784–92.

192. Cho, S.-H., Collet, J.-F. (2012). Many roles of the bacterial envelope reducing pathways. *Antioxid Redox Signal*.

193. Depuydt, M., Leonard, S.E., Vertommen, D., Denoncin, K., Morsomme, P., Wahni, K., Messens, J., Carroll, K.S., Collet, J.-F. (2009). A periplasmic reducing system protects single cysteine residues from oxidation. *Science (80-)* **326**:1109–11.

194. Erlendsson, L.S., Hederstedt, L. (2002). Mutations in the thiol-disulfide oxidoreductases BdbC and BdbD can suppress cytochrome c deficiency of CcdA-defective *Bacillus subtilis* cells. *J Bacteriol* **184**:1423–29.

195. Kouwen, T.R.H.M., Van der Goot, A., Dorenbos, R., Winter, T., Antelmann, H., Plaisier, M.-C., Quax, W.J., Van Dijl, J.M., Dubois, J.-Y.F. (2007). Thiol-disulphide oxidoreductase modules in the low-GC Gram-positive bacteria. *Mol Microbiol* **64**:984–99.

196. Christman, M.F., Morgan, R.W., Jacobson, F.S., Ames, B.N. (1985). Positive control of a regulon for defenses against oxidative stress and some heat-shock proteins in *Salmonella typhimurium*. *Cell* **41**:753–62.

197. Amábile-Cuevas, C.F., Demple, B. (1991). Molecular characterization of the soxRS genes of *Escherichia coli*: Two genes control a superoxide stress regulon. *Nucleic Acids Res* **19**:4479–84.

198. Dietrich, L.E.P., Teal, T.K., Price-Whelan, A., Newman, D.K. (2008). Redox-active antibiotics control gene expression and community behavior in divergent bacteria. *Science (80-)* **321**:1203–6.

199. Chen, H., Xu, G., Zhao, Y., Tian, B., Lu, H., Yu, X., Xu, Z., Ying, N., Hu, S., Hua, Y. (2008). A novel OxyR sensor and regulator of hydrogen peroxide stress with one cysteine residue in *Deinococcus radiodurans*. *PLoS One* **3**:e1602.

200. Kim, M., Hwang, S., Ryu, S., Jeon, B. (2011). Regulation of perR expression by iron and PerR in *Campylobacter jejuni*. *J Bacteriol* **193**:6171–78.

201. Flores-Cruz, Z., Allen, C. (2011). Necessity of OxyR for the hydrogen peroxide stress response and full virulence in *Ralstonia solanacearum*. *Appl Environ Microbiol* **77**:6426–32.

202. Daugherty, A., Suvarnapunya, A.E., Runyen-Janecky, L. (2012). The role of OxyR and SoxRS in oxidative stress survival in *Shigella flexneri*. *Microbiol Res* **167**:238–45.

203. Choi, H., Kim, S., Mukhopadhyay, P., Cho, S., Woo, J., Storz, G., Ryu, S.E. (2001). Structural basis of the redox switch in the OxyR transcription factor. *Cell* **105**:103–13.

204. Zheng, M., Wang, X., Templeton, L.J., Smulski, D.R., LaRossa, R.A., Storz, G. (2001). DNA microarray-mediated transcriptional profiling of the *Escherichia coli* response to hydrogen peroxide. *J Bacteriol* **183**:4562–70.

205. Anjem, A., Varghese, S., Imlay, J.A. (2009). Manganese import is a key element of the OxyR response to hydrogen peroxide in *Escherichia coli*. *Mol Microbiol* **72**:844–58.

206. Anjem, A., Imlay, J.A. (2012). Mononuclear iron enzymes are primary targets of hydrogen peroxide stress. *J Biol Chem* **287**:15544–56.

207. Sobota, J.M., Imlay, J.A. (2011). Iron enzyme ribulose-5-phosphate 3-epimerase in *Escherichia coli* is rapidly damaged by hydrogen peroxide but can be protected by manganese. *Proc Natl Acad Sci U S A* **108**:5402–7.

208. Liu, Y., Bauer, S.C., Imlay, J.A. (2011). The YaaA protein of the *Escherichia coli* OxyR regulon lessens hydrogen peroxide toxicity by diminishing the amount of intracellular unincorporated iron. *J Bacteriol* **193**:2186–96.

209. Körner, H., Sofia, H.J., Zumft, W.G. (2003). Phylogeny of the bacterial superfamily of Crp-Fnr transcription regulators: exploiting the metabolic spectrum by controlling alternative gene programs. *FEMS Microbiol Rev* **27**:559–92.

210. Gostick, D.O., Green, J., Irvine, a S., Gasson, M.J., Guest, J.R. (1998). A novel regulatory switch mediated by the FNR-like protein of Lactobacillus casei. *Microbiology* **144**:705–17.

211. Gostick, D.O., Griffin, H.G., Shearman, C. a, Scott, C., Green, J., Gasson, M.J., Guest, J.R. (1999). Two operons that encode FNR-like proteins in *Lactococcus lactis*. *Mol Microbiol* **31**:1523–35.

212. Stillman, T.J., Upadhyay, M., Norte, V.A., Sedelnikova, S.E., Carradus, M., Tzokov, S., Bullough, P.A., Shearman, C.A., Gasson, M.J., Williams, C.H., Artymiuk, P.J., Green, J. (2005). The crystal structures of *Lactococcus lactis* MG1363 Dps proteins reveal the presence of an N-terminal helix that is required for DNA binding. *Mol Microbiol* **57**:1101–12.

213. Nakano, S., Nakano, M.M., Zhang, Y., Leelakriangsak, M., Zuber, P. (2003). A regulatory protein that interferes with activator-stimulated transcription in bacteria. *Proc Natl Acad Sci U S A* **100**:4233–38.

214. Lamour, V., Westblade, L.F., Campbell, E. a, Darst, S. a (2009). Crystal structure of the *in vivo*-assembled *Bacillus subtilis* Spx/RNA polymerase alpha subunit C-terminal domain complex. *J Struct Biol* **168**:352–56.

215. Martin, P., DeMel, S., Shi, J., Gladysheva, T., Gatti, D.L., Rosen, B.P., Edwards, B.F. (2001). Insights into the structure, solvation, and mechanism of ArsC arsenate reductase, a novel arsenic detoxification enzyme. *Structure* **9**:1071–81.

216. Newberry, K.J., Nakano, S., Zuber, P., Brennan, R.G. (2005). Crystal structure of the *Bacillus subtilis* anti-alpha, global transcriptional regulator, Spx, in complex with the alpha C-terminal domain of RNA polymerase. *Proc Natl Acad Sci U S A* **102**:15839–44.

217. Nakano, M.M., Lin, A., Zuber, C.S., Newberry, K.J., Brennan, R.G., Zuber, P. (2010). Promoter recognition by a complex of Spx and the C-terminal domain of the RNA polymerase alpha subunit. *PLoS One* **5**:e8664.

218. Wegmann, U., O'Connell-Motherway, M., Zomer, A., Buist, G., Shearman, C., Canchaya, C., Ventura, M., Goesmann, A., Gasson, M.J., Kuipers, O.P., Van Sinderen, D., Kok, J. (2007). Complete genome sequence of the prototype lactic acid bacterium *Lactococcus lactis* subsp. *cremoris* MG1363. *J Bacteriol* **189**:3256–70.

219. Duwat, P., Ehrlich, S.D., Gruss, A. (1999). Effects of metabolic flux on stress response pathways in *Lactococcus lactis*. *Mol Microbiol* **31**:845–58.

220. Frees, D., Varmanen, P., Ingmer, H. (2001). Inactivation of a gene that is highly conserved in Gram-positive bacteria stimulates degradation of non-native proteins and concomitantly increases stress tolerance in *Lactococcus lactis*. *Mol Microbiol* **41**:93–103.

221. Turner, M.S., Tan, Y.P., Giffard, P.M. (2007). Inactivation of an iron transporter in *Lactococcus lactis* results in resistance to tellurite and oxidative stress. *Appl Environ Microbiol* **73**:6144–49.

222. Veiga, P., Bulbarela-Sampieri, C., Furlan, S., Maisons, A., Chapot-Chartier, M.-P., Erkelenz, M., Mervelet, P., Noirot, P., Frees, D., Kuipers, O.P., Kok, J., Gruss, A., Buist, G., Kulakauskas, S. (2007). SpxB regulates O-acetylation-dependent resistance of *Lactococcus lactis* peptidoglycan to hydrolysis. *J Biol Chem* **282**:19342–54.

223. Nakano, S., Erwin, K.N., Ralle, M., Zuber, P. (2005). Redox-sensitive transcriptional control by a thiol/disulphide switch in the global regulator, Spx. *Mol Microbiol* **55**:498–510.

224. Pamp, S.J., Frees, D., Engelmann, S., Hecker, M., Ingmer, H. (2006). Spx is a global effector impacting stress tolerance and biofilm formation in *Staphylococcus aureus*. *J Bacteriol* **188**:4861–70.

225. Ballal, A., Manna, A.C. (2010). Control of thioredoxin reductase gene (*trxB*) transcription by SarA in *Staphylococcus aureus*. *J Bacteriol* **192**:336–45.

226. Cheung, A.L., Nishina, K. a, Trotonda, M.P., Tamber, S. (2008). The SarA protein family of *Staphylococcus aureus*. *Int J Biochem Cell Biol* **40**:355–61.

227. Cocaign-Bousquet, M., Garrigues, C., Loubiere, P., Lindley, N.D. (1996). Physiology of pyruvate metabolism in *Lactococcus lactis*. *Antonie Van Leeuwenhoek* **70**:253–67.

228. Cotter, P.D., Hill, C., Ross, R.P. (2005). Bacteriocins: developing innate immunity for food. *Nat Rev Microbiol* **3**:777–88.

229. Dalié, D.K.D., Deschamps, A.M., Richard-Forget, F. (2010). Lactic acid bacteria – Potential for control of mould growth and mycotoxins: A review. *Food Control* **21**:370–80.

230. Lawrence, R.C., Creamer, L.K., Gilles, J. (1987). Texture development during cheese ripening. *Journal of Dairy Science* **70**:1748–60.

231. Van Kranenburg, R., Kleerebezem, M., Van Hylckama Vlieg, J., Ursing, B.M., Boekhorst, J., Smit, B.A., Ayad, E.H.E., Smit, G., Siezen, R.J. (2002). Flavour formation from amino acids by lactic acid bacteria: Predictions from genome sequence analysis. *Int Dairy J* **12**:111–21.

232. Makarova, K.S., Koonin, E. V (2007). Evolutionary genomics of lactic acid bacteria. *J Bacteriol* **189**:1199–208.

233. Ventura, M., Canchaya, C., Tauch, A., Chandra, G., Fitzgerald, G.F., Chater, K.F., Van Sinderen, D. (2007). Genomics of *Actinobacteria*: tracing the evolutionary history of an ancient phylum. *Microbiol Mol Biol Rev* **71**:495–548.

234. Marco, M.L., Pavan, S., Kleerebezem, M. (2006). Towards understanding molecular modes of probiotic action. *Curr Opin Biotechnol* **17**:204–10.

235. Sanders, M.E., Klaenhammer, T.R. (2001). Invited review: the scientific basis of *Lactobacillus acidophilus* NCFM functionality as a probiotic. *J Dairy Sci* **84**:319–31.

236. Gilad, O., Svensson, B., Viborg, A.H., Stuer-Lauridsen, B., Jacobsen, S. (2011). The extracellular proteome of *Bifidobacterium animalis* subsp. *lactis* BB-12 reveals proteins with putative roles in probiotic effects. *Proteomics* **11**:2503–14.

237. Andersen, J.M., Barrangou, R., Abou Hachem, M., Lahtinen, S., Goh, Y.J., Svensson, B., Klaenhammer, T.R. (2011). Transcriptional and functional analysis of galactooligosaccharide uptake by lacS in *Lactobacillus acidophilus*. *Proc Natl Acad Sci U S A* **108**:17785–90.

238. Cretenet, M., Laroute, V., Ulvé, V., Jeanson, S., Nouaille, S., Even, S., Piot, M., Girbal, L., Le Loir, Y., Loubière, P., Lortal, S., Cocaign-Bousquet, M. (2011). Dynamic analysis of the *Lactococcus lactis* transcriptome in cheeses made from milk concentrated by ultrafiltration reveals multiple strategies of adaptation to stresses. *Appl Environ Microbiol* **77**:247–57.

239. Linares, D.M., Kok, J., Poolman, B. (2010). Genome sequences of *Lactococcus lactis* MG1363 (revised) and NZ9000 and comparative physiological studies. *J Bacteriol* **192**:5806–12.

240. Kok, J., Buist, G., Zomer, A.L., Van Hijum, S. a F.T., Kuipers, O.P. (2005). Comparative and functional genomics of lactococci. *FEMS Microbiol Rev* **29**:411–33.

241. Mierau, I., Kleerebezem, M. (2005). 10 years of the nisin-controlled gene expression system (NICE) in *Lactococcus lactis*. *Appl Microbiol Biotechnol* **68**:705–17.

242. Bermúdez-Humarán, L.G., Kharrat, P., Chatel, J.-M., Langella, P. (2011). Lactococci and lactobacilli as mucosal delivery vectors for therapeutic proteins and DNA vaccines. *Microb Cell Fact* **10 Suppl 1**:S4.

243. Bahey-El-Din, M., Gahan, C.G.M. (2011). *Lactococcus lactis*-based vaccines: current status and future perspectives. *Hum Vaccin* **7**:106–9.

244. Condon, S. (1987). Responses of lactic acid bacteria to oxygen. *FEMS Microbiol Lett* **46**:269–80.

245. Jensen, N.B., Melchiorsen, C.R., Jokumsen, K. V, Villadsen, J. (2001). Metabolic behavior of *Lactococcus lactis* MG1363 in microaerobic continuous cultivation at a low dilution rate. *Appl Environ Microbiol* **67**:2677–82.

246. Thomas, T.D., Ellwood, D.C., Longyear, V.M. (1979). Change from homo- to heterolactic fermentation by *Streptococcus lactis* resulting from glucose limitation in anaerobic chemostat cultures. *J Bacteriol* **138**:109–17.

247. Garrigues, C., Loubiere, P., Lindley, N.D., Cocaign-Bousquet, M. (1997). Control of the shift from homolactic acid to mixed-acid fermentation in *Lactococcus lactis*: Predominant role of the NADH/NAD+ ratio. *J Bacteriol* **179**:5282–87.

248. Niimura, Y., Poole, L.B., Massey, V. (1995). *Amphibacillus xylanus* NADH oxidase and *Salmonella typhimurium* alkyl-hydroperoxide reductase flavoprotein components show extremely high scavenging activity for both alkyl hydroperoxide and hydrogen peroxide in the presence of <i>S. typhimuri. *J Biol Chem* **270**:25645–50.

249. Jiang, R., Riebel, B.R., Bommarius, A.S. (2005). Comparison of alkyl hydroperoxide reductase (AhpR) and water-forming NADH oxidase from *Lactococcus lactis* ATCC 19435. *Adv Synth Catal* **347**:1139–46.

250. Wang, L., Chong, H., Jiang, R. (2012). Comparison of alkyl hydroperoxide reductase and two water-forming NADH oxidases from *Bacillus cereus* ATCC 14579. *Appl Microbiol Biotechnol* **5**:1265–73.

251. Pedersen, M.B., Garrigues, C., Tuphile, K., Brun, C., Vido, K., Bennedsen, M., Møllgaard, H., Gaudu, P., Gruss, A. (2008). Impact of aeration and heme-activated respiration on *Lactococcus lactis* gene expression: identification of a heme-responsive operon. *J Bacteriol* **190**:4903–11.

252. Miyoshi, A., Rochat, T., Gratadoux, J.-J., Le Loir, Y., Oliveira, S.C., Langella, P., Azevedo, V. (2003). Oxidative stress in *Lactococcus lactis*. *Genet Mol Res* **2**:348–59.

253. Higuchi, M., Yamamoto, Y., Poole, L.B., Shimada, M., Sato, Y., Takahashi, N., Kamio, Y. (1999). Functions of two types of NADH oxidases in energy metabolism and oxidative stress of *Streptococcus mutans*. *J Bacteriol* **181**:5940–47.

254. Tachon, S., Brandsma, J.B., Yvon, M. (2010). NoxE NADH oxidase and the electron transport chain are responsible for the ability of *Lactococcus lactis* to decrease the redox potential of milk. *Appl Environ Microbiol* **76**:1311–19.

255. Parsonage, D., Desrosiers, D.C., Hazlett, K.R.O., Sun, Y., Nelson, K.J., Cox, D.L., Radolf, J.D., Poole, L.B. (2010). Broad specificity AhpC-like peroxiredoxin and its thioredoxin reductant in the sparse antioxidant defense system of *Treponema pallidum*. *Proc Natl Acad Sci U S A* **107**:6240–45.

256. Lopez de Felipe, F., Hugenholtz, J. (1999). Pyruvate flux distribution in NADH-oxidase-overproducing *Lactococcus lactis* strain as a function of culture conditions. *FEMS Microbiol Lett* **179**:461–66.

257. Derr, A.M., Faustoferri, R.C., Betzenhauser, M.J., Gonzalez, K., Marquis, R.E., Quivey, R.G. (2012). Mutation of the NADH oxidase gene (*nox*) reveals an overlap of the oxygen- and acid-mediated stress responses in *Streptococcus mutans*. *Appl Environ Microbiol* **78**:1215–27.

258. Murphy, M.G., Condon, S. (1984). Correlation of oxygen utilization and hydrogen peroxide accumulation with oxygen induced enzymes in *Lactobacillus plantarum* cultures. *Arch Microbiol* **138**:44–48.

259. Bolotin, A., Wincker, P., Mauger, S., Jaillon, O., Malarme, K., Weissenbach, J., Ehrlich, S.D., Sorokin, A. (2001). The complete genome sequence of the lactic acid bacterium *Lactococcus lactis* ssp. *lactis* IL1403. *Genome Res* **11**:731–53.

260. Price, C.E., Zeyniyev, A., Kuipers, O.P., Kok, J. (2011). From meadows to milk to mucosa - adaptation of *Streptococcus* and *Lactococcus* species to their nutritional environments. *FEMS Microbiol Rev* **36**:949–71.

261. Anders, R.F., Hogg, D.M., Jago, G.R. (1970). Formation of hydrogen peroxide by group N streptococci and its effect on their growth and metabolism. *Appl Microbiol* **19**:608–12.

262. Seki, M., Iida, K., Saito, M., Nakayama, H., Yoshida, S. (2004). Hydrogen peroxide production in *Streptococcus pyogenes*: involvement of lactate oxidase and coupling with aerobic utilization of lactate. *J Bacteriol* **186**:2046–51.

263. Barré, O., Mourlane, F., Solioz, M. (2007). Copper induction of lactate oxidase of *Lactococcus lactis*: A novel metal stress response. *J Bacteriol* **189**:5947–54.

264. Sijpesteijn, A.K. (1970). Induction of cytochrome formation and stimulation of oxidative dissimilation by hemin in *Streptococcus lactis* and *Leuconostoc mesenteroides*. *Antonie Van Leeuwenhoek* **36**:335–48.

265. Duwat, P., Sourice, S., Cesselin, B., Lamberet, G., Vido, K., Gaudu, P., Le Loir, Y., Violet, F., Loubière, P., Gruss, A. (2001). Respiration capacity of the fermenting bacterium *Lactococcus lactis* and its positive effects on growth and survival. *J Bacteriol* **183**:4509–16.

266. Pedersen, M.B., Gaudu, P., Lechardeur, D., Petit, M.-A., Gruss, A. (2012). Aerobic respiration metabolism in lactic acid bacteria and uses in biotechnology. *Annual Review of Food Science and Technology* **3**:37–58.

267. Archibald, F.S., Fridovich, I. (1981). Manganese, superoxide dismutase, and oxygen tolerance in some lactic acid bacteria. *J Bacteriol* **146**:928–36.

268. Yamamoto, Y., Poyart, C., Trieu-Cuot, P., Lamberet, G., Gruss, A., Gaudu, P. (2005). Respiration metabolism of Group B *Streptococcus* is activated by environmental haem and quinone and contributes to virulence. *Mol Microbiol* **56**:525–34.

269. Brooijmans, R.J.W., De Vos, W.M., Hugenholtz, J. (2009). *Lactobacillus plantarum* WCFS1 electron transport chains. *Appl Environ Microbiol* **75**:3580–85.

270. Huycke, M.M., Moore, D., Joyce, W., Wise, P., Shepard, L., Kotake, Y., Gilmore, M.S. (2001). Extracellular superoxide production by *Enterococcus faecalis* requires demethylmenaquinone and is attenuated by functional terminal quinol oxidases. *Mol Microbiol* **42**:729–40.

271. Gennis, R., Stewart, V. (1996). Respiration, p. 217–71. In Neidhardt, F (ed.), *Escherichia Coli and Salmonella*. ASM Press.

272. Gaudu, P., Vido, K., Cesselin, B., Kulakauskas, S., Tremblay, J., Rezaïki, L., Lamberret, G., Sourice, S., Duwat, P., Gruss, A. (2002). Respiration capacity and consequences in *Lactococcus lactis*. *Antonie Van Leeuwenhoek* **82**:263–69.

273. Rezaïki, L., Lamberet, G., Derré, A., Gruss, A., Gaudu, P. (2008). *Lactococcus lactis* produces short-chain quinones that cross-feed Group B *Streptococcus* to activate respiration growth. *Mol Microbiol* **67**:947–57.

274. Tachon, S., Michelon, D., Chambellon, E., Cantonnet, M., Mezange, C., Henno, L., Cachon, R., Yvon, M. (2009). Experimental conditions affect the site of tetrazolium violet reduction in the electron transport chain of *Lactococcus lactis*. *Microbiology* **155**:2941–48.

275. Koebmann, B., Blank, L.M., Solem, C., Petranovic, D., Nielsen, L.K., Jensen, P.R. (2008). Increased biomass yield of *Lactococcus lactis* during energetically limited growth and respiratory conditions. *Biotechnol Appl Biochem* **50**:25–33.

276. Vido, K., Le Bars, D., Mistou, M.-Y., Anglade, P., Gruss, A., Gaudu, P. (2004). Proteome analyses of heme-dependent respiration in *Lactococcus lactis*: Involvement of the proteolytic system. *J Bacteriol* **186**:1648–57.

277. Rezaïki, L., Cesselin, B., Yamamoto, Y., Vido, K., Van West, E., Gaudu, P., Gruss, A. (2004). Respiration metabolism reduces oxidative and acid stress to improve long-term survival of *Lactococcus lactis*. *Mol Microbiol* **53**:1331–42.

278. Vido, K., Diemer, H., Van Dorsselaer, A., Leize, E., Juillard, V., Gruss, A., Gaudu, P. (2005). Roles of thioredoxin reductase during the aerobic life of *Lactococcus lactis*. *J Bacteriol* **187**:601–10.

279. Serata, M., Iino, T., Yasuda, E., Sako, T. (2012). Roles of thioredoxin and thioredoxin reductase in the resistance to oxidative stress in *Lactobacillus casei*. *Microbiology* **158**:953–62.

280. Sanders, J.W., Leenhouts, K.J., Haandrikman, A.J., Venema, G., Kok, J. (1995). Stress response in *Lactococcus lactis*: Cloning, expression analysis, and mutation of the lactococcal superoxide dismutase gene. *J Bacteriol* **177**:5254–60.

281. Budin-Verneuil, A., Pichereau, V., Auffray, Y., Ehrlich, D., Maguin, E. (2007). Proteome phenotyping of acid stress-resistant mutants of *Lactococcus lactis* MG1363. *Proteomics* **7**:2038–46.

282. Wolf, G., Strahl, a, Meisel, J., Hammes, W.P. (1991). Heme-dependent catalase activity of lactobacilli. *Int J Food Microbiol* **12**:133–40.

283. Frankenberg, L., Brugna, M., Hederstedt, L. (2002). *Enterococcus faecalis* heme-dependent catalase. *J Bacteriol* **184**:6351–56.

284. Baureder, M., Hederstedt, L. (2012). Genes important for catalase activity in *Enterococcus faecalis*. *PLoS One* **7**:e36725.

285. Pugh, S.Y., Knowles, C.J. (1983). Synthesis of catalase by "*Streptococcus faecalis* subsp. *zymogenes*". *Arch Microbiol* **136**:60–63.

286. Kono, Y., Fridovich, I. (1983). Isolation and characterization of the pseudocatalase of *Lactobacillus plantarum*. *J Biol Chem* **258**:6015–9.

287. Johnston, M.A., Delwiche, E.A. (1965). Isolation and characterization of the cyanide-resistant and azide-resistant catalase of *Lactobacillus plantarum*. *J Bacteriol* **90**:352–56.

288. Whittaker, J.W. (2012). Non-heme manganese catalase--the "other" catalase. *Arch Biochem Biophys* **525**:111–20.

289. Magnani, D., Barré, O., Gerber, S.D., Solioz, M. (2008). Characterization of the CopR regulon of *Lactococcus lactis* IL1403. *J Bacteriol* **190**:536–45.

290. Mermod, M., Mourlane, F., Waltersperger, S., Oberholzer, A.E., Baumann, U., Solioz, M. (2010). Structure and function of CinD (YtjD) of *Lactococcus lactis*, a copper-induced nitroreductase involved in defense against oxidative stress. *J Bacteriol* **192**:4172–80.

291. Schroeter, R., Voigt, B., Jürgen, B., Methling, K., Pöther, D.-C., Schäfer, H., Albrecht, D., Mostertz, J., Mäder, U., Evers, S., Maurer, K.-H., Lalk, M., Mascher, T., Hecker, M., Schweder, T. (2011). The peroxide stress response of *Bacillus licheniformis*. *Proteomics* **11**:2851–66.

292. Lewis, J.P., Iyer, D., Anaya-Bergman, C. (2009). Adaptation of *Porphyromonas gingivalis* to microaerophilic conditions involves increased consumption of formate and reduced utilization of lactate. *Microbiology* **155**:3758–74.

293. Saikolappan, S., Das, K., Sasindran, S.J., Jagannath, C., Dhandayuthapani, S. (2011). OsmC proteins of *Mycobacterium tuberculosis* and *Mycobacterium smegmatis* protect against organic hydroperoxide stress. *Tuberculosis* **91**:S119–27.

294. Rallu, F., Gruss, A., Ehrlich, S.D., Maguin, E. (2000). Acid- and multistress-resistant mutants of *Lactococcus lactis*: Identification of intracellular stress signals. *Mol Microbiol* **35**:517–28.

295. Duwat, P., Ehrlich, S.D., Gruss, A. (1995). The *recA* gene of *Lactococcus lactis*: characterization and involvement in oxidative and thermal stress. *Mol Microbiol* **17**:1121–31.

296. Duwat, P., Cesselin, B., Sourice, S., Gruss, A. (2000). *Lactococcus lactis*, a bacterial model for stress responses and survival. *Int J Food Microbiol* **55**:83–86.

297. Cesselin, B., Ali, D., Gratadoux, J.-J., Gaudu, P., Duwat, P., Gruss, A., El Karoui, M. (2009). Inactivation of the *Lactococcus lactis* high-affinity phosphate transporter confers oxygen and thiol resistance and alters metal homeostasis. *Microbiology* **155**:2274–81.

298. O'Connell-Motherway, M., Van Sinderen, D., Morel-Deville, F., Fitzgerald, G.F., Ehrlich, S.D., Morel, P. (2000). Six putative two-component regulatory systems isolated from *Lactococcus lactis* subsp. *cremoris* MG1363. *Microbiology* **146**:935–47.

2 Chapter 2 – Two *Lactococcus lactis* thioredoxin paralogues play different roles in responses to arsenate and oxidative stress

Petr Efler[1], Mogens Kilstrup[2], Stig Johnsen[1], Birte Svensson[1], and Per Hägglund[1#]

[1] Enzyme and Protein Chemistry, Søltofts Plads Building 224, Department of Systems Biology, Technical University of Denmark, DK-2800, Kgs. Lyngby, Denmark

[2] Center for Systems Microbiology, Matematiktorvet Building 301, Department of Systems Biology, Technical University of Denmark, DK-2800 Kgs. Lyngby, Denmark

Corresponding author: Tel: +45 4525 5503; fax: +45 4588 6307; e-mail: ph@bio.dtu.dk

Formated for publication in Microbiology

Content category: Cell and Molecular Biology of Microbes

Running title: Different roles of two *Lactococcus lactis* thioredoxins

The number of words in the summary – 233; the main text – 6757; the number of tables and figures – 10 + supplementary data

Keywords: *Lactococcus lactis*, thioredoxin, oxidative stress, arsenate, redox

Abbreviations: ACN, acetonitrile; CHCA, α-cyano-4-hydroxycinnamic acid; DIGE, difference gel electrophoresis; EP, exponential phase; INT, iodonitrotetrazolium chloride; MALDI-TOF MS, matrix-assisted laser desorption ionization time-of-flight mass spectrometry; MetSO, methionine sulfoxide; NTR, NADPH-dependent thioredoxin reductase; SP, stationary growth phase; TFA, trifluoroacetic acid; Trx, thioredoxin; TV, tetrazolium violet; wt, wild type

2.1 Abstract (MAX 250 WORDS)

Thioredoxin (Trx) is a small universal disulfide reductase involved in a wide range of cellular processes including ribonucleotide reduction, sulphur assimilation, oxidative stress responses and arsenate detoxification. The industrially important lactic acid bacterium *Lactococcus lactis* contains two Trx paralogues (TrxA and TrxD). TrxA is similar to well characterized Trx homologues and contains a common WCGPC active site motif, while TrxD is atypical and contains an aspartate residue in the active site motif (WCGDC). In the present work Trx deletion mutants, Δ*trxA*, Δ*trxD* and Δ*trxA*Δ*trxD*, were investigated to elucidate the physiological roles of the two Trx paralogues in stress resistance. In general, the Δ*trxA*Δ*trxD* mutant was significantly more sensitive than either of the the Δ*trxA* and Δ*trxD* mutants suggesting partially overlapping functions of TrxA and TrxD. Upon exposure to oxidative stress the growth of the Δ*trxA* mutant was diminished while the Δ*trxD* mutant behaved similar to wild type. The lack of TrxA also appears to impair methionine sulfoxide reduction. Both Δ*trxA* and Δ*trxD* strains displayed growth inhibition after treatment with sodium arsenate and tellurite as compared to the wild type. Overall, the phenotype of the Δ*trxA* mutant match established functions of WCGPC-type Trx while TrxD appears to play a more restricted role in stress resistance of *L. lactis*. Proteome analysis of the Δ*trxD* mutant exposed to arsenate stress demonstrated a decrease in translation elongation factors and an increase in enzymes involved in nucleotide biosynthesis.

2.2 Introduction

Protein disulfide reductases such as thioredoxin (Trx) maintain the intracellular thiol redox environment and provide reducing equivalents to enzymes such as ribonucleotide reductase, peroxiredoxin, methionine sulfoxide reductase and arsenate reductase (Collet & Messens, 2010). Trx is a small protein (10–12 kDa) with a conserved redox-active WCGPC motif that reduces target protein disulfides in a so-called thiol-disulfide exchange reaction (Jensen *et al.*, 2009). The target disulfide is attacked by the thiolate anion of the cysteine at the N-terminal end of the active-site and forms an intermolecular disulfide, which is then attacked by the cysteine at the C-terminal end of the active-site. Consequently, the reduced target protein and oxidized Trx are formed. Trx is subsequently recycled by NADPH-dependent Trx reductase (NTR). In addition to Trx, disulfide bonds are reduced by glutaredoxin coupled to the tripeptide glutathione (GSH) and glutathione reductase (Lillig *et al.*, 2008). Most Gram-positive bacteria, however, lack GSH and some species produce alternative low molecular weight thiols such as mycothiol in *Actinomycetes* or bacillithiol in various *Bacilli*, *Staphylococcus aureus* and *Deinococcus radiodurans* (Fahey *et al.*, 1978; Newton *et al.*, 1996, 2009).

The industrially important Gram-positive lactic acid bacterium *L. lactis* also lacks the biosynthetic pathway for GSH but some strains can utilize exogenously supplied GSH (Fernándes & Steele, 1993; Li *et al.*, 2003; Newton *et al.*, 1996). *L. lactis* contains two Trx paralogues (TrxA, TrxD*)* and a glutaredoxin-like protein (NrdH), which functions as electron donor for the ribonucleotide reductase class Ib (NrdEF) in microbial cells (Jordan *et al.*, 1996). TrxA contains a common WCGPC active site motif and conserved residues important for Trx function. In contrast, TrxD displays low similarity to TrxA and contains an unconventional

WCGDC active site motif. *L. lactis* also produces an NTR (TrxB) that recycles TrxA, TrxD and NrdH *in vitro* (Efler, P., Björnberg, O., Ebong, E.D., Svensson, B. and Hägglund, P.; unpublished results). TrxB is important for oxidative stress resistance but not essential for viability under mild oxidative conditions (Vido *et al.*, 2005).

Here the physiological roles of TrxA and TrxD in *L. lactis* were investigated using strains lacking either one or both Trx (Δ*trxA*, Δ*trxD* and Δ*trxA*Δ*trxD*). Comparison of growth rates of these mutant strains and wild type after exposure to various stress conditions suggests a partial overlap in function between TrxA and TrxD. TrxA, however, appears to be of major importance for oxidative stress resistance whereas TrxD seems to play a role in arsenate detoxification.

2.3 Materials and methods

2.3.1 Strains and growth conditions

Unless stated otherwise *Lactococcus lactis* subsp. *cremoris* MG1363 (Gasson, 1983) wild type (wt), Δ*trxA*, Δ*trxD* and Δ*trxA*Δ*trxD* were maintained on agar plates containing M17 medium (Difco) with 1% (w/v) glucose (GM17), and grown in chemically defined SA medium (Jensen & Hammer, 1993) containing 1% (w/v) glucose and 4 µg/ml lipoic acid (GSAL medium). In order to obtain synchronized balanced cultures, colonies from fresh GM17 plates were inoculated into liquid GSAL medium, serially diluted (10^2, 10^3, 10^4, 10^5, 10^6) and grown under static conditions at 30°C overnight. The dilution with exponentially growing cells (optical density at 450 nm between 0.3 – 0.6) was used for further experiments. When performing phenotype screening on solid GSAL media, synchronized exponentially growing overnight cultures were used for making

serial dilutions (10^2, 10^3, 10^4, 10^5) in pre-warmed GSAL medium in a 96-well plate. From each well 10 µL was spotted to pre-warmed GSAL agar plates containing the particular stress compound (500 mM Na_2HAsO_4 or 300 mM K_2TeO_4) and incubated at 30°C for 24 h. *Escherichia coli* MC1061 was grown in Luria-Broth medium (LB) at 28°C, 30°C or 37°C. When relevant, LB was supplemented by erythromycin (150 µg/mL) and GM17 by erythromycin (5 µg/ml) + 1% NaCl.

2.3.2 Bioscreen assays

A Bioscreen C instrument (Oy Growth Curves Ab Ltd.) was used to monitor growth of *L. lactis* wt and *trx* mutants exposed to a range of different stress conditions. Synchronized exponentially growing cultures were diluted in preheated GSAL medium to an OD_{450} = 0.01, then 360 µL was mixed with 40 µL of a stress compound solution (listed in Table S2) or H_20 in a well of a pre-warmed honeycomb plate To monitor methionine sulfoxide (MetSO) assimilation a freshly grown single colony from a GM17 plate was resuspended in 5 mL GSAL medium without methionine and diluted ten times in the same medium. From this culture 360 µL aliquots were pipetted into wells of a pre-warmed honeycomb plate containing 40 µL of either methionine or MetSO at 1 mg/mL. The plates were incubated at 30ºC without shaking. OD_{450} was monitored at 40 min intervals with 10 s medium intense shaking prior to the measurement.

2.3.3 Construction of L. lactis ΔtrxA, ΔtrxD and ΔtrxAΔtrxD

DNA isolation, amplification and cloning were performed according to standard procedures (Sambrook & Russel, 2000) or the manufacturers' instructions. Upstream and downstream regions flanking the *trxA and trxD* genes were amplified from genomic DNA of *L. lactis* subsp. *cremoris* MG1363 by PCR (deletion by overlap extension) using primers listed in Table S1 and HotStar HiFidelity PCR kit (Qiagen). The PCR products of the upstream and downstream regions were fused and used as template for PCR using the forward primers for the upstream regions together with the reverse primers for the downstream regions (Table S1). The PCR products were digested with *Bam*HI and *Xho*I and ligated into pGHost4 (Appligene). The resulting plasmids were used to transform *E. coli* MC1061, and the correct sequences were confirmed by DNA sequencing (Eurofins). Plasmids were electroporated into *L. lactis* and the transformants were selected on GM17 plates containing erythromycin at 28˚C. After homologous recombination into the chromosome, and clearing of the plasmid as previously described (Biswas *et al.*, 1993), the deletions were confirmed by colony PCR amplification using the flanking primers binding to the chromosome outside the targeted region (Table S1). The Δ*trxA*Δ*trxD* double mutant was prepared using the Δ*trxA* strain as the template for homologous recombination of Δ*trxD* as described above.

2.3.4 Preparation of polyclonal primary antibodies against TrxA and TrxD

Purified recombinant *L. lactis* TrxA or TrxD produced in *E. coli* (Efler, P, Björnberg, O., Ebong, E.D., Svensson, B. and Hägglund, P.; unpublished results) were used for raising primary anti-TrxA or anti-TrxD antibodies. Prior to immunization the N-terminal His_6 tags of recombinant

TrxA and TrxD were removed by proteolytic digestion incubation overnight with immobilized thrombin (Calbiochem) as confirmed by matrix-assisted laser desorption ionization time-of-flight mass spectrometry (MALDI-TOF MS) and SDS-PAGE (data not shown). Cleaved His_6-tags and uncleaved His_6-Trx were subsequently removed on a HisTrap™ column (GE Healthcare) Non-His-tagged TrxA and TrxD were equilibrated in PBS using PD10 desalting columns (GE Healthcare) and 1.5 mL containing 120 µM TrxA or 65 µM TrxD was used for immunization of New Zealand white rabbits (3 – 3.5 kg). In the first immunization 500 µL of the antigen was mixed with 500 µL of the complete Freund's adjuvant and the solution was injected subcutaneously on five different spots on the back (0.2 mL/spot). The second and third boosters (given in two-week intervals) were performed similarly but using the incomplete Freund's adjuvant instead. Blood sera containing anti-TrxA or anti-TrxD primary antibodies were collected one week after the third booster and stored at -80°C.

2.3.5 Western blot analysis

Synchronized cultures of *L. lactis* wt, Δ*trxA* and Δ*trxD* strains were grown under static conditions in liquid GSAL medium at 30°C. From a total culture volume of 100 mL, 40 mL was harvested in the middle exponential phase (EP; OD_{450} = 0.4) and in the stationary phase (SP; $OD_{450} \approx 2$), respectively. The cell metabolism was quenched by pouring culture samples into pre-chilled flasks on ice and incubating for 15 min. Cultures were then centrifuged 10 min at 5000 g at 4˚C, and supernatants were removed. Pellets were washed by 1 mL of an ice-cold sterile 0.9% (w/v) NaCl solution, transferred into Eppendorf tubes and centrifuged again. Supernatants were discarded and pellets were stored at -20˚C until extraction. Frozen pellets were dried in SpeedVac

SPD1010 (Thermo Scientific) for 1–2 hours. Then 100 µL and 300 µL of glass beads ≤ 106 µm (Sigma) was added to the dry pellets from EP and SP cultures, respectively, followed by homogenization by aid of a micropestle (Eppendorf). Extraction buffer (0.2 M Tris/HCl, 0.2 M NaCl, 5% glycerol, 1 mM EDTA, pH 7.6) was added to obtain a final volume of 200 and 900 µL for the EP and SP samples, respectively. Following centrifugation (15 min at 14000 rpm, 4˚C) supernatants were collected and protein concentration was determined (Coomassie® plus protein assay reagent kit; Pierce Biotechnology) with BSA as standard. SDS-PAGE was performed with 25 µg of total protein from each cell extract and positive controls with 200 ng and 100 ng of His_6-tagged TrxA and TrxD, respectively. Western blotting was performed using a X-Cell II™ Blot Module (Invitrogen) and Amersham Hybond™ ECL™ nitrocellulose membrane (GE Healthcare). Membranes were incubated with non-purified rabbit sera containing primary anti-TrxA and anti-TrxD antibodies (see above) diluted 1:2000 in TBS buffer (100 mM Tris/HCl pH = 7.5, 150 mM NaCl) containing 0.1% Tween-20 for 1 h at RT. After several washes in TBS + Tween-20, buffer alkaline phosphatase conjugated polyclonal goat anti-rabbit IgG (c = 0.64 mg/ml; Dako) diluted 1:2000 in TBS was added and incubated 30 min. The membrane was again washed in the same buffer as previously followed by incubation for 10 min in 0.015 % (w/v) 5-bromo-4-chloro-3-indolyl phosphate and 0.030% (w/v) nitro blue tetrazolium chloride in 100 mM NaCl, 5 mM $MgCl_2$, 100 mM Tris/HCl pH 9.5 at RT. Reactions were stopped by transferring the membrane into 20 mM EDTA.

2.3.6 Tetrazolium salt reduction assay

L. lactis wt, Δ*trxA* and Δ*trxD* strains were examined for their ability to reduce tetrazolium salts in mid-EP and SP. Samples of synchronized cultures (0.9 mL) grown under static conditions at

30°C were collected in the middle EP (OD_{450} = 0.4) and in SP (OD_{450} ≈ 2), mixed with 100 µL of 5 mM tetrazolium violet (TV) or iodonitrotetrazolium chloride (INT) and incubated 15 min at RT in the dark. Samples were centrifuged (20000 g, 15 min, RT) and supernatants discarded. Pellets were resuspended in 1 mL DMSO and centrifuged again (20000 g, 15 min, RT). The absorbances at 510 nm (reduced TV) and 468 nm (reduced INT) in the supernatants were determined and divided by the OD_{450} values of the cultures at the harvesting points.

2.3.7 Difference gel electrophoresis (DIGE)

Synchronized cultures of *L. lactis* wt, Δ*trxA* and Δ*trxD* strains were grown in GSAL medium under static conditions at 30°C and samples were harvested in the middle EP (OD_{450} = 0.4). Cell pellets from 80 mL cultures washed in 0.9% NaCl were freeze-dried (Scanvac CoolSafe™ instrument; LaboGene) for 2 h. Thereafter 500 µL extraction buffer (0.2 M Tris/HCl, 0.2 M NaCl, 5% glycerol, 1 mM EDTA, pH 7.6) and 500 µL of glass beads ≤ 106 µm were added and cells were disrupted by 3 cycles in FastPrep® FP120 homogenizer (Qbiogene) set up at speed 4 and time 45 s (samples were kept for 2 min on ice between the cycles). The extracts were centrifuged (15 min at 14000 rpm at 4˚C), supernatants were collected, treated by Benzonase® (0.25 U/µL of extract) and proteins concentrations were determined (Coomassie® plus protein assay reagent kit; Pierce Biotechnology) with BSA as standard. The experiment was designed to compare four biological replicates each of *L. lactis* wt, Δ*trxA* and Δ*trxD* (see Table 1). For each replicate of these strains, 30 µg protein was precipitated by chloroform/methanol extraction (Wessel & Flügge, 1984). Pellets were dissolved in 105 µL rehydration buffer (7 M urea, 2 M thiourea, 10 mM Tris pH 8.5, 4% CHAPS) and 70 µL of each sample was labeled with 100 pmol (1 µL of 100 µM) of either the fluorescent dye Cy3 or Cy5 (CyDye DIGE Fluor; GE Healthcare)

194 in N,N-dimethylformamide. In addition, an internal standard containing 35 µL from each sample
195 was labelled with 600 pmol (6 µL of 100 µM) Cy2 dye (CyDye DIGE Fluor; GE Healthcare) in
196 N,N-dimethylformamide. Fluorophore labeling was carried out on ice in the dark for 30 min
197 followed by addition of 2 µL lysine (100 mg/mL) and incubation 10 min on ice in the dark.
198 Samples were mixed according to Table 1, 6 µL of 100 mg/mL DTT and 1 µL IPG buffer pH 4–7
199 (GE Healthcare) was added and isoelectric focusing with Immobiline™ DryStrip pH 4–7 11 cm
200 strips (GE Healthcare) was performed according to the following program: 6 h 30 V, 6 h 60 V, 1
201 h 200 V, 1 h 500 V, 1 h 1000 V, 1 h gradient from 1000 V to 8000 V followed by constant 8000
202 V until 20000 Vhrs. Prior to the second dimension, strips were incubated 15 min with
203 equilibration buffer (6 M urea, 30% v/v glycerol, 0.01% bromophenol blue, 2% w/v SDS, 100
204 mg/mL DTT, 50 mM Tris/HCl pH 8.8) and additional 15 min with the same buffer containing
205 iodoacetamide (250 mg/mL) instead of DTT. The second dimension was performed using
206 Criterion™ Precast 12.5% polyacrylamide gels (BioRad). Gels were fixed 30 min in 30% v/v
207 ethanol, 2% v/v phosphoric acid), scanned by Typhoon™ Trio (GE Healthcare) and stained by
208 Coomassie brilliant blue G-250 (Merck) as described previously (Candiano *et al.*, 2004).
209 Fluorescent images were analyzed by Progenesis SameSpots software (Nonlinear Dynamics).
210 Only spots displaying volume fold change > 1.5 and ANOVA p-value < 0.05 were selected for
211 identification by mass spectrometry.

212

213 **2.3.8 2D gel electrophoresis of [^{35}S]-L-methionine labeled proteins**

214 Serial dilutions (10^2, 10^3, 10^4, 10^5, 10^6) of *L. lactis* wt and Δ*trxD* strains were grown in GSAL
215 medium with reduced methionine concentration at 30°C overnight (20 µg/mL). The dilution with
216 exponentially growing cells was equilibrated in GSAL medium with further reduced methionine

concentration (5 µg/mL) and incubated under static conditions at 30°C until the middle EP (OD_{450} = 0.4) when sodium arsenate was added to a final concentration of 100 µM. Samples were labeled 60 min after arsenate exposure (**As**) and non-arsenate treated controls (**Ctrl**) were labeled at the same OD_{450} as the **As** sample. [^{35}S]-L-methionine labeling was performed essentially as previously described (Kilstrup *et al.*, 1997). Briefly, 150 µL of culture was mixed with 1.5 µL [^{35}S]-L-methionine (Hartmann Analytic GmbH) corresponding to radioactivity of 15 µCi (1000 Ci/mmol) and incubated 10 min in an Eppendorf tube equilibrated at 30°C. Then 13 µL of non-radioactive methionine was added and incubation continued 2 min, after which 10 µL chloramphenicol (20 mg/mL) was added. The sample was transferred to an ice-bath and centrifuged for 5 min at 20000 g and 4°C. The supernatant was discarded and the pellet was washed twice in 100 µL 0.9% NaCl, 30% ethanol and stored at -80°C until analysis. Cell pellets were freeze-dried by Scanvac CoolSafe™ instrument for 1 h. A small amount of glass beads ≤106 µm (10–20 µL) was added to each frozen pellet. The samples were ground by a melted Pasteur pipette for 5 min and added 20 µL extraction buffer (50 mM Tris/HCl 7.6, 50 mM NaCl, 0.25 mM EDTA, 1.25% glycerol, 0.3% DTT, 0.25U/µl benzonase, 15 mM $MgCl_2$) followed by incubation for 15 min at 37°C, and added 80 µL rehydration buffer containing 0.3% DTT and centrifuged (15 min at 20000 g at 4°C). Supernatants (85–90 µL) were mixed with an appropriate volume of rehydration buffer containing 0.3% DTT to a final volume of 200 µL, 1 µL IPG buffer pH = 4–7 was added and 2D gel electrophoresis was performed as described for DIGE above. Gels were fixed 30 min, incubated 30 min in a preservation solution (25% v/v ethanol, 10% v/v glycerol) and dried at RT for three days between Porous Cellophane sheets fixed in Gel Frames (GE Healthcare). Dried gels were cut out of the frames, exposed to Storage Phosphor Screens (GE Healthcare) for 18 days and scanned by Typhoon Trio scanner (GE Healthcare) at 50 µm

resolution. In parallel, 5 mL samples harvested at the same time points at the [^{35}S]-L-methionine labeled samples were processed as described above except labeling was omitted and protein concentrations were determined by 2DQuant kit (GE Healthcare) prior to 2D gel electrophoresis. The 2D gels for the ΔtrxD mutant (161 µg of total protein) and the wt strain (68 µg of total protein) exposed to arsenate, and the non-stressed wt strain (86 µg of total protein) were stained by Coomassie as described above, scanned by ScanMaker 9800XL in a transparent mode in 16-bit greyscale and 300 dpi resolution and kept in MilliQ water at 4°C. Two to four biological replicates per condition were used in the final image analysis. The radioactive images of 2D gels were processed by Progenesis SameSpots. The spot measurements were exported to MS Excel and normalization was performed manually. Normalized volume was defined as percentage of a given spot volume relative to the sum of all spot volumes within the gel. These values were used for calculation of means and variances, which were used as input for Welch's t-test, an adaptation of student's t-test for samples showing different variances and different number of replicates (Welch, 1947). Differences in spot volumes that corresponded to fold change > 1.5 and passed Welch's t-test (p-value under 0.05) were considered as significant.

2.3.9 In-gel trypsin digestion and MALDI-TOF MS analysis

Spot gel-plugs were manually picked from Coomassie stained gels and subjected to in-gel trypsin digestion as described previously (Majumder *et al.*, 2011). Briefly, the gel-plugs were washed by 40% ethanol, dried by 100% acetonitrile (ACN) and digested by 25 ng/µL porcine trypsin (Promega) in 10 µL 10 mM NH_4HCO_3 overnight at 37°C. 1 or 2 µL samples were loaded on an AnchorChip target plate (Bruker Daltonics) together with 1 µL of 0.5 µg/µL matrix solution (α-cyano-4-hydroxycinnamic acid (CHCA) in 70% ACN, 0.1% trifluoroacetic acid (TFA)). In some

cases, samples were desalted and concentrated by using a POROS R2 (Applied Biosystems) microcolumn prior to analysis. Samples were analyzed using an Ultraflex II MALDI-TOF/TOF MS instrument (Bruker Daltonics), spectra were processed by FlexAnalysis (v3.3) and BioTools (v3.2) software provided by the instrument manufacturer. Combination of MS and MS/MS data were used as input for databases searching for the spectra from MALDI-TOF-TOF using Mascot (www.matrixscience.com) with following setup: NCBInr database, trypsin digestion (1 partial cleavage), carbamidomethylation of Cys (global modification), oxidation of Met (variable modification), MS and MS/MS mass tolerance 80 ppm and 0.6 Da, respectively. Alternatively, the trypsin digests were analyzed on an LC-MS system composed to an EASY nLC 1000 chromatograph coupled on-line to a Q-Exactive MS (Thermo Scientific) and spectra were processed using Proteome Discoverer (Thermo Scientific). The setup of the Mascot database searching for LC/MS data was following: SwissProt database, trypsin digestion (1 partial cleavage), carbamidomethylation of Cys (global modification), oxidation of Met (variable modification), peptide and fragment mass tolerance 10 and 20 ppm, respectively. The significance threshold for protein identifications was $p < 0.05$.

2.4 Results and Discussion

2.4.1 Detection of TrxA and TrxD in *L. lactis* and construction of Δ*trxA*, Δ*trxD* and Δ*trxA*Δ*trxD* mutants

L. lactis MG1363 contains two putative thioredoxins, encoded by *trxA* and *trxD* (annotated as *trxH*). Expression of the genes was confirmed by western blot analysis, which further demonstrated that TrxA and TrxD were present in mid EP as well as in SP (Fig. 1, lanes 1 and 2). Deletions of *trxA* and *trxD* by overlap extension were constructed by PCR, followed by

286 homologous recombination into the chromosome, as verified by colony PCR (data not shown).
287 The identities of TrxA and TrxD detected in the Western blots were confirmed by the absence of
288 signal in protein extracts from Δ*trxA* and Δ*trxD* mutants, respectively using the appropriate
289 antibodies (Fig. 1). The growth of the wt strain and the *trx* mutants in chemically defined GSAL
290 medium under microaerophilic conditions was compared in the Bioscreen assay (Fig.2A; Tables
291 2 and 3). The Δ*trxA* mutant showed clear growth defects while the Δ*trxD* mutant was unaffected.
292 The *trxAtrxD* double mutant grew slower than the Δ*trxA* mutants. These results suggest that TrxA
293 can compensate for the loss of TrxD, but not *vice versa*.

294

295 **2.4.2 TrxA is important for oxidative stress resistance**

296 The *L. lactis* wt strain and the *trx* mutants were exposed to the oxidizing reagents hydrogen
297 peroxide, diamide and paraquat. In the presences of hydrogen peroxide (313 µM) the growth
298 rates of the strains were nearly the same as for the non-stressed cultures, but the lag phases before
299 reaching maximal growth rate were prolonged by 5 h for the wild type and Δ*trxD* mutant, and 30
300 h for the Δ*trxA* mutant (Fig. 2B). The Δ*trxA*Δ*trxD* mutant did not recover within 24 h after
301 addition of hydrogen peroxide. A similar pattern was observed upon exposure to the thiol specific
302 oxidant diamide. Thus wt and the Δ*trxD* mutant were affected almost identically by 1.25 mM
303 diamide while the Δ*trxA* mutant was more sensitive and the Δ*trxA*Δ*trxD* mutant did not recover
304 within 24 h (Tables 2 and 3). Surprisingly, concentrations of the superoxide producing reagent
305 paraquat < 1 mM exhibited no effect on the growth of wt, and the Δ*trxA* and Δ*trxD* mutants, but
306 had a positive effect on the growth of the Δ*trxA*Δ*trxD* mutant. At higher concentrations of
307 paraquat (5–20 mM), the Δ*trxA* mutant was affected to a higher extent than the wt and Δ*trxD*
308 cultures, and the Δ*trxA*Δ*trxD* mutant was the most severely affected (Tables 2 and 3). Thus,

overall TrxA appears to be the major thioredoxin involved in oxidative stress resistance in *L. lactis.*

2.4.3 Arsenate and tellurite-stress resistance is dependent upon TrxD

Exposure to sodium arsenate and potassium tellurite were the only stress conditions where the Δ*trxD* mutant had a phenotype that was clearly distinguishable from the wt. Arsenate-stressed (1.25 mM) and unstressed wt, Δ*trxA,* and Δ*trxD* cultures had similar growth rates but the lag phases of arsenate-treated cultures were prolonged by 3 h, 5 h and 9 h, respectively (Fig. 2AC). The Δ*trxA*Δ*trxD* mutant did not recover from arsenate-stress suggesting that at least one Trx is required for survival under arsenate-stress. Sensitivity to arsenate stress was also probed by aliquoting serially diluted cultures on GSAL agar plates containing arsenate and incubating at 30°C for 24h. (Fig. 2D). Whereas growth could be detected in a spot of 10^3-fold diluted cultures of both wt and the Δ*trxA* mutant in the presence of arsenate, no growth could be detected for the *trxD* mutant in spots of 10^2-fold diluted cultures. Arsenate is a toxic analog of phosphate and is reduced to arsenite(III) by arsenate reductase (ArsC) and exported out of the cell (Turner *et al.*, 1992). ArsC is grouped into four classes that are dependent on Trx, glutaredoxin, trypanothione and mycothiol, respectively, as electron donor. The amino-acid sequence of *L. lactis* ArsC is very similar to the Trx-dependent ArsC of *B. subtilis* (Li *et al.*, 2007) and *S. aureus* (Ji *et al.*, 1994). Although no direct evidence was obtained, the increased sensitivity to arsenate induced by the *trx* deletion mutants suggests that ArsC in *L. lactis* may be dependent on TrxD and TrxA as electron donors.

Addition of potassium tellurite prolonged the lag phase of the Δ*trxA* mutant more than the wt (Table 2). The Δ*trxD* mutant never recovered to reach its unstressed exponential growth rate following tellurite-stress, showing that TrxD is important for fast growth under these conditions (Table 3). Tests with agar plates containing tellurite indicated similar sensitivity of the Δ*trxD* and Δ*trxA* mutants (Fig. 2D). Tellurite causes intracellular production of superoxide (Pérez *et al.*, 2007), and is correlated with arsenate detoxification in *E. coli*, where the presence of a plasmid conferring arsenate resistance concomitantly increased the survival when exposed to tellurite (Turner *et al.*, 1992). Tellurite-resistant *L. lactis* strains were found to contain mutations in *e.g.* high-affinity phosphate (particularly *pstA* and *pstD*) and iron transporters (*mntH*), and in *trmA*, a homolog of the disulfide stress sensor *spx* (Turner *et al.*, 2007).

2.4.4 The influence of metal ions and formaldehyde on the growth of the *trx* mutants

A number of metal ions were added to probe their influence on the growth of the *trx* mutants. Cadmium was found to be extremely toxic even at 5 µM. (Table S2). The wt and the Δ*trxD* mutant were barely able to grow exponentially under these conditions. The Δ*trxA* mutant apparently remained in the lag phase while no apparent growth of the Δ*trxA*Δ*trxD* mutant was observed. When exposed to 313 µM zinc all strains were significantly inhibited and no growth was observed at 1.25 mM (Table S2). As observed for paraquat, sub-lethal concentrations (5 µM) of zinc had a slightly positive effect on the growth rate of Δ*trxA*Δ*trxD* double mutant. Zinc (Zn^{2+}) has been suggested to have a thiol-protective function since strains with impaired Zn-uptake were hypersensitive to oxidative stress (Scott *et al.*, 2000). Addition of iron in the range of concentrations tested (5–1250 µM) had only minor effects on the growth of Δ*trxA*, Δ*trxD*, Δ*trxA*Δ*trxD* mutants and wt (Table S2). Copper was found to be more toxic than iron causing

complete growth inhibition at 313 µM for Δ*trxA,* Δ*trxD* strains and wt, and at 78 µM for the Δ*trxA*Δ*trxD* mutant.

No significant difference between the effects on growth of Δ*trxA,* Δ*trxD,* and wt strains was observed upon exposure to formaldehyde (80–5000 µM). The Δ*trxA*Δ*trxD* mutant however was severely inhibited compared to the wt and the Δ*trxA* and Δ*trxD* mutants under these conditions. Formaldehyde is a reactive electrophilic species and has been shown to interact with thiol-based redox sensors and induce a disulfide stress response including up-regulation of e.g. Trx and NTR (Antelmann & Helmann, 2011; Nguyen *et al.*, 2009).

2.4.5 Methionine sulfoxide reduction is dependent on TrxA

The capacity of the *L. lactis trx* mutants to reduce oxidized methionine was tested in the Bioscreen assay using a medium where methionine was replaced by methionine sulfoxide (MetSO). *L. lactis* is auxotrophic for methionine (Jensen & Hammer, 1993; Seefeldt & Weimer, 2000), and the utilization of MetSO is therefore dependent upon disulfide reductase-coupled MetSO reductase (Msr) activity. When MetSO was supplied as the sole source of methionine, no significant difference was observed for the growth of the wt and Δ*trxD* mutant (Tables 2 and 3). However, both the Δ*trxA* and Δ*trxA*Δ*trxD* mutants exhibited significantly prolonged lag phases and reduced growth rates (reduced by 70±6% and 57±12%, respectively; Tables 2 and 3). Thus it is proposed that TrxA functions as an electron donor for Msr in *L. lactis*. However, since all the *trx* mutants were viable it may be suggested that *L. lactis* also can utilize an alternative Trx-independent MetSO reduction pathway. Oxidation of methionine to MetSO results in a racemic

mixture of (S)- and (R)-enantiomers that are reduced by two separate methionine sulfoxide reductases, MsrA and MsrB, respectively (Boschi-Muller *et al.*, 2008). However, certain bacteria such as *Neisseria gonorrhoeae* have a bifunctional protein PilB containing both MsrA and MsrB domains (Brot *et al.*, 2006). In *E. coli,* MsrA effectively reduces both bound and free Me-(S)-SO while MsrB reduce only peptide- or protein-bound Met-(R)-SO (Grimaud *et al.*, 2001). A novel Trx-dependent Met-(R)-SO reductase was discovered in *E. coli* when a strain lacking the *msrB* gene was found to utilize free Met-(R)-SO (Lin *et al.*, 2007). MsrA-independent reduction of free Met-(S)-SO is catalyzed in a Trx-independent manner by BisC in *E. coli* (Ezraty *et al.*, 2005). The genome of *L. lactis* contains genes encoding putative MsrA, MsrB and free methionine -(R)-sulfoxide reductase (*llmg_2480*) enzymes, but no BisC homologues.

2.4.6 Influence of *trx* mutants on reduction of tetrazolium salts

The ability of the *L. lactis* Δ*trxA* and Δ*trxD* mutants to reduce tetrazolium violet (TV) and *p*-iodonitrotetrazolium chloride (INT) were investigated (Fig. 3). These tetrazolium salts are colourless and water soluble compounds, that turn into coloured water-insoluble formazans upon reduction and can be monitored spectrophotometrically (Tachon *et al.*, 2009). Overall, the extent of INT and TV reduction was similar in wt and the Δ*trxD* mutant. On the other hand the Δ*trxA* mutant exhibited significantly increased reduction of INT in mid-EP compared to the wt. Both TV and INT were reduced significantly more efficiently by the Δ*trxA* mutant in SP, but TV reduction during exponential growth was similar for wt and the Δ*trxA* mutant. It is noteworthy that the tetrazolium reduction was 5 to 10-fold higher in mid-exponential phase than in stationary phase for the three strains. The increased INT and TV reduction by the Δ*trxA* mutant suggests that the overall cellular redox state in this strain is altered compared to the wt. From studies in *E.*

399 *coli* INT was suggested to be reduced by intracellular redox reactions (Smith & McFeters, 1996).
400 Reduction of TV is proposed to involve components in the electron transport chain of *L. lactis*,
401 particularly the membrane bound NADH dehydrogenases NoxAB and membrane embedded
402 menaquinones (Tachon *et al.*, 2009).

403

404 **2.4.7 Proteome profiles of thioredoxin null mutants during normal growth**

405 Protein profiles of wt, Δ*trxA* and Δ*trxD* mutants were analyzed in mid-EP phase under standard
406 (non-stressed) conditions. When the proteomes of the three strains were compared using
407 difference gel electrophoresis (DIGE), most differences were observed between the Δ*trxA* mutant
408 and wt (Fig. 4; Table 4). Several proteins involved in the oxidative stress response were up-
409 regulated in the Δ*trxA* mutant compared to the wt, including thioredoxin reductase (TrxB) and a
410 homolog of glutathione peroxidase (Gpo) (Table 4). TrxB has previously been observed to be
411 slightly up-regulated under respiratory conditions in *L. lactis* (Vido *et al.*, 2004). Gpo is most
412 probably Trx-dependent as demonstrated for homologous proteins from plants, fungi and bacteria
413 (Lee *et al.*, 2008). The pyruvate dehydrogenase E1 (PdhB) was likewise up-regulated in the
414 Δ*trxA* mutant. This protein has been observed to be up-regulated under respiratory conditions as
415 well as in a *trxB1* mutant of *L. lactis* (Vido *et al.*, 2004, 2005). Two hypothetical proteins
416 (Llmg_1475 and Llmg_2273) were also up-regulated in the Δ*trxA* mutant. Llmg_1475 was the
417 most up-regulated protein in Δ*trxA* vs wt (3.7-fold; Table 4). Llmg_1475 has not been linked to
418 stress responses in *L. lactis*, but a homologous protein in *B. subtilis* called YnzC (41% identity,
419 57.5% similarity) was previously suggested to be involved in the SOS DNA damage response
420 and was up-regulated upon H_2O_2 treatment in *Bacillus licheniformis* (Kawai *et al.*, 2003;
421 Schroeter *et al.*, 2011). The hypothetical protein llmg_2273 contains a histidine triad morif and

was annotated as a diadenosine tetraphosphate hydrolase. No bacterial homologue of Llmg_2273 has been characterized, but eukaryotic proteins containing histidine triad motifs influence the cell cycle through interactions with regulatory proteins such as MDM2 (Huebner *et al.*, 2011; Nishizaki *et al.*, 2004), and is associated with oxidative stress defence and DNA repair. Interestingly, Llmg_2273 was found to be down-regulated in both wt and Δ*trxD* mutant exposed to sodium arsenate (see below). The proteins in some spots displaying increased intensity in the Δ*trxA* mutant could not be unambiguously identified. For example 30S ribosomal protein S4 was identified in the same spot as nitroreductase and dihydrolipoamide dehydrogenase (PdhD) was identified in the same spot as pyruvate kinase (Pyk).

Down-regulated proteins in the Δ*trxA* mutant compared to the wt include pyruvate kinase (Pyk), formate-tetrahydrofolate ligase (Fhs), tyrosyl-tRNA synthetase (TyrS), as well as a putative tellurium resistance protein TelB, and a hypothetical protein llmg_0304 annotated as a potential RNA-binding protein (DUF1447 superfamily). It is noteworthy, that Fhs was overexpressed in *L. lactis* when growing under respiratory conditions, and highly overexpressed in *Porphyromonas gingivalis*, a Gram-negative bacterium living in the mouth cavity, at microaerophilic vs. anaerobic conditions (Lewis *et al.*, 2009; Vido *et al.*, 2004). Pyk was also observed in a spot together with aspartyl/glutamyl-tRNA amidotransferase (GatB), significantly down-regulated only when the Δ*trxA* mutant was compared to the Δ*trxD* mutant. The most down-regulated protein (2-fold) was a putative tellurium resistance protein (*telB*). Comparison to a partially characterized *E. coli* tellurium resistance determinant TelB (Walter *et al.*, 1991) showed only 9% sequence identity. However, *L. lactis* TelB exhibits around 50–55% identity with TerD homologs in *E. coli*, *Klebsiella pneumoniae*, *Yersinia pestis* and *Streptomyces coelicolor*.

2.4.8 Proteomic analysis of arsenate stress in *L. lactis*

Response to sodium arsenate was further analyzed by proteome analysis since this compound provided the most significant growth retardation phenotype of Δ*trxD* compared to wt. [^{35}S]-L-methionine was applied to exponentially growing cells after addition of arsenate (100 µM) to label *de novo* synthesized proteins and determine individual proteins synthesis rates. Samples were collected after 60 min of arsenate exposure. At the same time point samples were taken from non-stressed cultures growing at comparable OD_{450} as a control for growth phase effects (Fig. 5). Proteins were extracted, separated by 2D gel electrophoresis and radioactivity in the gel spots was quantified to compare protein synthesis rates in wt and the Δ*trxD* mutants. The relative signal intensity in four and six protein spots were significantly changed in the wt strain and the Δ*trxD* mutant, respectively upon arsenate stress (Table 5). The hypothetical protein Llmg_2273 was down-regulated in both wild type and Δ*trxD* mutant. As stated above this protein shows similarity to proteins involved in diadenosine tetraphosphate hydrolysis or RNA processing. In the wt, down-regulation was observed for ribonucleotide reductase (NrdEF) and a cell division initiation protein (DivIVA; Llmg_0769), while RNA polymerase (RpoA) was up-regulated during arsenate stress. NrdEF functions under aerobic conditions and accepts electrons from NTR *via* the specialized NrdH redox mediator protein (Jordan *et al.*, 1996). DivIVA is suggested to have various functions related to cell division in Gram-positive bacteria and was shown to be a substrate of the protein kinase StkP that controls growth and cell division in *Streptococcus pneumoniae* (Beilharz *et al.*, 2012; Kaval & Halbedel, 2012). Down-regulated proteins in the Δ*trxD* mutant upon arsenate stress include translation elongation factor (Ef-G) and glucose-1-phosphate thymidylyltransferase (RmlA). Lower signal intensities were also observed in two

spots that each contained AtpD protein, β subunit of the proton pumping ATP synthase, and either enolase or dipeptidase PepV. Only serine hydroxymethyltransferase (GlyA) was found to be up-regulated in Δ*trxD*.

Eight spots were up-regulated and seven spots down-regulated in the Δ*trxD* mutant when the protein synthesis rates of the arsenate stressed cultures were compared to the wt subjected to the same conditions (Table 5). Three of the up-regulated proteins are involved in nucleotide biosynthesis; GuaB (IMP dehydrogenase), Fhs (formate-tetrahydrofolate ligase), and GlyA (serine hydroxymethyltransferase). Among the up-regulated proteins in in the Δ*trxD* mutant were also PfkA (phosphofructokinase), MenB (naphthoate synthase), and a hypothetical protein (Llmg_1773). PfkA is a key glycolytic enzyme and has been shown to be involved in mRNA processing (Commichau *et al.*, 2009; Roux *et al.*, 2011). MenB is an enzyme involved in biosynthesis of menaquinone and was shown previously to be upregulated in *L. lactis trxB1* mutant (Vido *et al.*, 2005). Llmg_1773 is a CsbD-like bacterial stress protein and the gene was previously observed to be 3-fold and 11-fold up-regulated under aerobic conditions with and without heme in *L. lactis* respectively compared to static conditions (Pedersen *et al.*, 2008). CsbD of *B. subtilis* interacts with the alternative stress sigma factor, σ_B, and has been observed to be up-regulated during phosphate starvation (Prágai & Harwood, 2002). Down-regulated proteins in the Δ*trxD* mutant included Ef-G, Ef-Ts, RpoA, GroEL, and DnaK. Elongation factors in various organisms are often multifunctional and exhibit redox properties that are important for their regulation. Ef-G in *E. coli* is inactivated by oxidative stress and can be reactivated by Trx (Nagano *et al.*, 2012). The pattern of up-regulated proteins in nucleotide metabolism and down-

490 regulation of translation elongation factors is reminiscent of the pattern observed during purine
491 starvation in *L. lactis* (Beyer *et al.*, 2003).

492

493 **2.5 Conclusions**

494 The observed phenotypes of the *trx* mutants suggest that the two thioredoxins have different
495 functions in stress resistance in *L. lactis*. TrxA seems to be involved in responses to oxidative
496 stress while TrxD appears to be important for resistance towards arsenate and tellurite. The role
497 of TrxD in these processes is unknown but it is speculated that TrxD may act as an alternative
498 electron donor for arsenate reductase, an established Trx-target in *B. subtilis*. Even though both
499 TrxA and TrxD appear to be important for stress resistance, the strain lacking both Trx is viable,
500 suggesting the presence of an alternative thiol redox system in *L. lactis*.

501

502 **2.6 Acknowledgements**

503 Marzanna Pulka-Amin is acknowledged for technical assistance. The work was supported by the
504 Danish Council for Technology and Production Sciences (FTP, grant nr 274-08-0413) and the
505 Carlsberg Foundation. The PhD grant to PE was in part financed by the Technical University of
506 Denmark.

507

2.7 Tables

Table 1. DIGE experimental setup

	Cy3	**Cy5**	**Cy2**
gel 1	wt	ΔtrxD	IS
gel 2	ΔtrxA	wt	IS
gel 3	ΔtrxD	ΔtrxA	IS
gel 4	wt	ΔtrxD	IS
gel 5	ΔtrxA	wt	IS
gel 6	ΔtrxD	ΔtrxA	IS

Table 2. Selected results of the Bioscreen assay with wt and the *ΔtrxA* strains exposed to a range of stress compounds. Standard deviations are calculated based on three biological replicates.

		wild type				***ΔtrxA***					
		relative μ*		**lag phase**		**relative μ***			**lag phase**		
Compound	**c [μM]**	**% ctrl†**		**[h]**		**% ctrl†**		**% WT‡**	**[h]**		
Control	NA	100	± 3.9	3	± 1	100	± 2.8	72	4	±	1
Methionine sulfoxide	NA	96	± 3.3	4	± 1	30	± 5.6	22	12	±	3
Hydrogen peroxide	313	95	± 9.8	8	± 2	94	± 10.4	71	>24		
Sodium arsenate	1250	92	± 1.6	6	± 1	94	± 3.7	73	9	±	2
Potassium tellurite	1250	49	± 2.5	4	± 2	53	± 4.2	78	7	±	2
Diamide	1250	81	± 11.0	8	± 4	61	± 55.1	54	18	±	2
Paraquat	20000	61	± 10.1	8	± 3	29	± 30.9	35	11	±	1

* Relative growth rates (**μ**) of strains exposed to stress conditions were calculated as a percentage of the growth rate for the non-stressed control of the same strain (**†**) or a percentage of the growth rate for the wt exposed to the same stress condition (**‡**); 100% (wt) $\mu = 0.506\ h^{-1}$ and 100% (*ΔtrxA*) $\mu = 0.365\ h^{-1}$.

Table 3. Selected results of the Bioscreen assay with *ΔtrxD* and *ΔtrxAΔtrxD* strains. Standard deviations are based on three biological replicates.

		ΔtrxD			***ΔtrxAΔtrxD***		
		relative μ*		**lag phase**	**relative μ***		**lag phase**
Compound	**c [μM]**	**% ctrl†**	**% WT‡**	**[h]**	**% ctrl†**	**% WT‡**	**[h]**
Control	NA	100 ± 2.9	95	3 ± 1	100 ± 30.5	33	8 ± 1
Methionine sulfoxide	NA	95 ± 8.5	97	4 ± 1	57 ± 12.0	18	24 ± 5
Hydrogen peroxide	313	94 ± 7.9	94	9 ± 1	<10	NA	>24
Sodium arsenate	1250	90 ± 6.4	93	12 ± 1	<10	NA	>24
Potassium tellurite	1250	33 ± 1.4	64	4 ± 1	14 ± 0.9	10	>24
Diamide	1250	78 ± 11.9	91	9 ± 4	<10	NA	>24
Paraquat	20000	62 ± 6.1	96	10 ± 2	12 ± 2.1	7	>24

* Relative growth rates (**μ**) of strains exposed to stress conditions were calculated as a percentage of the growth rate for the non-stressed control of the same strain (**†**) or a percentage of the growth rate for the wt exposed to the same stress condition (**‡**); 100% (*ΔtrxD*) μ = 0.479 h^{-1} and 100% (*ΔtrxAΔtrxD*) μ = 0.167 h^{-1}.

Table 4. Up- and down regulated proteins identified by DIGE of non-stressed *trx* mutants vs. wt in mid-exponential phase.

Protein name	Fold*	pI/Mr [kDa]¤	Gene	Accession	p-value†	Score	SC¶	M#	F‡	Peptide sequences identifed by MS/MS	G$
hypothetical protein	+3.7	5.6/9.2	*llmg_1475*	gi|125624282	0.0002	87	21%	2	1	KAEGLSEAELEEQALLRR	5
dihydrolipoamide dehydrogenase (spot 915)	+2.6	4.9/49.9	*pdhD*	gi|125622950	0.0030	263	58%	19	1	MVVGAQATEVDLVVIGSGPGGYVAAIRA	X
pyruvate kinase (spot 915)	+2.6	5.21/54.3	*pyk*	gi|125623950	0.0030	95	39%	13	1	RFNFSHGDHPEQGARM	X
30S ribosomal protein S4 (spot 558)	+2.3	10.0/23.2	*rpsD*	gi|125623168	0.0002	174	57%	13	2	RNYVPGQHGPNNRS RVQPGQVISVRE	X
putative nitroreductase (spot 558)	+2.3	4.7/22.5	*llmg_2172*	gi|125624942	0.0002	153	50%	11	1	KAAMEAQGVPESAWDNTRA	X
gluthatione peroxidase	+2.1	5.2/18.1	*gpo*	gi|125623919	0.0002	84	28%	6	1	KFLIDRDGQVIERF	1
30S ribosomal protein S5	+1.7	10.2/17.6	*rpsE*	gi|125625124	0.0030	204	56%	11	3	RFAALVVVGDRN KAQEVPEAIRKA KSLGSNTPINVVRA	3
pyruvate dehydrogenase E1 component beta subunit	+1.6	4.8/35.1	*pdhB*	gi|125622952	0.0003	292	63%	19	2	KDKDALIFGEDVGQNGGVFRA RVVVVQEAQRT	2
TrxB1 protein	+1.5	4.8/34	*trxB1*	gi|125624390	0.0008	156	18%	4	1	RNQEILVIGGGDSAVEEALYLTRF	1
hypothetical protein	+1.5	5.4/14.9	*llmg_2273*	gi|125625038	0.0030	114	49%	5	1	KFTAHDYDLAEIAKQ	5
formate-tetrahydrofolate ligase	−1.6	5.7/59.7	*fhs*	gi|125623054	0.0050	615	53%	34	3	KSTVTVGLADAFARQ ; RIVIAQNYDRK; KTQYSFSDQANLLAAPEGFEVTVRE	4
pyruvate kinase	−1.6	5.2/54.3	*pyk*	gi|125623950	0.0050	465	53%	26	3	KIVSTLGPAVEIRG RTELFTDGADSISVVTGDKFRV KLIVALTESGNTARL	2
tyrosyl-tRNA synthetase	−1.6	5.38/47.3	*tyrS*	gi|125624396	0.0090	323	37%	16	2	KTSEILFGGGDLRQ RVQELDYVLTDSDKIENRL	3
pyruvate kinase	−1.6	5.2/54.3	*pyk*	gi|125623950	0.0060	335	57%	31	2	KLIVALTESGNTARL KIPFPALAERDDADIRF	2
hypothetical protein	−1.7	4.5/8.8	*llmg_0304*	gi|125623269	0.0110	236	88%	8	1	RETTDALYLDLDVATKEEGVILARE	5
formate-tetrahydrofolate ligase	−1.7	5.7/59.7	*fhs*	gi|125623950	0.0010	169	28%	15	2	K.STVTVGLADAFARQ RIVIAQNYDRK	4
aspartyl/glutamyl-tRNA amidotransferase subunit B (spot 895)	−1.7"	5.2/53.4	*gatB*	gi|125623950	0.0030	238	53%	26	1	RAHLEEDAGKNTHGTDGYSYVDLNRQ	X
pyruvate kinase (spot 895)	−1.7"	5.2/54.3	*pyk*	gi|125624396	0.0070	214	53%	22	2	RFNFSHGDHPEQGARM KLIVALTESGNTARL	X
putative tellurium resistance protein	−1.9	4.38/21.1	*telB*	gi|125624170	0.0310	241	48%	9	2	KVRNDDDFIFYNHKI RNDDDFIFYNHKI	1

* Ratio *ΔtrxA* vs. wt unless marked differently; ± mark up- and down-regulation, respectively
" Ratio *ΔtrxA* vs. *ΔtrxD*
¤ Calculated values
† ANOVA p-value from the image analysis
¶ Sequence coverage in peptide mass fingerprinting (PMF)
# Number of matched peptides in PMF
‡ Number of peptides fragmented and analyzed by MS/MS
$ Groups: 1 - stress; 2 - carbon metabolism; 3 - translation; 4 - other; X - two proteins in a spot

Table 5. Differential protein expression in wt and the *ΔtrxD* mutant upon treatment by 100 µM sodium arsenate

ΔtrxD versus wild type; both exposed to arsenate (As vs As)										
Protein name	RTR*	pI/Mr [kDa]¤	Gene	Accession	p-value†	Score	SC¶	M#	F‡	Peptide sequences identifed by MS/MS"	G$
phosphopyruvate hydratase (spot 3013)	−3.4	4.7/46.9	*enoA*	gi|125623478	0.0080	708	54%	20	5	SIITDIYAR GNPTLEVEVYTEDGAFGR GMVPSGASTGEHEAVELR AVDNVNNIIAEAIIGYEVTDQQAIDR EAGFTAIVSHR	X
ATP synthase F0F1 subunit beta (spot 3013)	−3.4	5.0/52.7	*atpD*	gi|125624725	0.0080	157	53%	21	0		X
elongation factor G	−2.6	4.8/77.9	*fusA*	gi|125625309	0.0349	424	46%	28	2	EFKVEANVGAPQVAYR VTITVPEENLGDIMGHVTAR	4
dipeptidase PepV (spot 3039)	−2.2	4.7/51.9	*pepV*	gi|116511662	0.0271	110	34%	16	0		X
ATP synthase F0F1 subunit beta (spot 3039)	−2.2	5.0/52.7	*atpD*	gi|125624725	0.0271	107	39%	18	0		X
hypothetical protein llmg_1773	+2.0	5.9/8.6	*llmg_1773*	gi|125624563	0.0128	128	49%	3	1	ASDLAEDVAEKFNDTVDSVK	5
Inosine-5'-monophosphate dehydrogenase	+1.9	52.8	*guaB*	gi|125623107	0.0188	184	9%	10§	10§	KVGIGPGSICTTRV; RKLVGIITNRD; KLVPEGIEGRV; KTIIADGGIKY; LVGIITNRD; RGMGSIAAMKK; GMGSIAAMKK (M)	2
formate-tetrahydrofolate ligase	+1.8	5.7/59.7	*fhs*	gi|125624396	0.0113	270	21%	9	3	STVTVGLADAFAR IVIAQNYDR TQYSFSDQANLLAAPEGFEVTVR	2
DNA-directed RNA polymerase subunit alpha	−1.8	4.9/34.2	*rpoA*	gi|125625115	0.0229	315	26%	14	5	FDESENYGKFVVEPLER GYGTTLGNSLR VNYQVEPAR VLDKIIEEMDFSVR VLDKIIEEMDFSVR (M)	6
elongation factor Ts	−1.7	5.0/36.1	*tsf*	gi|125625187	0.0198	504	50%	17	3	ALVETDGNMEAAAELLR VLVNKPELPHHEYGSK FEVGEGIEKAETDFAAEVEAAK	4
molecular chaperone GroEL	−1.6	4.8/51.2	*groEL*	gi|125623278	0.0398	415	21%	27	2	TNDIAGDGTTTATVLTQAIVR TNRPLLIVADDVDGEALPTLVLNK	3
molecular chaperone DnaK	−1.6	4.6/64.9	*dnaK*	gi|125624376	0.0410	256	37%	16	1	QALSDAGLSTSDIDEVLLVGGSTR	3
naphthoate synthase	+1.6	5.7/31.1	*menB*	gi|116511535	0.0155	205	35%	8	2	ITINRPEVR GNGGYVGEDQIPR	5
serine hydroxymethyltransferase	+1.6	5.6/44.8	*glyA*	gi|125623428	0.0295	486	50%	21	3	YAEGYPGKR YYGGTEAVDVVENLAIDR ALVNHDNQEKLEEVR	2
phosphofructokinase	+1.5	35.8	*pfkA*	gi|125623949	0.0155	123	35%	32§	32§	RYPEFAQVEGQLAGIEQLKKF; RIAVLTSGGDAPGMNAAIRA; RAVELLRDGIGGVAVGIRN; KFENVVNNINKGYEKG; RLNSALNNLNLN; KFENVVNNINKG; RTFVVEVMGRN; RDGIGGVAVGIRN; RVSVLGHIQRG; KEAGYKGDLRV; RGGTFLYSARY; KAGLELYRL; RAVELLRD	1, 6

Table 5. (continued)

ΔtrxD; arsenate stressed samples vs. control (As vs C)											
Protein name	RTR*	pI/Mr [kDa]¤	Gene	Accession	p-value†	Score	SC¶	M#	F‡	Peptide sequences identifed by MS/MS"	G$
phosphopyruvate hydratase (spot 3013)	−2.1	4.7/46.9	*enoA*	gi|125623478	0.0262	708	54%	20	5	SIITDIYAR GNPTLEVEVYTEDGAFGR GMVPSGASTGEHEAVELR AVDNVNNIIAEAIIGYEVTDQQAIDR EAGFTAIVSHR	X
ATP synthase F0F1 subunit beta (spot 3013)	−2.1	5.0/52.7	*atpD*	gi|125624725	0.0262	157	53%	21	0		X
elongation factor G	−1.8	4.8/77.9	*fusA*	gi|125625309	0.0484	424	46%	28	2	EFKVEANVGAPQVAYR VTITVPEENLGDIMGHVTAR	4
serine hydroxymethyltransferase	+1.7	5.6/44.8	*glyA*	gi|125623428	0.0007	486	50%	21	3	YAEGYPGKR YYGGTEAVDVVENLAIDR ALVNHDNQEKLEEVR	2
hypothetical protein	−1.7	5.4/14.9	*llmg_2273*	gi|125625038	0.0176	251	51%	6	2	VYEDDDVVAFLDITQTTK FTAHDYDLAEIAK	6
dipeptidase PepV (spot 3039)	−1.6	4.7/51.9	*pepV*	gi|116511662	0.0075	110	34%	16	0		X
ATP synthase F0F1 subunit beta (spot 3039)	−1.6	5.0/52.7	*atpD*	gi|125624725	0.0075	107	39%	18	0		X
glucose-1-phosphate thymidylyltransferase	−1.5	4.7/32.2	*rmlA*	gi|125623083	0.0384	394	47%	17	4	GATVFGYHVPDPER GELEITDVNKAYLER MGYITEEDVR NEYGQYLLR	7

Table 5. (continued)

wild type; arsenate stressed samples vs. control (As vs C)

Protein name	RTR*	pI/Mr [kDa]¤	Gene	Accession	p-value†	Score	SC¶	M#	F‡	Peptide sequences identifed by MS/MS"	G$
DivIVA cell division initiation protein	−1.8	4.7/14.9	*llmg_0769*	gi|125623623	0.0242	93	74%	8	0		6
DNA-directed RNA polymerase subunit alpha	+1.8	4.9/34.2	*rpoA*	gi|125625115	0.0337	315	26%	14	5	FDESENYGKFVVEPLER GYGTTLGNSLR VNYQVEPAR VLDKIIEEMDFSVR VLDKIIEEMDFSVR (M)	6
ribonucleotide-diphosphate reductase subunit alpha	−1.5	5.2/81.8	*nrdE*	gi|125624346	0.0252	88	2%	1	1	ALTFISETSNLDTVPTVR	2
hypothetical protein	−1.5	5.4/14.9	*llmg_2273*	gi|125625038	0.0124	251	51%	6	2	VYEDDDVVAFLDITQTTK FTAHDYDLAEIAK	6

* Relative translation rate; ± mark up- and down-regulation, respectively

¤ Calculated values

† Result of the Welch's t-test (see Materials and Methods)

¶ Sequence coverage in peptide mass fingerprinting (PMF)

Number of matched peptides in PMF

‡ Number of peptides fragmented and analyzed by MS/MS; "0" means that the protein was identified based on PMF only

§ Spot identified by LC/MS

" (M) - oxidation of methionine

$ Group: 1 - carbon metabolism; 2 - nucleotide metabolism; 3 - ATPases; 4 - GTPases; 5 - stress/aerobiosis; 6 - other; X - two proteins in a spot

2.8 Figure legends

Fig. 1 Detection of TrxA and TrxD. Protein extracts from wt, Δ*trxA* and Δ*trxD* strains harvested in mid-exponential phase (EP) or stationary phase (SP) were subjected to western blot analysis. Recombinant TrxA and TrxD were used as positive controls. Slower migration of the recombinant proteins are due to the presence of N-terminal His_6-tags. 1 – wt EP; 2 – wt SP; 3 - Δ*trxA* EP; 4 - Δ*trxA* SP; 5 - Δ*trxD* EP; 6 - Δ*trxD* SP; 7 – 200 ng TrxA; 8 – 100 ng TrxD. Proteins were transferred from identically prepared SDS-PAGE gels. Primary antibodies used in each experiment are on the left side. No apparent cross-reaction between the antibodies and the two His_6-tagged recombinant thioredoxins or the native proteins was observed.

Fig. 2 Trx mutant phenotypes. Growth curves display wt (♦), Δ*trxA* (▲), Δ*trxD* (○) and Δ*trxA*Δ*trxD* (×) strains without stress (**A**) or when exposed to hydrogen peroxide (**B**) and sodium arsenate (**C**). For more details see text. (**D**) Plate assays showing three biological replicates of wt, Δ*trxA* and Δ*trxD* strains exposed to sodium arsenate and potassium tellurite. Each section contains four dilutions of exponentially growing cultures (See materials and methods). The Δ*trxA* and Δ*trxD* mutants are more affected by sodium arsenate and potassium tellurite than wt. White background was chosen for the tellurite experiment, because formed Te^0 made the colonies black.

Fig. 3 Reduction of tetrazolium salts. Reduction of tetrazolium violet (TV) and *p*-iodonitrotetrazolium chloride (INT) added to wild type, Δ*trxA* and Δ*trxD* strains in mid-exponential phase (A) and stationary phase (B) was monitored spectrophotometrically at 510 nm (TV) and 468 nm (INT). Error bars represent standard deviation of at least three biological replicates.

Fig. 4 Proteome profile of Δ*trxA* vs. wt. Representative DIGE gel of soluble cytosolic proteins in the acidic range (pI=4–7) of wild type and Δ*trxA* strains. Proteins up- or down-regulated in Δ*trxA* mutant vs. wt are marked red or purple, respectively. For details see Table 4.

Fig. 5 [^{35}S]-L-methionine labeling of Δ*trxD* and wt exposed to arsenate. Representative radioactive images of control (**Ctrl**) (**A**, **B**) and arsenate (**As**) treated (**C**, **D**) samples are shown. Up- and down-regulated proteins upon arsenate exposure in each strain (**As** vs. **Ctrl**) are marked red or purple, respectively. Up- and down-regulated proteins in stressed ΔtrxD mutant vs. wt (**As** vs. **As**) are marked green or orange, respectively.

2.9 Figures

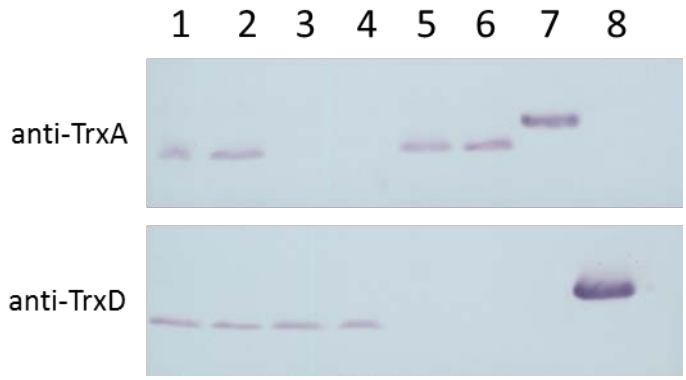

Fig.1

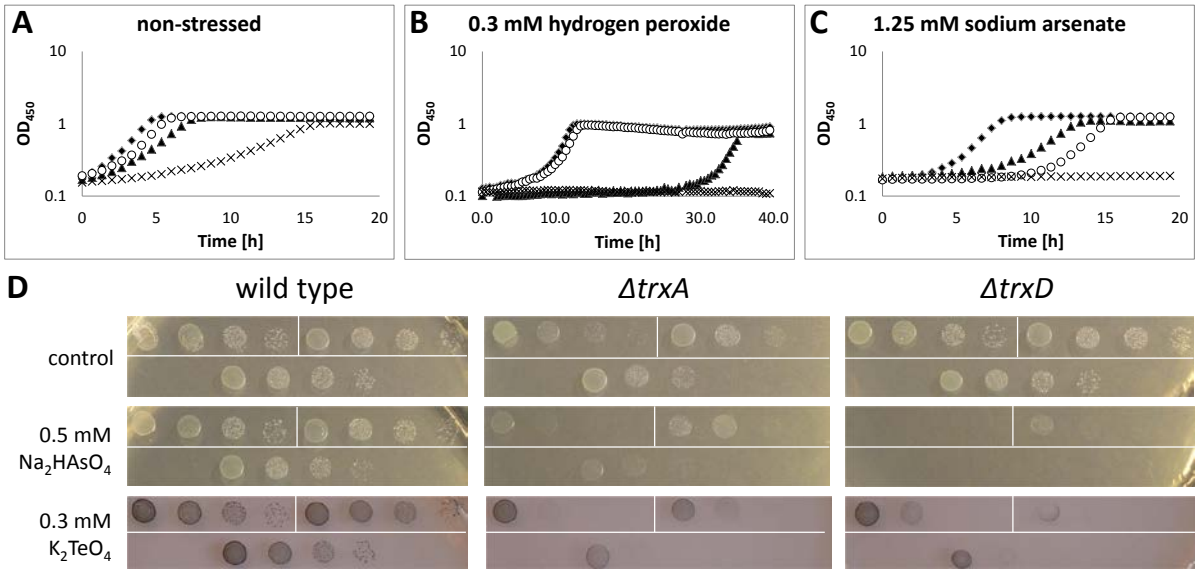
A
non-stressed
B
0.3 mM hydrogen peroxide
C
1.25 mM sodium arsenate
OD450
Time [h]
D
wild type
ΔtrxA
ΔtrxD
control
0.5 mM Na2HAsO4
0.3 mM K2TeO4

Fig.2

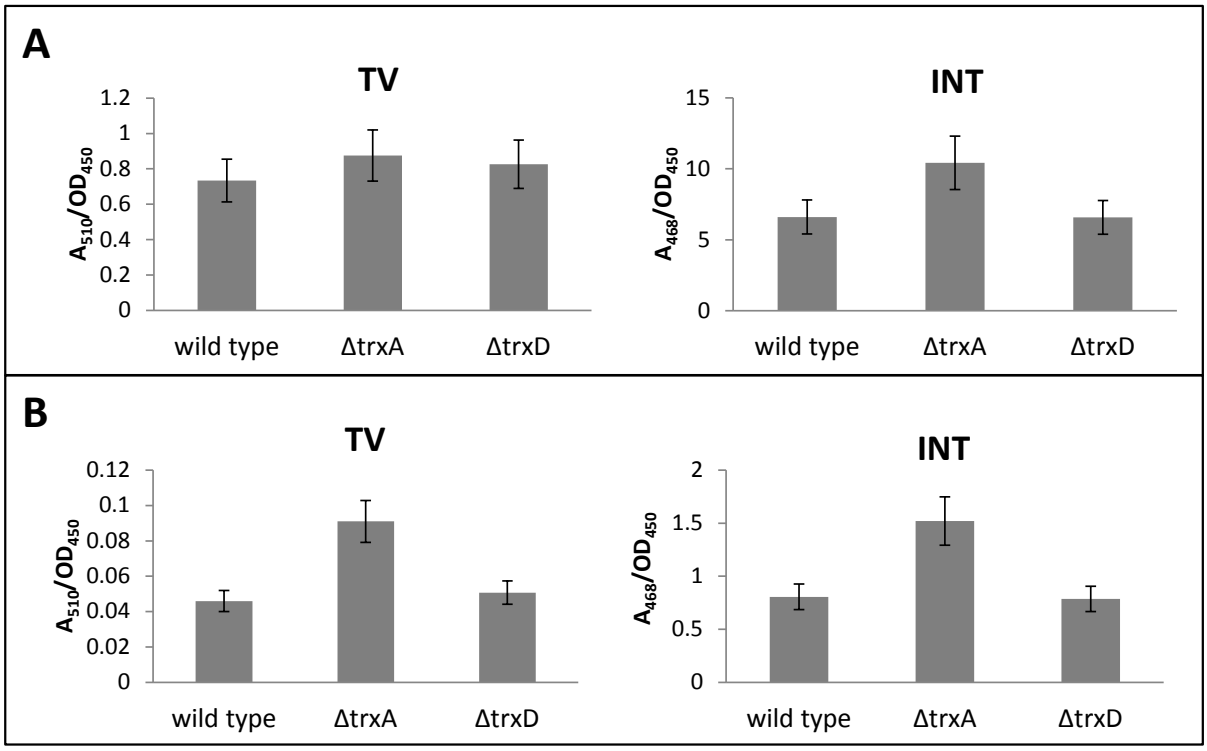
A
TV
INT
1.2
1
0.8
0.6
0.4
0.2
0
15
10
5
0
A510/OD450
A468/OD450
wild type
ΔtrxA
ΔtrxD
B
TV
INT
0.12
0.1
0.08
0.06
0.04
0.02
0
2
1.5
1
0.5
0
A510/OD450
A468/OD450
wild type
ΔtrxA
ΔtrxD

Fig.3

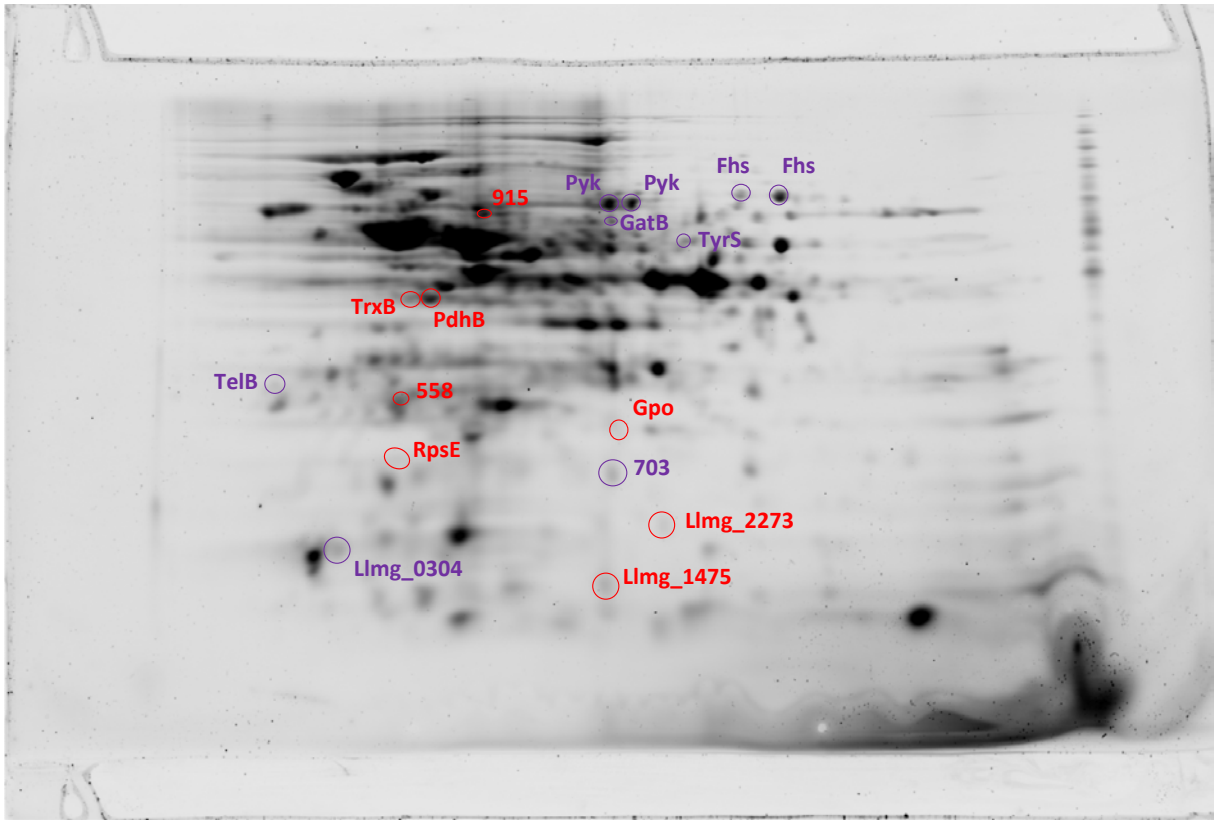
Fhs
Fhs
Pyk
Pyk
915
GatB
TyrS
TrxB
PdhB
TelB
558
Gpo
RpsE
703
Llmg_2273
Llmg_0304
Llmg_1475

Fig.4

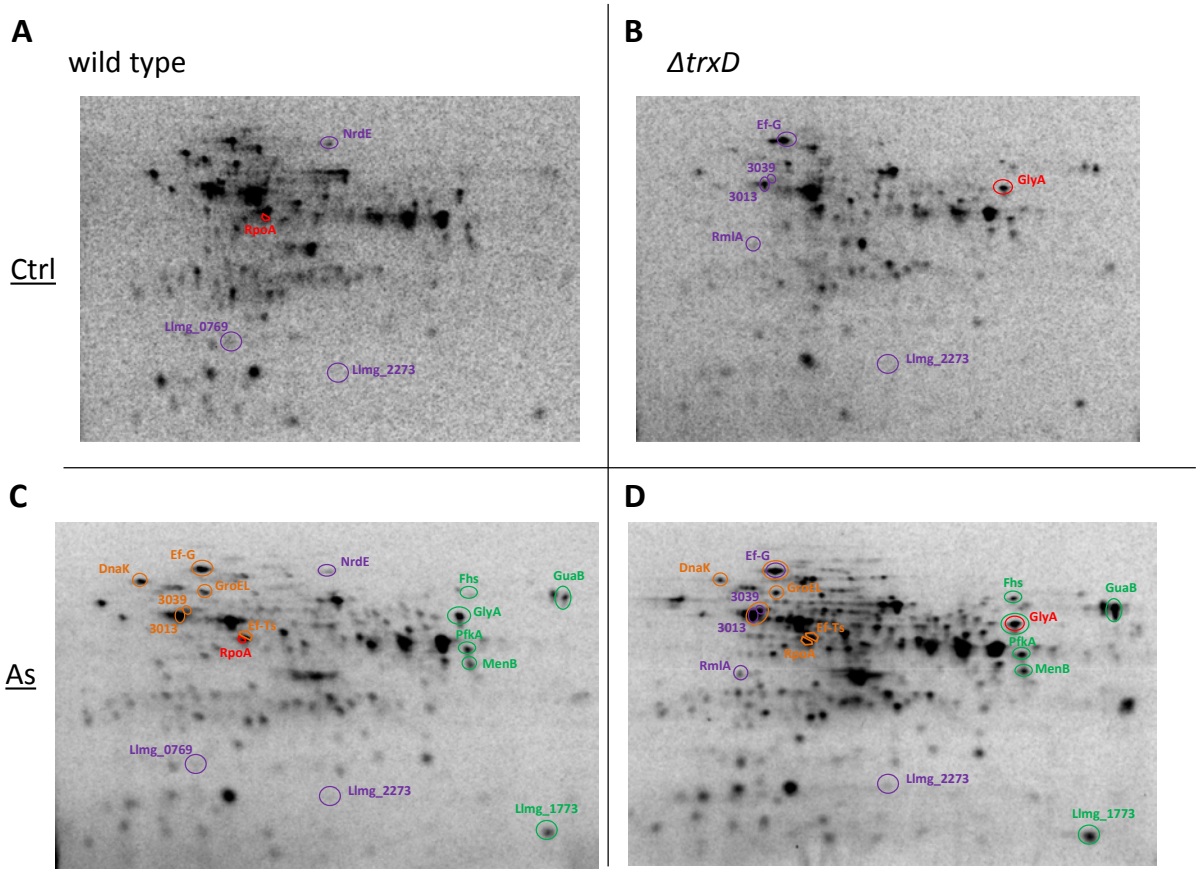
A
wild type
B
ΔtrxD
Ctrl
NrdE
RpoA
Llmg_0769
Llmg_2273
Ef-G
3039
3013
GlyA
RmlA
Llmg_2273
C
D
As
DnaK
Ef-G
GrdEL
3039
3013
Ef-Ts
RpoA
NrdE
Fhs
GlyA
PfkA
MenB
GuaB
Llmg_0769
Llmg_2273
Llmg_1773
RmlA

Fig.5

2.10 Supplementary material

Table S1. PCR primers

trxA upstream region	Product size [bp]
Fw - 5-CCGGATCCATTGATTCGTTTAGAAAAAGATGG -3	494
Rev - 5-GTAAATTTTATTATGATAATTCAGATTCCATTATATCTCCTTCATTGAA-3	
*trxA down*stream region	
Fw - 5-CTGAATTATCATAATAAAATTTACTGACAG-3	447
Rev - 5-AAAACTCGAGCAAGAAATATTTTACCAAAAACCCTC-3	
trxA outside primers	
Fw - 5-CCTTTAAAGTTTTTTTACTGG-3	1433 / 1121*
Rev - 5-CTCAAGAAGTAGTTAAAAAAG-3	
trxD upstream region	
Fw - 5-CCGGATCCGTCAAATTCTGGTTGATAGCCTAG-3	564
Rev - 5-GAAATCAGTCTTATTTTGCACGAATAATCATTCTGTATTTCCTTTCG-3	
trxD downstream region	
Fw - 5-GTGCAAAATAAGACTGATTTCTTG-3	510
Rev - 5-AAAACTCGAGCACCACAAACAATTTGTACTGG-3	
trxD outside primers	
Fw - 5-GACTTTTGAAGCTTTTGTC-3	1477/1162*
Rev - 5-CCATTAGGCATCATTGC-3	
Other primers	
T3 - 5-ATTAACCCTCACTAAAG-3	-
T7 - 5-AATACGACTCACTATAG-3	

* product size in case of the presence or absence of the particular gene on the chrosome

Table S2. Bioscreen assay with wt, *ΔtrxA*, *ΔtrxD* and *ΔtrxAΔtrxD* strains. Standard deviations (SD) are based on three biological replicates.

Stress conditions \ strains		**wild type**				**ΔtrxA**				
		relative µ*		**lag phase**		**relative µ***			**lag phase**	
compound	**c [µM]**	**% ctrl†**	**SD [%]**	**[h]**	**SD [h]**	**% ctrl†**	**SD [%]**	**% WT‡**	**[h]**	**SD [h]**
Control	NA	100	3.9	3	1	100	2.8	72	4	1
Methionine sulfoxide	NA	96	3.3	4	1	30	5.6	22	12	3
Formaldehyde	78	90	4.9	3	1	79	2.4	63	5	1
	313	54	3.2	6	2	47	7.0	62	9	2
	1250	<10	NA	>24	NA	<10	NA	NA	>24	NA
	5000	<10	NA	>24	NA	<10	NA	NA	>24	NA
Hydrogen peroxide	78	100	9.2	4	1	102	10.0	73	7	2
	313	95	9.8	8	2	94	10.4	71	>24	NA
	1250	<10	NA	>24	NA	<10	NA	NA	>24	NA
	5000	<10	NA	>24	NA	<10	NA	NA	>24	NA
Sodium arsenate	78	100	2.1	3	1	102	5.7	74	4	1
	313	100	2.2	4	1	100	7.9	72	5	1
	1250	92	1.6	6	1	94	3.7	73	9	2
	5000	64	9.4	19	1	21	34.6	24	>24	NA
Potassium tellurite	78	101	6.4	3	1	103	10.2	74	4	1
	313	86	3.8	3	1	90	2.9	75	5	1
	1250	49	2.5	4	2	53	4.2	78	7	2
	5000	<10	NA	>24	NA	<10	NA	NA	>24	NA
Diamide	20	101	6.1	3	1	100	4.4	71	4	1
	78	102	4.9	3	1	97	5.0	68	5	1
	313	105	1.5	4	2	104	6.1	72	11	5
	1250	81	11.0	8	4	61	55.1	54	18	2
	5000	<10	NA	>24	NA	<10	NA	NA	>24	NA

* Relative growth rates (µ) were calculated by dividing µ of a strain at a stress condition by µ of non-stressed control (†) or µ of wt at the same stress condition (‡); 100% (wt) = 0.506 h^{-1} and 100% (*ΔtrxA*) = 0.365 h^{-1}.

Table S2 (continued)

Stress conditions \ strains		wild type				ΔtrxA				
		relative µ*		lag phase		relative µ*			lag phase	
compound	**c [µM]**	**% ctrl†**	**SD [%]**	**[h]**	**SD [h]**	**% ctrl†**	**SD [%]**	**% WT‡**	**[h]**	**SD [h]**
Paraquat	20	101	2.3	3	1	96	5.5	69	4	1
	78	102	9.8	3	1	99	4.5	70	4	1
	313	97	3.5	3	1	99	14.0	74	4	1
	1250	91	5.8	4	2	103	2.4	82	5	2
	5000	81	5.9	6	2	82	3.8	73	8	2
	20000	61	10.1	8	3	29	30.9	35	11	1
Cadmium(II)chloride	5	13	6.5	5	1	10	7.6	54	>24	NA
	20	<10	NA	>24	NA	<10	NA	NA	>24	NA
	78	<10	NA	>24	NA	<10	NA	NA	>24	NA
	313	<10	NA	>24	NA	<10	NA	NA	>24	NA
	1250	<10	NA	>24	NA	<10	NA	NA	>24	NA
Zinc(II)chloride	5	108	7.2	3	1	98	5.6	66	4	1
	20	110	9.3	3	1	96	10.4	63	4	1
	78	95	6.5	3	1	88	3.0	66	4	1
	313	46	34.7	4	2	44	33.8	68	6	2
	1250	<10	NA	>24	NA	<10	NA	NA	>24	NA
Iron(II)sulfate	5	102	2.1	3	1	91	3.6	64	4	1
	20	98	3.5	3	1	86	2.0	63	4	1
	78	97	5.2	3	1	81	1.2	60	4	1
	313	91	13.3	3	1	77	3.7	61	5	1
	1250	77	16.9	4	1	61	2.8	57	5	1
Copper(II)sulfate	5	103	3.0	3	1	90	1.4	63	4	1
	20	100	12.4	3	1	88	2.9	64	4	1
	78	61	15.7	4	2	53	20.0	63	5	1
	313	<10	NA	>24	NA	<10	NA	NA	>24	NA
	1250	<10	NA	>24	NA	<10	NA	NA	>24	NA

* Relative growth rates (µ) were calculated by dividing µ of a strain at a stress condition by µ of non-stressed control (†) or µ of wt at the same stress condition (‡); 100% (wt) = 0.506 h^{-1} and 100% (*ΔtrxA*) = 0.365 h^{-1}.

Table S2 (continued)

Stress conditions \ strains		ΔtrxD					ΔtrxAΔtrxD				
		relative µ*			lag phase		relative µ*			lag phase	
compound	**c [µM]**	**% ctrl†**	**SD [%]**	**% WT‡**	**[h]**	**SD [h]**	**% ctrl†**	**SD [%]**	**% WT‡**	**[h]**	**SD [h]**
Control	NA	100	2.9	95	3	1	100	30.5	33	8	1
Methionine sulfoxide	NA	95	8.5	97	4	1	57	12.0	18	24	5
Formaldehyde	78	86	7.9	91	4	1	55	21.6	20	12	1
	313	48	5.2	84	>24	3	11	1.1	7	>24	NA
	1250	<10	NA	NA	>24	NA	<10	NA	NA	>24	NA
	5000	<10	NA	NA	>24	NA	<10	NA	NA	>24	NA
Hydrogen peroxide	78	102	10.2	96	5	1	75	15.8	25	16	1
	313	94	7.9	94	>24	1	<10	NA	NA	>24	NA
	1250	<10	NA	NA	>24	NA	<10	NA	NA	>24	NA
	5000	<10	NA	NA	>24	NA	<10	NA	NA	>24	NA
Sodium arsenate	78	101	3.3	96	4	1	111	13.4	37	11	1
	313	103	2.1	98	5	1	75	9.3	25	16	2
	1250	90	6.4	93	>24	1	<10	NA	NA	>24	NA
	5000	<10	NA	NA	>24	NA	<10	NA	NA	>24	NA
Potassium tellurite	78	98	0.7	92	4	1	124	5.5	41	12	1
	313	79	4.1	87	4	1	81	21.5	31	16	1
	1250	33	1.4	64	>24	1	14	0.9	10	>24	NA
	5000	<10	NA	NA	>24	NA	<10	NA	NA	>24	NA
Diamide	20	102	3.4	96	3	1	116	6.0	38	11	2
	78	102	5.2	94	4	1	151	55.7	49	17	2
	313	103	1.4	92	>24	1	<10	NA	NA	>24	NA
	1250	78	11.9	91	>24	4	<10	NA	NA	>24	NA
	5000	<10	NA	NA	>24	NA	<10	NA	NA	>24	NA

* Relative growth rates (µ) were calculated by dividing µ of a strain at a stress condition by µ of non-stressed control (†) or µ of wt at the same stress condition (‡); 100% (*ΔtrxD*) = 0.479 h^{-1} and 100% (*ΔtrxAΔtrxD*) = 0.167 h^{-1}.

Table S2 (continued)

Stress conditions \ strains		ΔtrxD					ΔtrxAΔtrxD				
		relative µ*			lag phase		relative µ*			lag phase	
compound	**c [µM]**	**% ctrl†**	**SD [%]**	**% WT‡**	**[h]**	**SD [h]**	**% ctrl†**	**SD [%]**	**% WT‡**	**[h]**	**SD [h]**
Paraquat	20	105	3.2	98	4	1	133	8.9	43	9	1
	78	103	6.0	96	4	1	127	15.2	41	10	2
	313	99	7.6	96	4	1	128	11.2	44	10	1
	1250	93	10.4	96	4	0	120	5.7	44	11	1
	5000	80	2.0	93	6	1	33	20.9	13	>24	NA
	20000	62	6.1	96	10	2	<10	NA	NA	>24	NA
Cadmium(II)chloride	5	29	4.7	206	10	2	<10	NA	NA	>24	NA
	20	<10	NA	NA	>24	NA	<10	NA	NA	>24	NA
	78	<10	NA	NA	>24	NA	<10	NA	NA	>24	NA
	313	<10	NA	NA	>24	NA	<10	NA	NA	>24	NA
	1250	<10	NA	NA	>24	NA	<10	NA	NA	>24	NA
Zinc(II)chloride	5	106	9.6	93	4	1	127	8.7	39	9	1
	20	107	7.5	92	4	1	120	13.6	36	9	1
	78	97	5.9	96	4	1	99	19.4	34	10	1
	313	46	34.3	94	4	1	28	19.8	20	11	3
	1250	<10	0.4	400	>24	NA	<10	NA	NA	>24	NA
Iron(II)sulfate	5	105	4.9	98	4	1	99	4.2	32	9	1
	20	101	2.8	97	4	1	101	10.9	34	9	1
	78	97	5.8	95	4	1	105	16.4	36	10	2
	313	90	5.7	93	4	1	101	14.6	37	11	1
	1250	64	8.8	79	4	1	85	10.5	37	12	1
Copper(II)sulfate	5	103	4.9	94	3	1	100	11.2	32	8	1
	20	91	5.7	87	3	1	63	11.0	21	8	1
	78	66	9.1	102	4	0	<10	NA	NA	>24	NA
	313	<10	NA	NA	>24	NA	<10	NA	NA	>24	NA
	1250	<10	NA	NA	>24	NA	<10	NA	NA	>24	NA

* Relative growth rates (µ) were calculated by dividing µ of a strain at a stress condition by µ of non-stressed control (†) or µ of wt at the same stress condition (‡); 100% (Δ*trxD*) = 0.479 h^{-1} and 100% (Δ*trxA*Δ*trxD*) = 0.167 h^{-1}.

2.11 References

Antelmann, H. & Helmann, J. D. (2011). Thiol-based redox switches and gene regulation. *Antioxid Redox Signal* **14**, 1049–63.

Beilharz, K., Nováková, L., Fadda, D., Branny, P., Massidda, O. & Veening, J.-W. (2012). Control of cell division in *Streptococcus pneumoniae* by the conserved Ser/Thr protein kinase StkP. *Proc Natl Acad Sci U S A* **109**, E905–13.

Beyer, N. H., Roepstorff, P., Hammer, K. & Kilstrup, M. (2003). Proteome analysis of the purine stimulon from *Lactococcus lactis*. *Proteomics* **3**, 786–97.

Biswas, I., Gruss, A., Ehrlich, S. D. & Maguin, E. (1993). High-efficiency gene inactivation and replacement system for Gram-positive bacteria. *J Bacteriol* **175**, 3628–35.

Boschi-Muller, S., Gand, A. & Branlant, G. (2008). The methionine sulfoxide reductases: Catalysis and substrate specificities. *Arch Biochem Biophys* **474**, 266–73.

Brot, N., Collet, J.-F., Johnson, L. C., Jönsson, T. J., Weissbach, H. & Lowther, W. T. (2006). The thioredoxin domain of *Neisseria gonorrhoeae* PilB can use electrons from DsbD to reduce downstream methionine sulfoxide reductases. *J Biol Chem* **281**, 32668–75.

Candiano, G., Bruschi, M., Musante, L., Santucci, L., Ghiggeri, G. M., Carnemolla, B., Orecchia, P., Zardi, L. & Righetti, P. G. (2004). Blue silver: a very sensitive colloidal Coomassie G-250 staining for proteome analysis. *Electrophoresis* **25**, 1327–33.

Collet, J.-F. & Messens, J. (2010). Structure, function, and mechanism of thioredoxin proteins. *Antioxid Redox Signal* **13**, 1205–16.

Commichau, F. M., Rothe, F. M., Herzberg, C., Wagner, E., Hellwig, D., Lehnik-Habrink, M., Hammer, E., Völker, U. & Stülke, J. (2009). Novel activities of glycolytic enzymes in *Bacillus subtilis*: interactions with essential proteins involved in mRNA processing. *Mol Cell Proteomics* **8**, 1350–60.

Ezraty, B., Bos, J., Barras, F. & Aussel, L. (2005). Methionine sulfoxide reduction and assimilation in *Escherichia coli*: new role for the biotin sulfoxide reductase BisC. *J Bacteriol* **187**, 231–37.

Fahey, R. C., Brown, W. C., Adams, W. B. & Worsham, M. B. (1978). Occurrence of glutathione in bacteria. *J Bacteriol* **133**, 1126–29.

Fernándes, L. & Steele, J. L. (1993). Glutathione content of lactic acid bacteria. *J Dairy Sci* **76**, 1233–42.

Gasson, M. J. (1983). Plasmid complements of *Streptococcus lactis* NCDO 712 and other lactic streptococci after protoplast-induced curing. *J Bacteriol* **154**, 1–9.

Grimaud, R., Ezraty, B., Mitchell, J. K., Lafitte, D., Briand, C., Derrick, P. J. & Barras, F. (2001). Repair of oxidized proteins. Identification of a new methionine sulfoxide reductase. *J Biol Chem* **276**, 48915–20.

Huebner, K., Saldivar, J. C., Sun, J., Shibata, H. & Druck, T. (2011). Hits, Fhits and Nits: beyond enzymatic function. *Adv Enzyme Regul* **51**, 208–17.

Jensen, K. S., Hansen, R. E. & Winther, J. R. (2009). Kinetic and thermodynamic aspects of cellular thiol-disulfide redox regulation. *Antioxid Redox Signal* **11**, 1047–58.

Jensen, P. R. & Hammer, K. (1993). Minimal requirements for exponential growth of *Lactococcus lactis*. *Appl Environ Microbiol* **59**, 4363–66.

Ji, G., Garber, E. A., Armes, L. G., Chen, C. M., Fuchs, J. A. & Silver, S. (1994). Arsenate reductase of *Staphylococcus aureus* plasmid pI258. *Biochemistry* **33**, 7294–99.

Jordan, A., Pontis, E., Åslund, F., Hellman, U., Gibert, I. & Reichard, P. (1996). The ribonucleotide reductase system of *Lactococcus lactis*. Characterization of an NrdEF enzyme and a new electron transport protein. *J Biol Chem* **271**, 8779–85.

Kaval, K. & Halbedel, S. (2012). Architecturally the same, but playing a different game: The diverse species-specific roles of DivIVA proteins. *Virulence* 405–19.

Kawai, Y., Moriya, S. & Ogasawara, N. (2003). Identification of a protein, YneA, responsible for cell division suppression during the SOS response in *Bacillus subtilis*. *Mol Microbiol* **47**, 1113–22.

Kilstrup, M., Jacobsen, S., Hammer, K. & Vogensen, F. K. (1997). Induction of heat shock proteins DnaK, GroEL, and GroES by salt stress in *Lactococcus lactis*. *Appl Environ Microbiol* **63**, 1826–37.

Lee, S.-Y., Song, J.-Y., Kwon, E.-S. & Roe, J.-H. (2008). Gpx1 is a stationary phase-specific thioredoxin peroxidase in fission yeast. *Biochem Biophys Res Commun* **367**, 67–71.

Lewis, J. P., Iyer, D. & Anaya-Bergman, C. (2009). Adaptation of *Porphyromonas gingivalis* to microaerophilic conditions involves increased consumption of formate and reduced utilization of lactate. *Microbiology* **155**, 3758–74.

Li, Y., Hugenholtz, J., Abee, T. & Molenaar, D. (2003). Glutathione protects *Lactococcus lactis* against oxidative stress. *Appl Environ Microbiol* **69**, 5739–45. Am Soc Microbiol.

Li, Y., Hu, Y., Zhang, X., Xu, H., Lescop, E., Xia, B. & Jin, C. (2007). Conformational fluctuations coupled to the thiol-disulfide transfer between thioredoxin and arsenate reductase in *Bacillus subtilis*. *J Biol Chem* **282**, 11078–83.

Lillig, C. H., Berndt, C. & Holmgren, A. (2008). Glutaredoxin systems. *Biochim Biophys Acta* **1780**, 1304–17.

Lin, Z., Johnson, L. C., Weissbach, H., Brot, N., Lively, M. O. & Lowther, W. T. (2007). Free methionine-(R)-sulfoxide reductase from *Escherichia coli* reveals a new GAF domain function. *Proc Natl Acad Sci U S A* **104**, 9597–602.

Majumder, A., Sultan, A., Jersie-Christensen, R. R., Ejby, M., Schmidt, B. G., Lahtinen, S. J., Jacobsen, S. & Svensson, B. (2011). Proteome reference map of *Lactobacillus acidophilus* NCFM and quantitative proteomics towards understanding the prebiotic action of lactitol. *Proteomics* **11**, 3470–81.

Nagano, T., Kojima, K., Hisabori, T., Hayashi, H., Morita, E. H., Kanamori, T., Miyagi, T., Ueda, T. & Nishiyama, Y. (2012). Elongation factor G is a critical target during oxidative damage to the translation system of *Escherichia coli*. *J Biol Chem* **287**, 28697–704.

Newton, G. L., Arnold, K., Price, M. S., Sherrill, C., Delcardayre, S. B., Aharonowitz, Y., Cohen, G., Davies, J., Fahey, R. C. & Davis, C. (1996). Distribution of thiols in microorganisms: mycothiol is a major thiol in most actinomycetes. *J Bacteriol* **178**, 1990–95.

Newton, G. L., Rawat, M., La Clair, J. J., Jothivasan, V. K., Budiarto, T., Hamilton, C. J., Claiborne, A., Helmann, J. D. & Fahey, R. C. (2009). Bacillithiol is an antioxidant thiol produced in *Bacilli*. *Nat Chem Biol* **5**, 625–27.

Nguyen, T. T. H., Eiamphungporn, W., Mäder, U., Liebeke, M., Lalk, M., Hecker, M., Helmann, J. D. & Antelmann, H. (2009). Genome-wide responses to carbonyl electrophiles in *Bacillus subtilis*: control of the thiol-dependent formaldehyde dehydrogenase AdhA and cysteine proteinase YraA by the MerR-family regulator YraB (AdhR). *Mol Microbiol* **71**, 876–94.

Nishizaki, M., Sasaki, J.-I., Fang, B., Atkinson, E. N., Minna, J. D., Roth, J. A. & Ji, L. (2004). Synergistic tumor suppression by coexpression of FHIT and p53 coincides with FHIT-mediated MDM2 inactivation and p53 stabilization in human non-small cell lung cancer cells. *Cancer Res* **64**, 5745–52.

Pedersen, M. B., Garrigues, C., Tuphile, K., Brun, C., Vido, K., Bennedsen, M., Møllgaard, H., Gaudu, P. & Gruss, A. (2008). Impact of aeration and heme-activated respiration on *Lactococcus lactis* gene expression: identification of a heme-responsive operon. *J Bacteriol* **190**, 4903–11.

Prágai, Z. & Harwood, C. R. (2002). Regulatory interactions between the Pho and sigma(B)-dependent general stress regulons of *Bacillus subtilis*. *Microbiology* **148**, 1593–602.

Pérez, J. M., Calderón, I. L., Arenas, F. A., Fuentes, D. E., Pradenas, G. A., Fuentes, E. L., Sandoval, J. M., Castro, M. E., Elías, A. O. & Vásquez, C. C. (2007). Bacterial toxicity of potassium tellurite: unveiling an ancient enigma. *PLoS One* **2**, e211.

Roux, C. M., DeMuth, J. P. & Dunman, P. M. (2011). Characterization of components of the *Staphylococcus aureus* mRNA degradosome holoenzyme-like complex. *J Bacteriol* **193**, 5520–26.

Sambrook, J. & Russel, D. (2000). *Molecular Cloning – A Laboratory Manual*, Third. New York: Cold Spring Harbor Laboratory Press.

Schroeter, R., Voigt, B., Jürgen, B., Methling, K., Pöther, D.-C., Schäfer, H., Albrecht, D., Mostertz, J., Mäder, U. & other authors. **(2011).** The peroxide stress response of *Bacillus licheniformis*. *Proteomics* **11**, 2851–66.

Scott, C., Rawsthorne, H., Upadhyay, M., Shearman, C. a, Gasson, M. J., Guest, J. R. & Green, J. (2000). Zinc uptake, oxidative stress and the FNR-like proteins of *Lactococcus lactis*. *FEMS Microbiol Lett* **192**, 85–89.

Seefeldt, K. E. & Weimer, B. C. (2000). Diversity of sulfur compound production in lactic acid bacteria. *J Dairy Sci* **83**, 2740–46.

Smith, J. J. & McFeters, G. A. (1996). Effects of substrates and phosphate on INT (2-(4-iodophenyl)-3-(4-nitrophenyl)-5-phenyl tetrazolium chloride) and CTC (5-cyano-2,3-ditolyl tetrazolium chloride) reduction in *Escherichia coli*. *J Appl Bacteriol* **80**, 209–15.

Tachon, S., Michelon, D., Chambellon, E., Cantonnet, M., Mezange, C., Henno, L., Cachon, R. & Yvon, M. (2009). Experimental conditions affect the site of tetrazolium violet reduction in the electron transport chain of *Lactococcus lactis*. *Microbiology* **155**, 2941–48.

Turner, M. S., Tan, Y. P. & Giffard, P. M. (2007). Inactivation of an iron transporter in *Lactococcus lactis* results in resistance to tellurite and oxidative stress. *Appl Environ Microbiol* **73**, 6144–49.

Turner, R., Hou, Y. & Weiner, J. (1992). The arsenical ATPase efflux pump mediates tellurite resistance. *J Bacteriol* **174**, 3092–94.

Vido, K., Le Bars, D., Mistou, M.-Y., Anglade, P., Gruss, A. & Gaudu, P. (2004). Proteome analyses of heme-dependent respiration in *Lactococcus lactis*: Involvement of the proteolytic system. *J Bacteriol* **186**, 1648–57.

Vido, K., Diemer, H., Van Dorsselaer, A., Leize, E., Juillard, V., Gruss, A. & Gaudu, P. (2005). Roles of thioredoxin reductase during the aerobic life of *Lactococcus lactis*. *J Bacteriol* **187**, 601–10.

Walter, E., Thomas, C., Ibbotson, J. & Taylor, D. (1991). Transcriptional analysis, translational analysis, and sequence of the kilA-tellurite resistance region of plasmid RK2Ter. *J Bacteriol* **173**, 1111. Am Soc Microbiol.

Welch, B. L. (1947). The generalisation of student's problems when several different population variances are involved. *Biometrika* **34**, 28–35.

Wessel, D. & Flügge, U. I. (1984). A method for the quantitative recovery of protein in dilute solution in the presence of detergents and lipids. *Anal Biochem* **138**, 141–43.

3 Chapter 3 – Redox potential and catalytic properties of three thioredoxin superfamily disulfide reductases from *Lactococcus lactis*

Petr Efler[†], Olof Björnberg[†], Epie Denis Ebong, Birte Svensson and Per Hägglund*

Enzyme and Protein Chemistry, Department of Systems Biology, Søltofts Plads, Building 224, Technical University of Denmark, DK-2800 Kgs. Lyngby, Denmark

[†] These authors contributed equally to this work

* To whom correspondence should be addressed. Tel: +45 4525 5503; fax: +45 4588 6307; e-mail: ph@bio.dtu.dk

Formated for publication in FEBS journal

Running title: Three thioredoxin superfamily proteins from *Lactococcus lactis*

Abbrevations: DTNB, 5,5'-dithiobis-(2-nitrobenzoic acid); EcNTR, *E. coli* NADPH-dependent thioredoxin reductase; EcTrx1, *E. coli* thioredoxin 1; HvTrxh1, barley thioredoxin h1; IAM, Iodoacetamide LlTrxA, *Lactococcus lactis* thioredoxin A; LlNrdH, *Lactococcus lactis* NrdH; LlNTR, *Lactococcus lactis* NADPH-dependent thioredoxin reductase; LlTrxA, *Lactococcus lactis* thioredoxin A; wild type, wt

Keywords: thioredoxin, lactic acid bacteria, redox potential, disulfide reduction, thiol-disulfide exchange

3.1 Abstract

Thioredoxins are protein disulfide reductants found in all domains of life. Here we investigate three thioredoxin superfamily proteins with active site CXXC motifs (LlTrxA, LlTrxD and LlNrdH) from the industrially important microorganism *Lactococcus lactis* and compare these to the well characterized thioredoxin from *Escherichia coli* (EcTrx1) with respect to thiol-disulfide exchange reactivity and redox potential. LlTrxA resembles EcTrx1 and contains a WCGPC active site and other key residues conserved among classical thioredoxins. By contrast LlTrxD has the atypical WCGDC active site sequence apparently overrepresented in a group of Trx-like proteins from Gram-positive bacteria. The LlNrdH is established as electron donor for ribonucleotide reductase class Ib, has sequence similiarity to glutaredoxin and contains a CMQC active site motif. Both LlTrxA and EcTrx1 have high capacity to reduce insulin disulfides and their exposed active site thiol is alkylated at similar rate at pH 7.0. LlTrxA, however, has significantly higher redox potential ($E°´$=-259 mV) than EcTrx1 ($E°´$=-270 mV). LlTrxD on the other hand, is alkylated (at pH 7.0) by iodoacetamide almost 100 fold more rapidly than TrxA and EcTrx1, shows no insulin disulfide reduction and has a high redox potential ($E°´$=-243 mV). Finally, LlNrdH has only weak activity towards insulin and a higher redox potential ($E°´$=-238 mV) than *E. coli* NrdH ($E°´$=-248 mV). LlTrxA, LlTrxD and LlNrdH are all efficiently reduced by the NADPH dependent thioredoxin reductase (LlNTR). With LlTrxD as notable exception a high level of cross-reactivity towards *E. coli* NTR was observed.

3.2 Introduction

Cysteine sulfhydryl groups are highly reactive and prone to oxidative damage. Thiols in the intracellular environment are thus maintained in reduced state by low molecular weight antioxidants such as the tripeptide glutathione (GSH) and redoxins, *i.e.* protein disulfide reductases such as thioredoxin (Trx) and glutaredoxin (Grx) containing redox active C_NXXC_C motifs [1]. In addition to their role as general disulfide reductants these redoxins act as hydrogen donors to enzymes such as methionine sulfoxide reductase, peroxiredoxins and ribonucleotide reductase [2]. In deprotonated thiolate form the exposed C_N of Trx attacks target disulfides and forms an intermolecular disulfide in turn reduced by Trx C_C. In the cytosol, the reducing power for Trx and Grx is provided in an NADPH-dependent manner by thioredoxin reductase (NTR) and glutathione reductase (GR), respectively. Trx and Grx belong to the Trx superfamily of proteins with similar overall fold and a core motif of a four-stranded β-sheet flanked by three α-helices [3], which includes proteins catalyzing formation and isomerization of disulfide bonds, *e.g.* Dsb proteins in the periplasm of bacteria. The Trx superfamily covers a wide range of thiol-disulfide exchange equilibria spanning from reductants such as *Escherchia coli* Trx1 (WCGPC, -270 mV) and Grx1 (WCPYC, -233 mV) to oxidants like DsbA (WCPHC, -120 mV) [4-6]. The amino acid sequence of the CXXC motif is an important determinant for the reactivity of Trx family proteins, but target specificity also appears to be guided by specific intermolecular interactions involving key residues in the vicinity of the active site [7, 8].

The industrially important microaerophilic bacterium *Lactococcus lactis* contains two Trx-like proteins (LlTrxA, LlTrxD), a smaller redoxin (LlNrdH), and an NTR (LlNTR). LlTrxA has a WCGPC active site motif and resembles the well characterized thioredoxin from *E. coli* (EcTrx1), whereas the atypical active site WCGDC is found in LlTrxD. Phenotype screening of *Lactococcus*

lactis knock-out strains suggests different but partially overlapping roles for these Trx-like proteins; LlTrxA seems to be involved in oxidative stress resistance whereas LlTrxD appears to be important for arsenate detoxification (Efler, P, Kilstrup, M, Johnsen, S; Svensson, B & Hägglund, P, unpublished work). LlNrdH (CMQC) represents a group of Grx-like proteins providing reducing equivalents to ribonucleotide reductase Ib (NrdEF) as first demonstrated in *L. lactis* [9, 10]. Despite being related to Grx, NrdH from *E. coli* is recycled by NTR and not by GSH and GR [9]. Similarly to many other Gram-positive bacteria *L. lactis* cannot synthesise GSH, and production of alternative low-molecular weight thiols such as bacillithiol [11] has not yet been reported in this species [12, 13]. It can therefore be expected that LlNTR is essential but a mutant lacking NTR was demonstrated to be viable and tolerant to oxygen [13]. In contrast deletion of NTR in *Staphylococcus aureus* is lethal suggesting fundamental differences in the disulfide reduction pathways among Gram-positive bacteria [12]. To further the understanding of thiol reduction in *L. lactis* we characterized and compared the biophysical and catalytic properties of three potentials targets of LlNTR with those of EcTrx1.

3.3 Results and discussion

3.3.1 **Sequence analysis of two *L. lactis* thioredoxins**

The genome of *L. lactis* MG1363 contains two open reading frames, *trxA* and *trxH,* annotated as thioredoxins, and a smaller Grx-like *nrdH*; the corresponding encoded redoxins are here referred to as LlTrxA, LlTrxD and LlNrdH, respectively. The sequence of LlNrdH has been described elsewhere [9, 10] and will not be analyzed in detail here. The amino acid sequence of LlTrxA is similar to other reported thioredoxins containing the canonical WCGPC motif and shows 42%

identity to the well characterized EcTrx1 (Fig. S1). Conserved residues include D26, F27, A29, P40, D61, P76, T77, G84, G92 (EcTrx1 numbering). LlTrxD on the other hand has a WCGDC motif, is more distantly related to EcTrx1 and LlTrxA (25% and 28% sequence identity, respectively) and lacks D26, T77 and G92 conserved among the "WCGPC"-thioredoxins (Fig. S1). $D26_{EcTrx1}$ has been studied extensively and is proposed to play an important role as acid/base in the catalytic mechanism of thioredoxin [14, 15]. G92 as well as the *cis*-proline (P76) preceeding T77 are both conserved among a wide range of Trx-fold proteins including Trx and Grx [3, 7, 16]. In an attempt to define and place LlTrxD in an evolutionary context, the amino acid sequence was subjected to BLAST analysis yielding 294 NCBI accessions with >50% sequence identity ($e<1*10^{-16}$; BLAST score>76.6 bits) originating mainly from the phylum *Firmicutes*. Most of these sequences display a WC[G/P]DC active site motif (Fig. S2). As observed for LlTrxD, residues corresponding to EcTrx1 D26 and G92 are not conserved and $T77_{EcTrx1}$ is apparently replaced by an invariant serine residue. Other conserved residues include P40, E43, F51, R56, R91, F100 and L101 (LlTrxD numbering) (Fig. S2).

Thioredoxin-like proteins with atypical active site motifs is not a rare phenomenon; 5330 out of a total of 10856 sequences with WCXXC motifs in the pfam thioredoxin (PF00085) do not match WCGPC and 823 sequences contain WC[G/P]DC motifs (Table 1). 745 of these 823 sequences derive from bacterial species in the phylum *Firmicutes*, suggesting overrepresentation in this phylogenetic group which includes a wide range of Gram positive bacteria including *L. lactis*. Characterized thioredoxin-like proteins with WC[G/P]DC active sites include Trx2 from *Helicobacter pylori* (WCPDC, 39% identity to LlTrxD) and Trx2 from *Bacillus anthracis* (WCPDC, 58% identity to LlTrxD) [17, 18]. WCPDC active site motifs are also present in more distantly related redoxins including *Saccharomyces cerevisae* glutaredoxin 8 (30% identity to

LlTrxD) and the well characterized, structure-determined human Trx-like protein HsTRP14 (21% identity to LlTrxD) [19-21].

3.3.2 Insulin disulfide reduction

Protein disulfide reductase activity was tested using a qualitative turbidity assay with insulin as model substrate and DTT as electron donor [22]. Whereas LlTrxA reduces insulin with similar apparent efficiency as EcTrx1, LlNrdH reduces insulin comparatively inefficiently (Fig. 1A). A similar trend was previously observed when comparing the relative insulin disulfide reduction efficiency of EcTrx1 and *E. coli* NrdH [9]. With LlTrxD, no insulin reduction was detected even at elevated Trx concentration (10 µM), and with LlNTR and NADPH as reductants instead of DTT (data not shown). In order to probe the influence of the active site aspartate conserved among proteins related to LlTrxD (Fig. S2), site-directed mutagenesis was employed to exchange this residue by proline or asparagine. For LlTrxD D31N no apparent insulin reduction was detected but with D31P (10 µM), however, a low but significant rate of disulfide reduction was found (Fig. 1B). Among Trx-like proteins with WC[G/P]DC motifs insulin disulfide reduction activity was observed in Trx2 of *H. pylori*, but not in Trx2 of *B. anthracis* [17, 18]. Low activity towards insulin was determined for the distantly related HsTRP14 and ScGrx8 [19, 20].

3.3.3 Recycling by NTRs from *L. lactis* and *E. coli*

LlTrxA, LlTrxD, LlNrdH and EcTrx1 were assayed as substrates for NTR from *L. lactis* and *E. coli* using Ellmans reagent (5,5'-dithiobis-(2-nitrobenzoic acid); DTNB) as final electron acceptor. This assay is a good tool to obtain kinetic parameters of NTR, since DTNB is very reactive towards the EcTrx1 dithiol [14], but not with the dithiol in bacterial NTR. The EcTrx1/EcNTR redox couple

serve as a reference and cross-reactivity was studied between the components of the two Trx systems. Importantly, the *L. lactis* and *E. coli* NTRs displayed similar k_{cat} values (~25 s^{-1}) and the parameters for EcTrx1/EcNTR (Table 2 and Fig. 2A, K_m 2.2 µM and k_{cat} 26 s^{-1}) agree with literature values [15, 23, 24]. LlTrxA and LlNrdH were quite reasonably reduced by EcNTR, with loss of efficiency of less than one order of magnitude compared to EcTrx1. By contrast, EcNTR hardly accepted LlTrxD as substrate and a 1000 fold reduction in k_{cat}/K_m relative to EcTrx1 was observed (Fig. 2A). The LlTrxD D31N and D31P mutants showed unchanged parameters with LlNTR and improved marginally with EcNTR compared to LlTrxD wild type (wt). *E. coli* has no LlTrxD homologue but the strikingly low reactivity for the LlTrxD/EcNTR couple is surprising and suggests substantial differences in substrate recognition between the two NTRs. In all cases a hyperbolic function was used to fit the kinetic data (Fig. 2 and Table 2) although for LlNrdH/LlNTR, a better fit is obtained by including a term of substrate inhibition. Nevertheless, LlNrdH displayed the highest catalytic efficiency as substrate of LlNTR (6.1 x 10^{-7} $M^{-1}s^{-1}$) with a seven fold lower K_m compared to LlTrxA (Table 2). This stands in sharp contrast to *B. anthracis* where a WCGPC Trx (BaTrx1) was recycled 10 times more efficiently than BaNrdH [18]. In the *E.coli*, system, the EcNrdH/EcNTR couple was significantly more efficient (1.5 fold) than the EcTrx1/EcNTR couple [9].

3.3.4 Reduction of low molecular weight disulfide substrates

Four low molecular weight thiol compounds forming intermolecular disulfides (cystine, oxidized GSH (GSSG), hydroxyethyl disulfide (HED) and cystamine) and two homologues peptide hormones (vasopressin and oxytocin) resembling protein disulfide targets were tested as model substrates. Activity was monitored spectrophotometrically at 340 nm as NADPH oxidation rates in an NTR coupled assay and the results are given as turnover (min^{-1}) at a fixed substrate

concentration (Table 3). Considering the low concentration (0.1 mM), vasopressin and oxytocin in general appears among the most efficiently reduced low molecular weight substrate compounds. Interestingly, despite its inability to reduce insulin disulfides, LlTrxD displayed the highest turnover rates with four out of the six substrates examined (Table 3) and most strikingly, the rate of reduction of cystamine (10 min^{-1}) was six-fold higher than for the second best redoxin (*i.e.* LlTrxA). If converted to second order rate constant (170 $M^{-1}s^{-1}$), it is clearly above the rates of some non-cognate disulfide exchange reactions (0.1 - 10 $M^{-1}s^{-1}$) [25, 26]. It can be speculated that the positively charged cystamine may be attracted through electrostatic interactions with the active site aspartate in LlTrxD. LlNrdH is restricted compared to EcTrx1, LlTrxA and LlTrxD, and displays the lowest rates of disulfide reduction (Table 3). The composition of the low molecular weight thiol pool in *L. lactis* has not been established. Although *L. lactis* does not synthesise glutathione, it has a putative GSSG reductase and uptake of glutathione has been demonstrated [27]. Reduction of GSSG by Trx has been shown to be physiologically relevant in *Saccharomyces cerevisae* [28].

3.3.5 Determination of redox potential (E°') by direct protein-protein equilibrium

Redox potentials were determined according to Åslund et al [4] by HPLC-quantification of reduced and oxidized protein species at equilibrium using EcTrx1 ($E°'$= -270 mV) as reference [5]. From eight reactions between either reduced LlTrxA and oxidized EcTrx1 or *vice versa*, an equilibrium constant (K) of 0.428 +/- 0.034 was obtained, which corresponds to $E°'$ = -259.2 +/-0.98 mV for LlTrxA. Considering the high degree of sequence homology, the approximate difference of 10 mV from the well characterized EcTrx1 is noteworthy. A representative chromatogram of the separation of reduced and oxidised proteins is shown in Fig. 3A.

Reactions between EcTrx1 and LlTrxD suggested slow and insufficient equilibration. Although duplicate samples were consistent, different *K* values were obtained depending on starting conditions (reduced reference or oxidized reference) and the time of incubation. Some consistency was obtained, however, at a prolonged incubation time (69 hrs). Four samples at the two concentrations of 25 and 50 µM, respectively, starting with reduced reference (EcTrx1) and oxidized LlTrxD indicated a *K* value of 0.1184 +/- 0.0014 (Fig. 3B). As expected for a longer incubation time, control samples of reduced EcTrx1 and LlTrxD, incubated in parallel, showed a substantially higher level of oxidation (10 and 18%, respectively). If the above mentioned *K* value represents an equilibrium, it gives *E*°' = -243 mV for LlTrxD. Noticeably, failure to reach equilibrium by this approach has been reported previously, *e.g.* no transfer of redox equivalents was observed between human Grx1 and EcGrx1 after 24 hrs of incubation [29]. When reference samples of oxidized and reduced LlTrxD were analyzed, it was noticed that the oxidized form eluted earlier than the reduced form. Among the redoxins investigated here, this was only observed for LlTrxD and it is contradictory to the expectation that the disulfide bond makes the protein appear more hydrophobic during chromatography (Fig. 3B). However, a mutant form of EcTrx1, $Trx^{"PDI"}$ also displayed this property [4].

With 91 amino acid residues, including the pentahistidine tag, LlNrdH is the smallest protein in the present study. Less acetonitrile was required to elute it from the C18 column and the separation between reduced and oxidized forms was unsatisfactory. To avoid overlapping peaks EcTrx1 was replaced as reference protein by recombinant HvTrxh1 fr om barley [30]. Reaction between EcTrx1 and HvTrxh1 resulted in *K* = 1.054 +/- 0.014 corresponding to an *E*°' = -270.7 mV (Fig. S3). LlNrdH was then incubated with HvTrxh1 in eight reactions yielding *K* = 0.0787 +/- 0.0039 and

E°'=-237.6 +/- 0.8 (Fig. 3C). The obtained *E*°' is significantly more positive than that of NrdH from *E. coli* (*E*°'=-248.5 +/- 1.5 mV) determined by equilibration with the NADPH/$NADP^+$ couple [9].

3.3.6 Redox potential *E*°' by equilibrium to the NADPH/$NADP^+$ couple via NTR

Using the equilibrium with the NADPH/$NADP^+$ redox couple catalyzed by EcNTR, we reproduced the parameter for EcTrx1 reasonably well (*E*°´=-270.3 +/ - 1.8 mV; Fig. S4A). The $E^{0'}$ value of LlTrxA was also determined by this approach (-258.1 +/- 0.3 mV, Fig. 4A) which is in good agreement with the value obtained from protein-protein equilibrium (-259.2 +/- 0.98 mV). Determination of LlNrdH was attempted by the same method but very little NADPH was generated when $NADP^+$ was added to reverse the reaction (Fig. S4B). Thus, consistent with the finding using the protein-protein equilibrium HPLC method described above, LlNrdH is the least reducing protein of those characterized in the present study.

EcNTR is a poor reductant of LlTrxD, and was thus replaced by LlNTR for redox potential determination of LlTrxD (Fig. 2A). However, stable baselines of NADPH absorbance (A340 nm) were not obtained, and the absorbance of NADPH decreased continuously within the time frame of the experiment. A comparison of EcNTR and LlNTR showed that the unstable baseline stems from an approximately 10-fold higher reduction rate of O_2 by the *L. lactis* enzyme (0.4 NADPH oxidized per second). We therefore turned to a semi-anaerobic buffer system to reduce the concentration of oxygen in the solution. Glucose (10 mM), and the two enzymes glucose oxidase and catalase (both at 0.05 mg/mL) were added in the reaction mixture causing the recorded oxygen-dependent NADPH consumption to be reduced by at least a factor of 15. As the LlNTR is severely light-sensitive compared to EcNTR (O.B., unpublished observation), the concentration of LlNTR was

increased 6 fold to 300 nM. Sufficiently stable baselines of NADPH absorbance were thus obtained, comparable to those with EcNTR under aerobic conditions. The semi-anaerobic system (with LlNTR) was first validated with LlTrxA yielding a similar value ($E°'$=-257.8 +/- 2.05 mV; Fig. S4C) as was obtained with EcNTR (-258.1 +/- 0.3 mV). For LlTrxD, a redox potential of -241.7 +/- 2.2 mV was obtained (Fig. 4C), thus supporting the determination by HPLC (protein-protein equilibrium) in one direction (-243.0 +/-0.2 mV).

Thus, two independent methods have here been used to determine redox potentials. The method based on direct protein-protein equilibrium with a known reference has strong advantages as determination of absolute reactant concentration is not critical and experiments are varied with respect to time, protein concentration and reactant status (*i.e.* starting with reduced or oxidized reference). However, there are both kinetic and thermodynamic limitations. Equilibrium must be reached within a reasonable time and the two dithiol/disulfide proteins cannot be too far apart on the redox scale, *i.e.* the equilibrium constant (*K)* should not differ from 1.0 much more than one order of magnitude.

LlTrxA and LlNrdH both display higher redox potentials in comparison to their *E. coli* counterparts. These observations may potentially reflect differences in the intracellular redox environment in the two bacteria. The higher redox potential of LlTrxD in comparison to LlTrxA is important as this may limit the ability of LlTrxD to reduce potential target disulfides *in vivo*. LlTrxD is apparently incapable of reducing insulin disulfides despite having a higher redox potential than LlNrdH (Fig. 1). Thus it is hypothesized that the lack of activity with LlTrxD is due to steric or electrostatic constrains rather than thermodynamic limitations.

3.3.7 Iodoacetamide alkylation kinetics

Thiol groups in the *L. lactis* redoxins were subjected to iodoacetamide (IAM) alkylation followed by acid quenching and HPLC separation of unmodified and carbamidomethylated species [31]. MALDI TOF analysis of alkylated LlTrxD verified carbamidomethylation of a single cysteine residue (data not shown), most likely a nucleophilic C_N in the active site C_NXXC_C motif, as previously demonstrated for EcTrx1 [32]. The second order reaction rate for IAM alkylation of LlTrxD (k = 1050.4 $M^{-1}s^{-1}$) is 80 and 70 times higher than LlTrxA (k = 12.8 $M^{-1}s^{-1}$) and EcTrx1 (k = 14.8 $M^{-1}s^{-1}$), respectively (Fig.2; Tab.2). The LlTrxD D31N mutant showed a more than ten times decreased alkylation rate (k = 88.4 $M^{-1}s^{-1}$) compared to wt, suggesting a strong influence of the active site aspartate residue on thiol reactivity. Data for LlTrxD D31P mutant and LlNrdH was not obtained due to failure to obtain reproducible chromatographic separation and quantification of the alkylated and non-alkylated forms (data not shown).

The reactivity of cysteine residues is determined by the p*K*a and the intrinsic nucleophilicity of the thiol group [33]. pH-dependent IAM alkylation assays were conducted (not shown) and did not exhibit a major shift in comparison with EcTrx1 [32], but the data could not be fitted to obtain a reliable pK_a value. Irrespective of the thiol p*K*a of LlTrxD, the IAM alkylation rate is exceptionally high in comparison to previous values obtained for Trx family proteins [32, 34, 35] and model peptides [36]. The reactivity of thiol groups in this type of bimolecular nucleophilic substition (S_N2) is influenced by the electrostatic environment and steric constrains. A comparison of the primary structure of LlTrxD and EcTrx1 reveals replacements of charged residues at several positions (Fig. S1) but since no three-dimensional structure of a close homolog to LlTrxD is available it is very

difficult judge what effects these substitutions may have on thiol reactivity. High thiol IAM reactivity (k = 1200 M^{-1} s^{-1} at RT) was previously observed in the human Trx-like protein TRP-14 containing a WCPDC active site motif [20].

3.4 Conclusion

This comparative study demonstrates that all the three *L. lactis* redoxins investigated are efficient substrates of the LlNTR. LlTrxD differs from classical thioredoxins in terms of primary structure and biochemical reactivity and is suggested to belong to a distinct subgroup of Trx-like proteins with WC[P/G]DC active site motifs present in related bacteria. The active site aspartate is conserved and appears to be important for the thiol reactivity and the redox potential of LlTrxD is intermediate (-248 mV) between classical glutaredoxins and thioredoxins. The physiological importance of LlTrxD and related proteins and their roles in reduction of putative protein disulfide targets remains to be investigated.

3.5 Experimental procedures

3.5.1 Bacterial strains and reagents

E. coli strains XL10-gold (Novagen) and Rosetta DE3 (Stratagene) were maintained on LB agar plates and cultivated in LB medium. When appropriate, ampicillin (100 µg/mL) and chloramphenicol (20 µg/mL solid media; 5 µg/mL liquid media) was added. Unless stated otherwise all chemicals and reagents were from Sigma.

Sequence analysis

Sequence alignments were performed using the ClustalW2 algorithm (http://www.ebi.ac.uk/Tools/msa/clustalw2/). Percentage sequence identity is calculated by dividing the number of identical residues by the total number of positions in the sequence alignments. Logo-representation of aligned output sequences (http://www.ncbi.nlm.nih.gov/tools/cobalt/cobalt.cgi) from Protein BLAST of LlTrxD against nrNCBI was generated using Weblogo (http://weblogo.berkeley.edu/logo.cgi) [37]. The phylogenetic lineage of proteins annotated in the thioredoxin (PF00085) pfam (vers 26.0: 20121004) was obtained from the corresponding Uniprot entries [38].

Cloning and site-directed mutagenesis

Genes encoding LlTrxA, LlTrxD, LlNrdH and LlNTR were amplified by PCR from genomic DNA of *L. lactis* subsp. *cremoris* MG1363 (kindly provided by Mogens Kilstrup) using primers flanked by *Nde*I and *Bam*HI sites listed in Table S1. PCR products were either i) digested with *Nde*I /*Bam*HI and ligated with *Nde*I /*Bam*HI treated pET15b (Novagen), ii) subcloned into TA-cloning vector pCR2.1 (Invitrogen) or *Eco*RV linearized, antarctic phosphatase treated pBluescript SK+ (Stratagene), digested with *Nde*I /*Bam*HI and ligated into *Nde*I /*Bam*HI treated pET15b. D31P and D31N mutants of LlTrxD were constructed with QuikChange® Site-Directed Mutagenesis Kit (Stratagene) using the plasmid with LlTrxD in pET15b as template and designed primers listed in Table S1. Plasmids containing genes encoding EcTrx1 and *E. coli* NTR (EcNTR) for expression in pET14b and pET15b, respectively, were purchased (Eurofins, Germany). The plasmid and procedure to obtain recombinant barley HvTrxh1 has been described previously [7]. All constructs were verified by bidirectional sequencing (Eurofins) and transformed into *E. coli* Rosetta DE3.

3.5.2 Protein expression and purification

Single colonies of *E. coli* Rosetta DE3 strains containing the constructs outlined above were inoculated into 50 mL LB medium and incubated at 37^0C overnight, followed by inoculation into fresh LB medium to reach OD 0.1. Cultures were incubated until an OD_{600} of 0.6, IPTG (100 µM) was added and growth continued for 5 h at 30^0C or overnight at 20^0C. The culture was placed on ice for 30 min, centrifuged 30 min at 3000 g and cell pellets were stored at -20^0C. Cell pellets were resuspended in Bugbuster protein extraction reagent (Novagen) containing 25 U Benzonase nuclease (Merck) and incubated at RT for 30 min with slow shaking followed by 30 min centrifugation at 20000 g and 4^0C. In extractions of the NTRs, FAD (0.1 mM) was included. Supernatants were filtered (pore size 0.45 µm) and loaded on HisTrap columns (GE Healthcare) equilibrated with loading buffer (30 mM Tris/HCl pH 8, 500 mM NaCl, 10 mM imidazole). Target proteins were eluted in a linear gradient from 10–50% elution buffer (30 mM Tris/HCl pH 8, 500 mM NaCl, 400 mM imidazole). Selected pooled fractions were dialyzed against 30 mM Tris/HCl, pH 8, concentrated to approximately 5 mL (Amicon Ultra 6-8 MWCO), applied to a Superdex 75 26/60 column and eluted by 30 mM Tris/HCl, pH 8, 200 mM NaCl at a flow rate of 0.5 mL/min. Selected fractions were pooled, dialyzed against 30 mM Tris/HCl, pH 8, concentrated to at least 100 µM and stored in aliquots at -80^0C. Protein concentrations were determined by aid of amino acid analysis and by absorbance at 280 nm. The molar extinction coefficients used were 13700, 14400, 7210, and 14200 $M^{-1}cm^{-1}$ for LlTrxA, LlTrxD, LlNrdH and EcTrx1, respectively. For purification of LlNTR, 20 mM potassium phosphate pH 7.4 (instead of Tris buffer) was used for the HisTrap column. After dialysis against 0.1 M potassium phosphate, 1 mM EDTA, pH 7.4, LlNTR was concentrated (Amicon Ultra 6-8 MWCO) without further purification. The concentration of active LlNTR and EcNTR was determined by FAD absorbance (ε_{456} = 11300 $M^{-1}cm^{-1}$).

3.5.3 Insulin disulfide reduction assay

Reduction of insulin disulfide bonds was performed essentially as described previously [22] but adapted to a 96-well plate format [39]. Reactions were started by addition of 50 µL 1.66 mM DTT to obtain final concentrations of final 0.33 mM DTT, 1 µM target protein, 0.1 M potassium phosphate, pH 7.0, 0.2 mM EDTA, 1 mg/ml insulin in 250 µL and OD_{650} was recorded at 1 min intervals in an ELISA plate reader (Power Wave XS, BIO-TEK®, Holm & Halby). Sample containing 12.5 µL 30 mM Tris/HCl, pH 8 instead of target protein was used as a negative control. For LlTrxD wt and mutants, experiments were also performed with 53 µL of 47 µM target protein (final 10 µM). All experiments were performed in duplicates.

3.5.4 Interaction of redoxins with thioredoxin reductase

The redoxins were assayed as substrates for LlNTR and EcNTR at RT in 0.1 M potassium phosphate, pH 7.5, 2 mM EDTA, BSA (0.1 mg/mL), 0.2 mM NADPH with 0.2 mM DTNB as the final electron acceptor. The formation of TNB anion was measured at 412 nm (ε_{412}=13600 $M^{-1}cm^{-1}$). To determine the apparent k_{cat} and K_M, substrate concentration was varied between 0.1 and 5 µM at fixed concentrations of NTR (10 or 20 nM). The Michaelis-Menten equation was fitted to the data using Kaleidagraph (Synergy Software, Reading, PA, USA).

3.5.5 Reduction of disulfide bonds in compounds of low molecular weight

The redoxins from *L. lactis* and EcTrx were compared (at 1.0 µM) in their ability to reduce low molecular weight disulfides. The substrate concentration was 1 mM (hydroxyethyl disulfide, GSSG and cystamine) and 0.5 mM for cystine. The assay (at RT) of 1.0 mL contained 0.1 M potassium

phosphate, pH 7.5, 2 mM EDTA, BSA (0.1 mg/mL), 0.2 mM NADPH and LlNTR (20 nM). Under the same conditions, but in a format of 120 µL (quartz cuvette), the peptide hormones vasopressin and oxytocin were tested at 0.1 mM. The disappearance of NADPH was followed at 340 nm (ε_{340}=6220 $M^{-1}cm^{-1}$). The results are expressed as the number of disulfides reduced per thioredoxin molecule min^{-1}.

3.5.6 Determination of redox potential (E°') by direct protein protein equilibrium

Reduced and oxidized forms of thioredoxin were separated and quantified by reversed phase chromatography and a thioredoxin (Trxref) with an established $E^{0'}$ value was used to determine the corresponding value of another thioredoxin (Trx) or a related protein, essentially as described previously [4]. The difference, $\Delta E^{0'}$, between the two proteins is obtained from the equilibrium constant and the Nernst equation:

$$E°'(Trxref) - E°'(Trx) = \Delta E°' = \frac{RT}{nF} \ln \frac{[\mathrm{Trx(S)_2}][\mathrm{Trxref(SH)_2}]}{[\mathrm{Trx(SH)_2}][\mathrm{Trxref(S)_2}]} \quad (1)$$

Here, R is the gas constant (1.987 cal K^{-1} mol^{-1}), T the (room) incubation temperature (294 K= 21°C), n is the number of electrons transferred (2), and F is the Faraday´s constant (23,040.612 cal mol^{-1} V^{-1}). The reference $E^{0'}$ value for EcTrx1, -270 mV, was according to Krause *et al.* [5]. Proteins were reduced by 10 mM DTT for 30 min in the dark. Excess DTT was removed by gel filtration (NAP-5 column, GE Healthcare) equilibrated in argon-purged reaction buffer (0.1 M sodium phosphate, 0.2 mM EDTA, pH 7.0). The redox reaction was initiated by mixing one protein in the reduced state with the other protein in its oxidized state in a 1:1 molar ratio. Two protein concentrations were used (25 and 50 µM) and the reaction was also run in the reverse order. The reaction (100 µL) was allowed to equilibrate for 4 hrs or O.N. until quenching by phosphoric acid

(0.67 M, 100 µL) to a final pH of ~2.0. In order to gauge the loss of reducing equivalents to molecular oxygen during the incubation, samples with reduced protein alone were included. Typically, they retained about 95% of the reduced form after O.N. incubation. The mixture (150 µL) was loaded on a C18 RP-HPLC column (3 µm, 300 Å, 4.6 x150 mm; Dionex) at 30°C using a Dionex Ultimate 3000 HPLC system. The column was equilibrated in 5% (v/v) acetonitrile and 0.1% (v/v) trifluoroacetic acid and the proteins were eluted by a gradient of acetonitrile in 0.1% (v/v) trifluoroacetic acid during 25 min at a flow rate of 1 mL/min. The gradient was typically between 40–60% (v/v) acetonitrile, and adapted to improve separation of the four protein species to be analysed. Only in the case of the separation between LlNrdH and HvTrxh1, a much lower concentration of acetonitrile was used (36–49.5% (v/v) during 25 min). Column effluent was monitored at 215 and 280 nm. The relative amount of reduced and oxidized protein was obtained from the peak areas at 215 nm after integration by the software Chromeleon (Dionex).

3.5.7 Determination of redox potentials *E°'* by equilibrium to the NADPH/NADP+ couple *via* EcNTR and LlNTR

Redox potential of the redoxins were determined by equilibrium with the NADPH/$NADP^+$ redox couple *via* EcNTR and LlNTR based on the spectrophotometric approach developed by Krause *et al* [5]. In a volume of 499 µL Trx-S_2 (30 µM) was mixed with NADPH (50 µM) in reaction buffer (0.1 M sodium phosphate, 0.2 mM EDTA, pH 7.0) and after one min a catalytic amount of NTR (1 µl to final 50 nM EcNTR) was added to reduce Trx. When a new stable baseline at 340 nm was attained (after approximately 3 min) it was assumed that the reduction of Trx-S_2 was complete and 15 µL $NADP^+$ (40 mM based on the molar extinction coefficient at 260 nm (ε_{260}=15300 $M^{-1}cm^{-1}$)) was added to final 1.16 mM to reverse the reaction. The resulting increase in NADPH concentration determined from the absorbance at 340 nm (ε_{340}=6220 $M^{-1}cm^{-1}$) and corrected for dilution (3%)

corresponds to the equilibrium concentration of Trx-S_2. The concentrations of all four participating reactants (Trx-$(SH)_2$, Trx-S_2, NADPH and $NADP^+$) were thus calculated and the defined standard state of NADPH ($E°´$ =-315 mV) translated to $E°´$ values according to the Nernst equation:

$$E°´(Trx) - E°´(NADP) = \Delta E°´ = \frac{RT}{nF} \ln \frac{[\mathrm{Trx(SH)_2}][\mathrm{NADP}]}{[\mathrm{TrxS_2}][\mathrm{NADPH}]} \quad (2)$$

Using a single beam spectrophotometer, the contribution to absorbance from additions of $NADP^+$ (Δ340 nm=0.052) and NTR (no detectable change) was determined separately, and subtracted. Determinations were based on triplicates unless otherwise stated. In order to use LlNTR to catalyse the equilibration with LlTrxD, a semi-anaerobic buffer system was introduced containing glucose (10 mM), and the two enzymes glucose oxidase and catalase (both at 0.05 mg/ml) in the reaction buffer (0.1 M sodium phosphate, 0.2 mM EDTA, pH 7.0). A 6-fold higher concentration (0.3 µM) of LlNTR was used. Because of the light sensitivity of LlNTR it was added both after approximately 1 min (1 µl 82 µM) and together with the $NADP^+$ after 4 min (15 µL and 1 µL). The cuvette was taken out from the spectrophotometer during mixing.

3.5.8 Iodoacetamide alkylation kinetics

Kinetics of the reaction between IAM and protein cysteine residues was determined essentially as described previously [31]. Proteins (12 µM) equilibrated in 1 – 5 mL reducing buffer (0.5 mM tris(2-carboxyethyl)phosphine, 50 mM NaCl, 5 mM HEPES, pH 7.5) were incubated for at least 1 h at RT and chilled on ice. Samples (50 µL) were removed, mixed with 100 µL of ice-cold reaction buffer (45 mM HEPES, 1.5 mM EDTA, 300 mM NaCl, 30 µM IAM, pH 7), and incubated on ice for various lengths of time followed by addition of 50 µl 40% (v/v) acetic acid (final concentration 10%). Unmodified and carbamidomethylated proteins were separated on an Acclaim® 300 reversed

phase column (C18, 300 Å, 3 µM, 4.6x150 mm; Dionex) connected to Ultimate 3000 HPLC system (Dionex) using an appropriate Acclaim® guard cartridge. The column was pre-warmed to 30°C and equilibrated with 95% solution A (0.1% trifluoroacetic acid) + 5% solution B (100% acetonitrile). Samples were separated by a 25 min linear gradient (37-54%) of solution B. The separation was monitored by absorption at 215 nm. Peak areas were evaluated using Chromeleon software (Dionex), and second order reaction constants *k* were obtained by fitting data into equation 3:

$$\frac{1}{A_0 - B_0} \cdot ln \frac{A \cdot B_0}{B \cdot A_0} = kt \qquad \textbf{(3)}$$

(A= [IAM], B = [Trx]).

Two independent experiments were performed for each protein. IAM alkylation of a single cysteine residue in LlTrxD was confirmed by MALDI TOF analysis (data not shown).

3.6 Acknowledgements

Aida Curovic is acknowledged for technical assistance. Anne Blicher is thanked for performing amino acid analysis and we are grateful to Alexander Viborg for constructing algorithms to extract lists of phylogenetic information from large datasets of Uniprot entries. The work was supported by the Danish Council for Technology and Production Sciences (FTP, grant nr 274-08-0413) and the Carlsberg Foundation. The PhD grant to PE was in part financed by the Technical University of Denmark.

3.7 Tables

Table 1. Phylogenetic distribution of Trx-like proteins with selected active site WCXXC motifs annotated in the thioredoxin pfam (PF00085) database.

	WCXXC	**WCGPC**	**WCXDC**	**WC[G/P]DC**	**WCGDC**
Eukaryota	4293	1147	19	1	1
Archaea	149	79	8	4	3
Bacteria*	6373	4280	851	818	232
Firmicutes	1867	909	771	745	227
Viruses	17	4	0	0	0
Unclassified	24	16	0	0	0
TOTAL	10856	5526	878	823	236

Includes *Firmicutes

Table 2. Saturation kinetics of LlNTR and EcNTR with redoxin substrates.

Saturation kinetics with LlNTR

Redoxin	Km (µM)	Kcat (s^{-}	Efficiency ($M^{-1}s^{-1}$)
LlTrxA	3.48+/- 0.33	26.8	7.7 x10^{6}
LlNrdH	0.48+/-0.05	29.3	6.1 x 10^{7}
LlTrxD	1.80+/-0.13	26.2	1.5 x 10^{7}
LlTrxD D31N	2.10+/-0.25	30.3	1.44 x 10^{7}
LlTrxD D31P	1.63+/-0.18	22.2	1.36 x 10^{7}
EcTrx1	6.05+/-0.49	24.4	4.0 x 10^{6}

Saturation kinetics with EcNTR

Redoxin	Km (µM)	Kcat (s^{-}	Efficiency ($M^{-1}s^{-}$
LlTrxA	4.17+/-0.64	21.9	5.3 x10^{6}
LlNrdH	9.96+/-1.44	42	4.2 x10^{6}
LlTrxD	<1.0	ca 0.01	ca 1x 10^{4}
LlTrxD D31N	0.15 +/-0.04	0.014	< 1x 10^{5}
LlTrxD D31P	0.93+/- 0.08	0.017	ca 2 x 10^{4}
EcTrx1	2.20+/-0.14	26.3	1.2 x 10^{7}

* The relative errors of k_{cat} values are comparable or lower than those on the K_m values and therefore not displayed

Table 3. Low molecular weight disulfides as substrates for redoxins. Standard deviations (%) are based on duplicate assays.

Compound	MW (Da)	EcTrx1 (min^{-1})	StDev (%)	LlTrxA (min^{-1})	StDev (%)	LlTrxD (min^{-1})	StDev (%)	LlNrdH (min^{-1})	StDev (%)
Cystamine (1 mM)	152.28	1.4	4	1.5	1	10	14	0.82	9
Hydroxyethyl-disulfide (1 mM)	154.25	0.77	2	1.0	6	0.38	16	0.15	16
Cystine (0.5 mM)	240.30	2.7	3	5.6	6	11	7	0.62	14
GSSG (1 mM)	612.63	1.9	2	3.9	2	2.4	17	0.28	36
Oxytocin (0.1 mM)	1007.19	3.2	7	9.4	1.3	13.7	3.3	5.2	1.8
Vasopressin (0.1 mM)	1084.25	3.6	3.2	10.9	2.3	13.1	8.0	0.39	20

Table 4. Second order rates for IAM alkylation reactions. Reduced redoxins (4 µM) were reacted with IAM (20 µM) at pH = 7; T = 0°C (see Experimental Procedures). Standard deviations (%) are based on two independent measurements.

Redoxin	***k*** **[$M^{-1}s^{-1}$]**	**StDev [%]**
LlTrxD wt	1050.4	5.6
LlTrxD D31N	88.4	7.3
LlTrxA	12.8	2.2
EcTrx1	14.8	6

3.8 Figure legends

Fig. 1. Insulin disulfide reduction assay with redoxins in 0.1 M potassium phosphate, pH 7.0, 0.2 mM EDTA, 0.33 mM DTT and 1 mg/mL insulin (**A**) 1 µM LlTrxA (●), EcTrx1 (■), LlNrdH (–), LlTrxD (▲), LlTrxD D31N (+), LlTrxD D31P (**X**), control without Trx (**—**). (**B**) 10 µM LlTrxD D31N (+), LlTrxD D31P (**X**) control without Trx (**—**). Turbidity was monitored as absorbance at 650 nm in an ELISA plate reader at 1 min intervals.

Fig. 2. Michaelis-Menten plot of the redoxins as substrates of EcNTR (**A**) and LlNTR (**B**). The concentration of NTR was constant (10 or 20 nM) whereas concentrations of the redoxins were varied. The rate of absorbance decrease at 412 nm was transferred to NTR turnover (s^{-1}). The symbols denote LlNrdH (empty circles), LlTrxA (empty squares), LlTrxD (empty triangles) and EcTrx1 (filled triangles).

Fig. 3. Redox potential by direct protein protein equilibria (HPLC). **A.** Determination of the redox potential of LlTrxA. Reduced LlTrxA and oxidized EcTrx1, both at 25 µM, were incubated O.N. before analysis by HPLC with a gradient of 38.7-61.2 % actetonitrile. Integration of the peaks yielded K=0.446 corresponding to a difference of +10.2 mV from the reference EcTrx1. **B.** Determination of redox potential for LlTrxD. Reduced LlTrxD and oxidized EcTrx1, both at 25 µM, were incubated 70 hrs before analysis by HPLC. It is noteworthy that the oxidized form of LlTrxD elutes before the reduced form in the gradient (of 36–61.2% actetonitrile). Integration of the peaks yielded K=0.117 corresponding to a difference of +27.2 mV in comparison to the reference EcTrx1. **C.** Determination of redox potential for LlNrdH using HvTrxh1 as reference. Reduced LlNrdH and oxidized HvTrxh1, both at 25 µM, were incubated O.N. (16.5 hrs) before analysis by HPLC in which a gradient of 36–49.5% actetonitrile was employed. Integration of the peaks yielded K=0.0733 corresponding to a difference of +33.1 mV from the reference HvTrxh1 (-270.7 mV).

Fig. 4. Determination of redox potentials for LlTrxA and LlTrxD by equilibration with NADPH/$NADP^+$ *via* EcNTR and LlNTR, respectively. The concentrations of the four reactants, Trx-$(SH)_2$, Trx-S_2, NADPH, and $NADP^+$ were calculated to obtain an equilibrium constant. **A.** Equilibrium with LlTrxA catalyzed by EcNTR (1 µl 25 µM) yielding *K*=83.2 (E0'=-258.4 mV). **B.** Equilibrium with LlTrxD catalyzed by LlNTR yielding *K*=292 (E0´=-242.3 mV). The expected contribution of absorbance from LlNTR was about 0.0015 and neglected.

Fig. 5. IAM alkylation kinetics. LlTrxD (diamond), LlTrxA (triangle), EcTrxA (square) and LlTrxD D31N (cross) were subjected to IAM alkylation. Samples were withdrawn at specified time points and the fraction of carbamidomethylated protein was determined spectrophotometrically at 215 nm following HPLC separation of alkylated and unmodified protein.

3.9 Figures

Figure 1

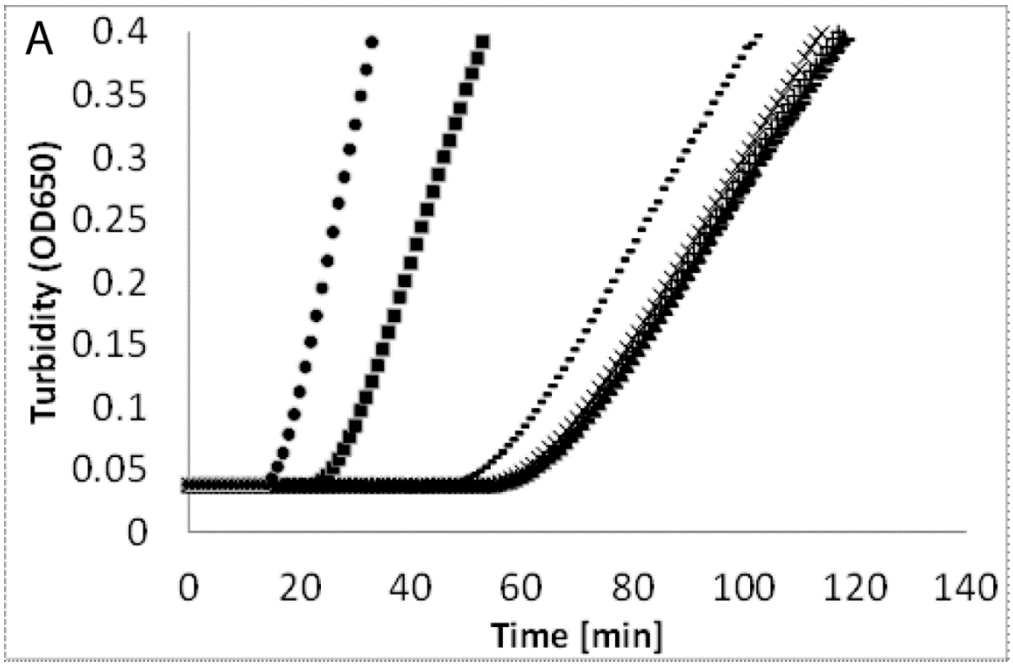

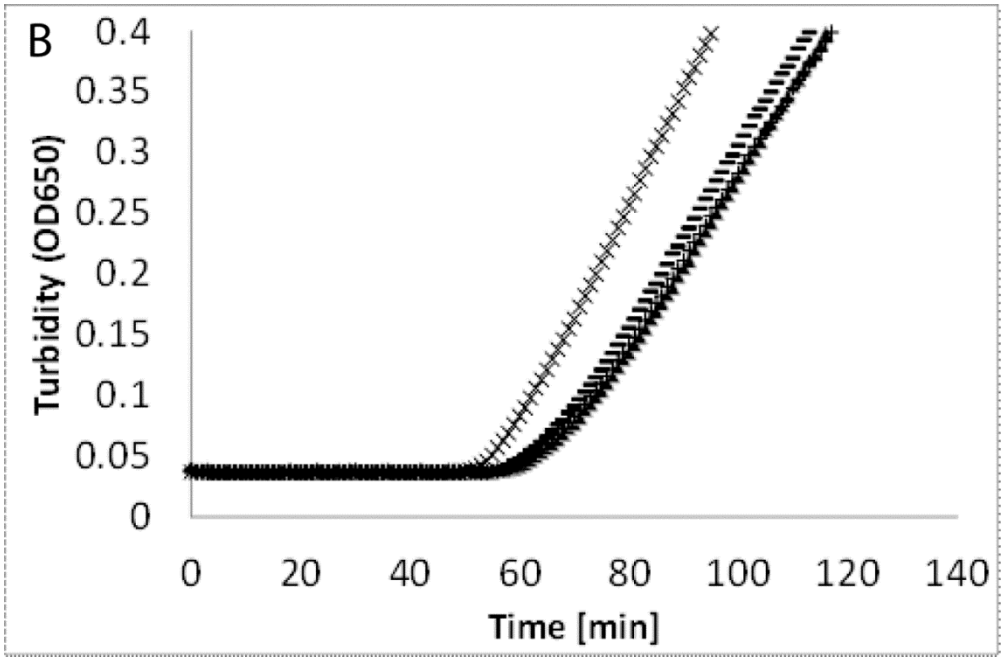

Figure 2

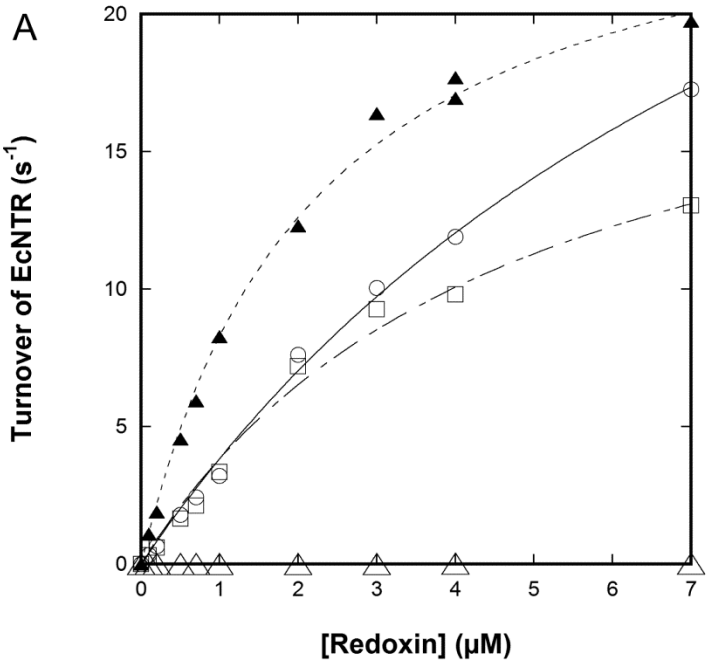
A
Turnover of EcNTR (s-1)
[Redoxin] (μM)
0
5
10
15
20
0
1
2
3
4
5
6
7

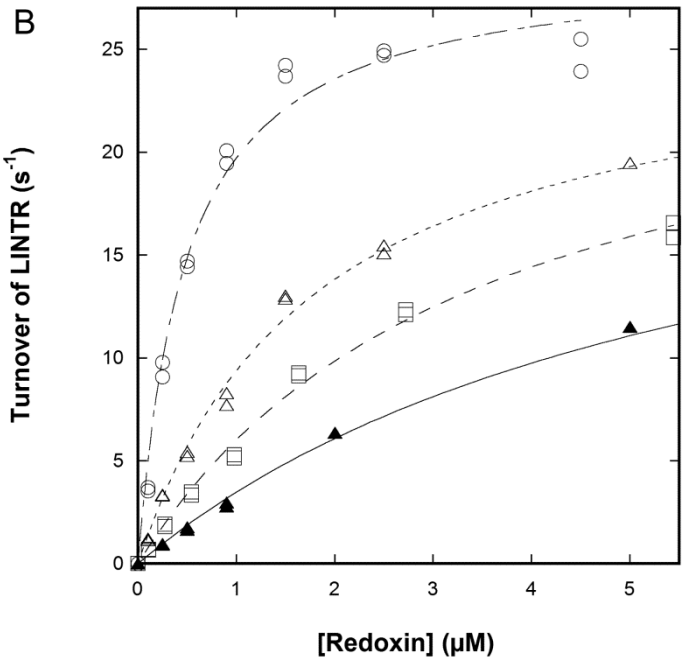
B
Turnover of LINTR (s-1)
[Redoxin] (μM)
0
5
10
15
20
25
0
1
2
3
4
5

Figure 3

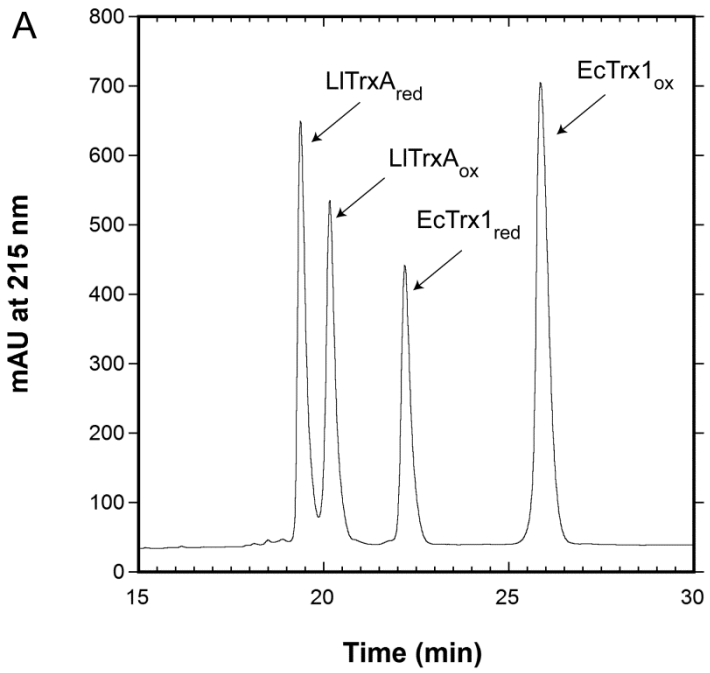
A
mAU at 215 nm
Time (min)
LlTrxA$_{red}$
LlTrxA$_{ox}$
EcTrx1$_{red}$
EcTrx1$_{ox}$

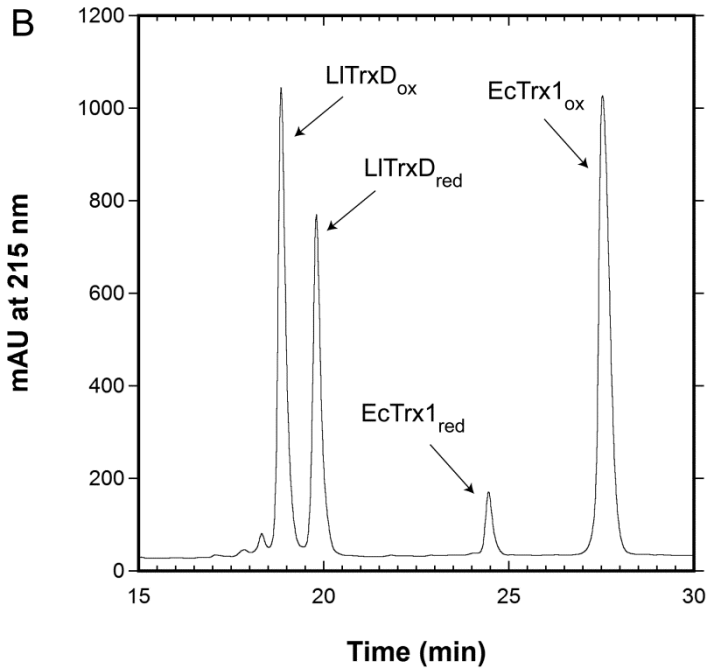
B
mAU at 215 nm
Time (min)
LlTrxD$_{ox}$
LlTrxD$_{red}$
EcTrx1$_{red}$
EcTrx1$_{ox}$

C

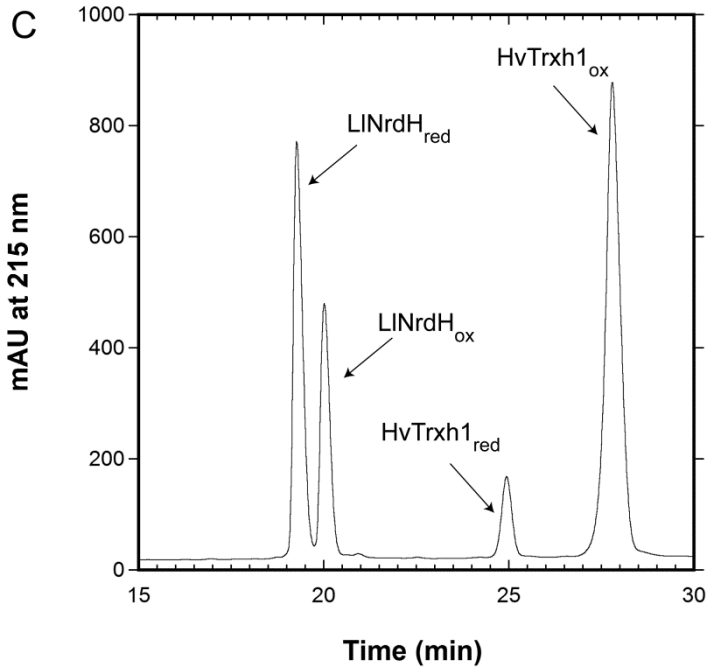
1000
800
600
400
200
0
15
20
25
30
mAU at 215 nm
Time (min)
HvTrxh1ox
LlNrdHred
LlNrdHox
HvTrxh1red

Figure 4

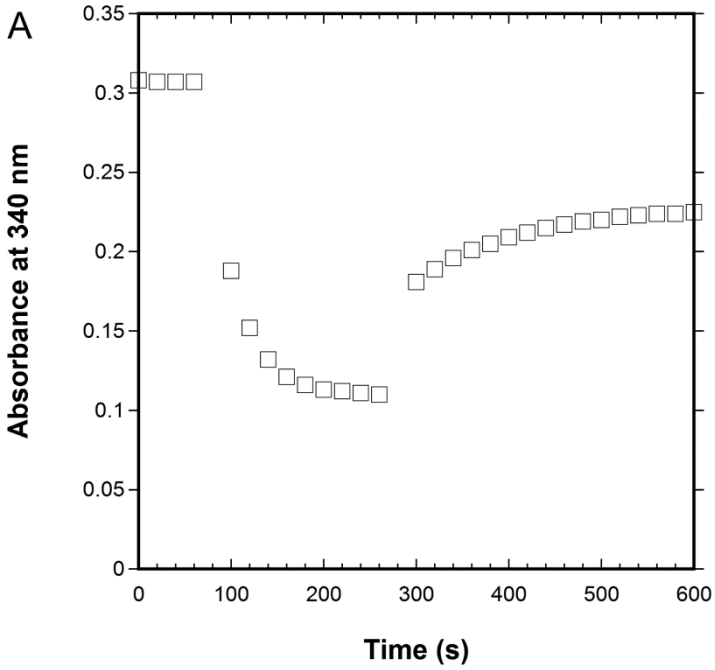
A
Absorbance at 340 nm
0.35
0.3
0.25
0.2
0.15
0.1
0.05
0
0
100
200
300
400
500
600
Time (s)

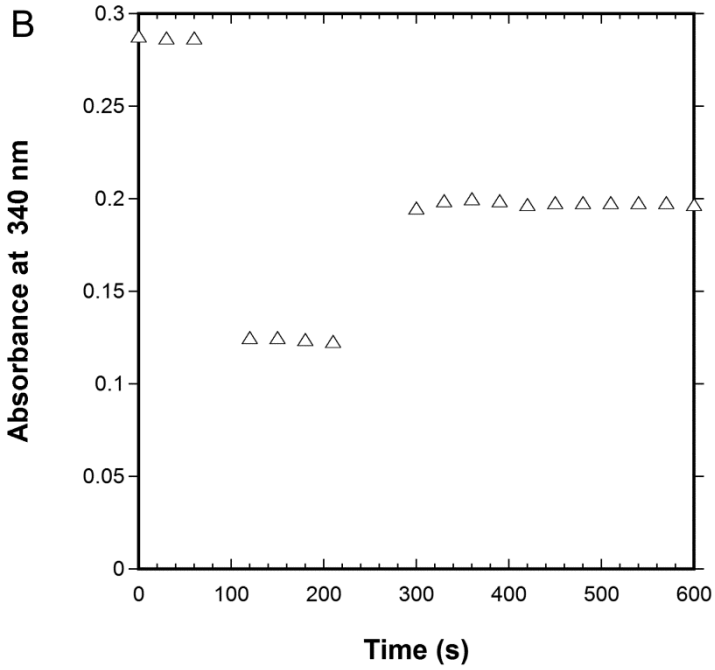
B
Absorbance at 340 nm
0.3
0.25
0.2
0.15
0.1
0.05
0
0
100
200
300
400
500
600
Time (s)

3.10 Supplementary material

Table S1 Primers used for cloning and mutagenesis.

Name	Sequence[$]	T_M [°C]
TrxA1	5′-atacatatggaatataatattactgatgcaacgtttg-3′	64.2
TrxA2	5′-aggatccttcatttcaataagaaaaaattctgtc-3′	65.7
TrxH1	5′-atacatatgattattccagaaaatattgaaaatttagc–3′	63.2
TrxH2	5′-aggatccattttacctcaagaaatcagtc-3′	63.6
NrdH1	5′-gatacatatggttacagtttattctaaaaacaattg-3′	61.4
NrdH2	5′-aggatccatctctaaatcatcgtca-3′	60.9
TrxB1	5′-atacatatgacagaaaagaaatatgatgttgtca-3′	62.8
TrxB2	5′-aggatcctttaacaaaaaattactgacttctttg-3′	64.4
LlTrxB-D31P 1	5'- tttttcacagctggttggtgtggaccttgtaattttatcaaacct -3'	77
LlTrxB-D31P 2	5'- aggtttgataaaattacaaggtccacaccaaccagctgtgaaaaa -3'	77
LlTrxB-D31P 1	5'- tttttcacagctggttggtgtggaaattgtaattttatcaaacct -3'	75.7
LlTrxB-D31P 2	5'- aggtttgataaaattacaatttccacaccaaccagctgtgaaaaa -3'	75.7

[$]=Restriction sites for NdeI or BamHI respectively are underlined.

Fig. S1. Sequence alignment of, LlTrxD LlTrxA, and a range of WCGPC thioredoxins.

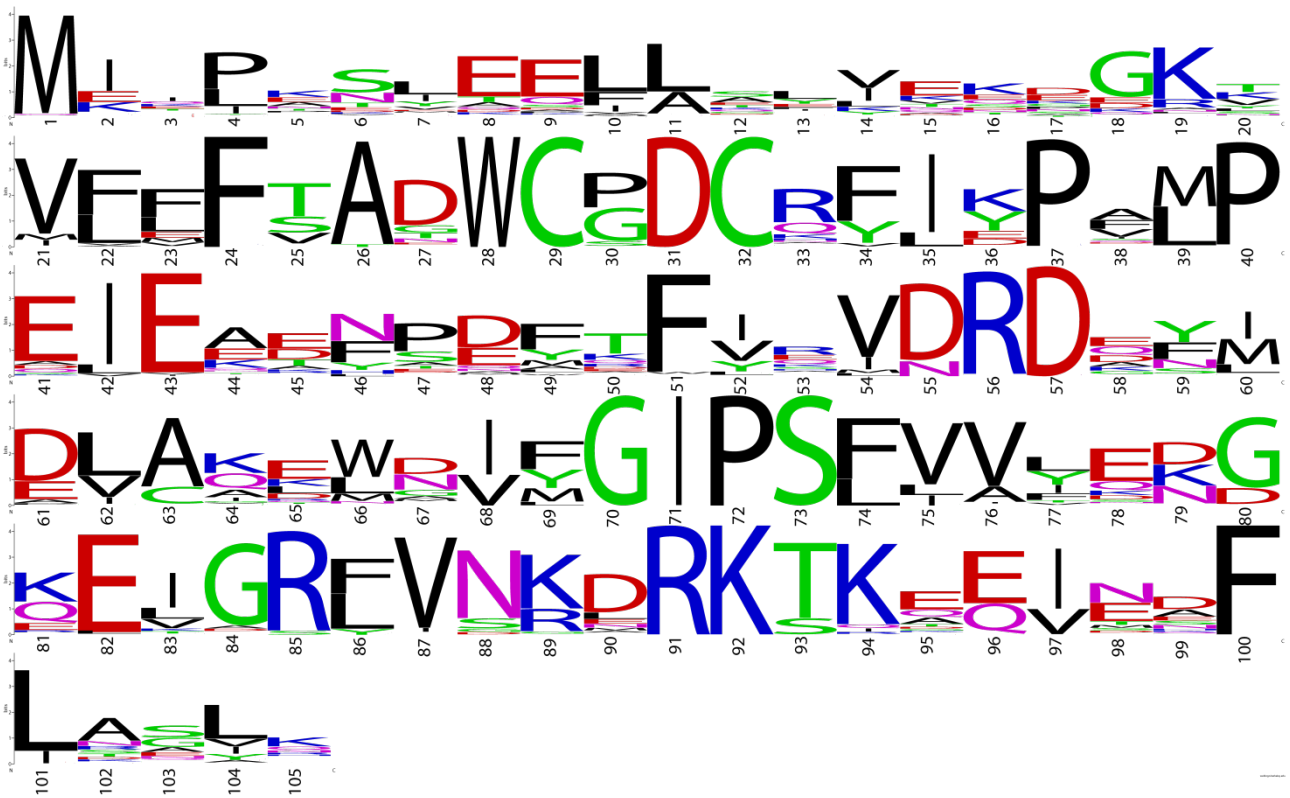

Fig. S2. Sequence LOGO representation of the top 294 sequences matching LlTrxD from BLAST. Numbering below characters refer to sequence positions in LlTrxD.

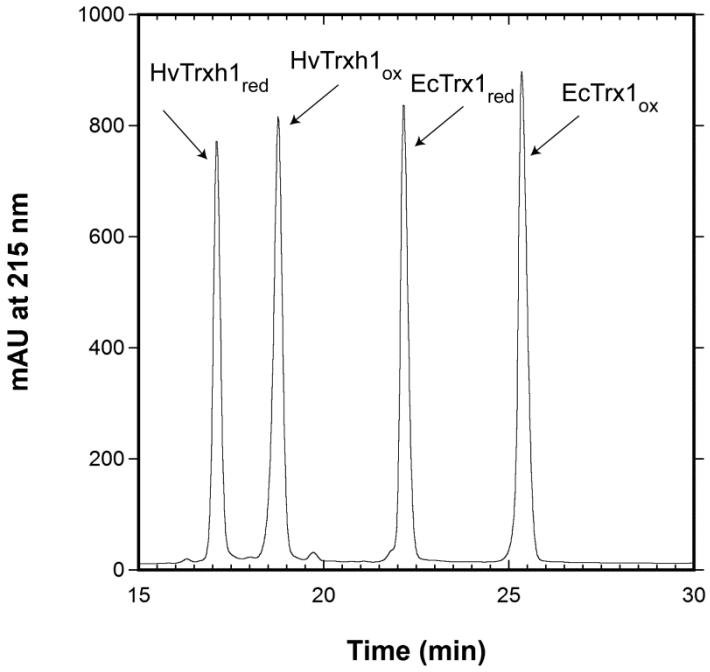

Fig. S3. Determination of the redox potential of HvTrxh1 using EcTrx1 as reference. Reduced HvTrxh1 and oxidized EcTrx1, both at 25 µM, were incubated 4 hrs before analysis by HPLC with a gradient of 37.8–63% actetonitrile. Integration of the peaks yielded *K*=1.055 corresponding to a $E^{\circ\prime}$ difference of -0.7 mV from the reference EcTrx1

A

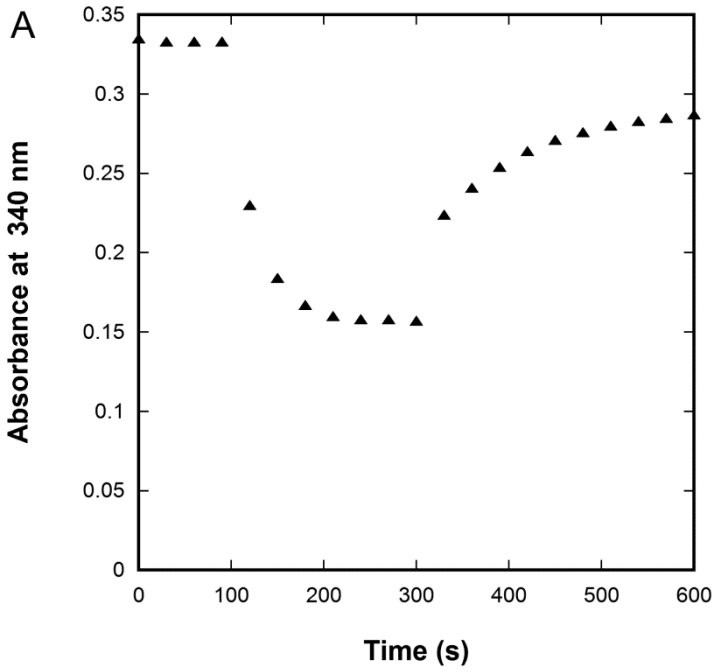
Absorbance at 340 nm
0.35
0.3
0.25
0.2
0.15
0.1
0.05
0
0
100
200
300
400
500
600
Time (s)

B

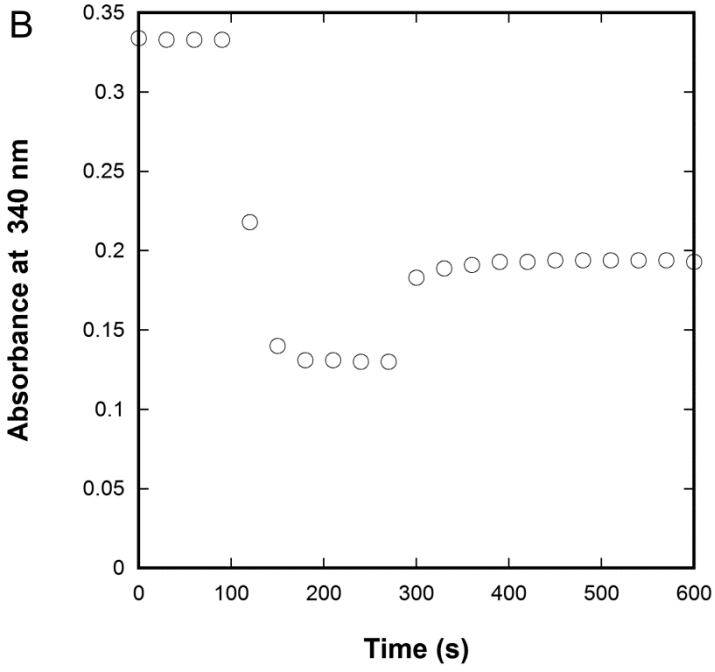
Absorbance at 340 nm
0.35
0.3
0.25
0.2
0.15
0.1
0.05
0
0
100
200
300
400
500
600
Time (s)

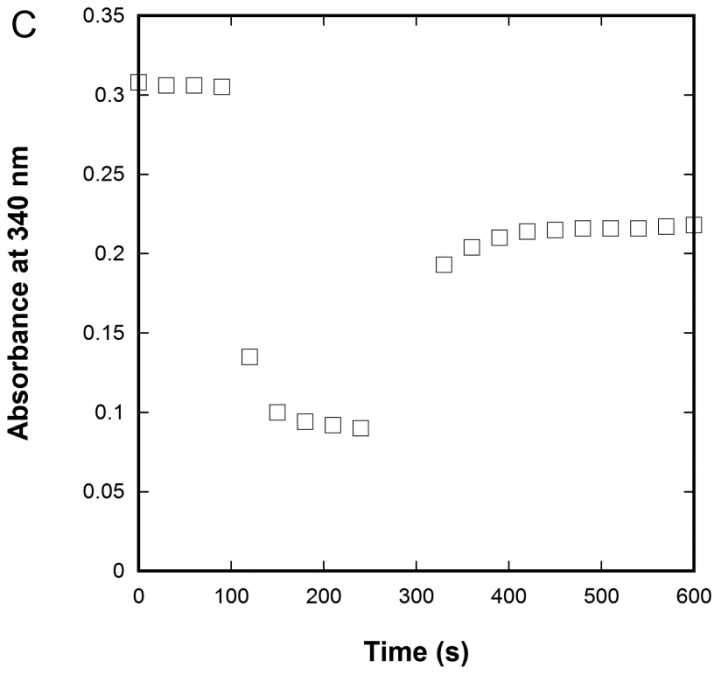

Fig. S4. Determination of the redox potential of EcTrx1 **(A)** and LlNrdH **(B)** using EcNTR (50 nM) and of LlTrxA **(C)** using LlNTR (0.3 µM) by equilibration with NADPH/$NADP^+$. **A**. The experiment suggests a *K* = 35.2 and $E^{\circ\prime}$=-269.41 mV for EcTrx1 **B.** LlNrdH was readily reduced but the reverse reaction was too weak. The increase in absorbance (0.064) seen after addition of $NADP^+$ is primarily caused by the intrinsic absorbance from $NADP^+$ (0.052) and thus subtracted in these experiments. The absorbance difference of 0.012, was judged to be too small for an accurate determination of the equilibrium constant (*K)*. **C.** The experiment suggests a *K* = 77.6 and a redox potential of $E^{0\prime}$ = -259.3 mV for LlTrxA.

3.11 References

1. Holmgren, A & Morgan, FJ (1976) Enzyme reduction of disulfide bonds by thioredoxin. The reactivity of disulfide bonds in human choriogonadotropin and its subunits, *Eur J Biochem.* **70**, 377-383.
2. Arnér, ESJ & Holmgren, A (2000) Physiological functions of thioredoxin and thioredoxin reductase, *Eur J Biochem.* **267**, 6102-6109.
3. Martin, JL (1995) Thioredoxin - a fold for all reasons, *Structure.* **3**, 245-250.
4. Åslund, F, Berndt, KD & Holmgren, A (1997) Redox potentials of glutaredoxins and other thiol-disulfide oxidoreductases of the thioredoxin superfamily determined by direct protein-protein redox equilibria, *J Biol Chem.* **272**, 30780-30786.
5. Krause, G, Lundström, J, Barea, JL, Pueyo de la Cuesta, C & Holmgren, A (1991) Mimicking the active site of protein disulfide-isomerase by substitution of proline 34 in *Escherichia coli* thioredoxin, *J Biol Chem.* **266**, 9494-9500.
6. Zapun, A, Bardwell, JC & Creighton, TE (1993) The reactive and destabilizing disulfide bond of DsbA, a protein required for protein disulfide bond formation *in vivo*, *Biochemistry.* **32**, 5083-5092.
7. Maeda, K, Hägglund, P, Finnie, C, Svensson, B & Henriksen, A (2006) Structural basis for target protein recognition by the protein disulfide reductase thioredoxin, *Structure.* **14**, 1701-1710.
8. Ren, G, Stephan, D, Xu, Z, Zheng, Y, Tang, D, Harrison, RS, Kurz, M, Jarrott, R, Shouldice, SR, Hiniker, A, Martin, JL, Heras, B & Bardwell, JC (2009) Properties of the thioredoxin fold superfamily are modulated by a single amino acid residue, *J Biol Chem.* **284**, 10150-10159.
9. Jordan, A, Åslund, F, Pontis, E, Reichard, P & Holmgren, A (1997) Characterization of *Escherichia coli* NrdH. A glutaredoxin-like protein with a thioredoxin-like activity profile, *J Biol Chem.* **272**, 18044-18050.
10. Jordan, A, Pontis, E, Åslund, F, Hellman, U, Gibert, I & Reichard, P (1996) The ribonucleotide reductase system of *Lactococcus lactis*. Characterization of an NrdEF enzyme and a new electron transport protein, *J Biol Chem.* **271**, 8779-8785.
11. Newton, GL, Rawat, M, La Clair, JJ, Jothivasan, VK, Budiarto, T, Hamilton, CJ, Claiborne, A, Helmann, JD & Fahey, RC (2009) Bacillithiol is an antioxidant thiol produced in Bacilli, *Nature chemical biology.* **5**, 625-627.
12. Uziel, O, Borovok, I, Schreiber, R, Cohen, G & Aharonowitz, Y (2004) Transcriptional regulation of the *Staphylococcus aureus* thioredoxin and thioredoxin reductase genes in response to oxygen and disulfide stress, *J Bacteriol.* **186**, 326-334.
13. Vido, K, Diemer, H, Van Dorsselaer, A, Leize, E, Juillard, V, Gruss, A & Gaudu, P (2005) Roles of thioredoxin reductase during the aerobic life of *Lactococcus lactis*, *J Bacteriol.* **187**, 601-610.
14. Chivers, PT & Raines, RT (1997) General acid/base catalysis in the active site of Escherichia coli thioredoxin, *Biochemistry.* **36**, 15810-15816.
15. Dyson, HJ, Jeng, MF, Tennant, LL, Slaby, I, Lindell, M, Cui, DS, Kuprin, S & Holmgren, A (1997) Effects of buried charged groups on cysteine thiol ionization and reactivity in Escherichia coli thioredoxin: Structural and functional characterization of mutants of Asp 26 and Lys 57, *Biochemistry.* **36**, 2622-2636.
16. Eklund, H, Cambillau, C, Sjöberg, BM, Holmgren, A, Jörnvall, H, Höög, JO & Branden, CI (1984) Conformational and functional similarities between glutaredoxin and thioredoxins, *EMBO J.* **3**, 1443-1449.
17. Baker, LM, Raudonikiene, A, Hoffman, PS & Poole, LB (2001) Essential thioredoxin-dependent peroxiredoxin system from *Helicobacter pylori*: genetic and kinetic characterization, *J Bacteriol.* **183**, 1961-1973.
18. Gustafsson, TN, Sahlin, M, Lu, J, Sjöberg, BM & Holmgren, A (2012) *Bacillus anthracis* thioredoxin systems, characterization and role as electron donors for ribonucleotide reductase, *J Biol Chem.* **287**, 39686-39697.
19. Eckers, E, Bien, M, Stroobant, V, Herrmann, JM & Deponte, M (2009) Biochemical characterization of dithiol glutaredoxin 8 from *Saccharomyces cerevisiae*: the catalytic redox mechanism redux, *Biochemistry.* **48**, 1410-1423.

20. Jeong, W, Yoon, HW, Lee, SR & Rhee, SG (2004) Identification and characterization of TRP14, a thioredoxin-related protein of 14 kDa. New insights into the specificity of thioredoxin function, *J Biol Chem.* **279**, 3142-3150.
21. Woo, JR, Kim, SJ, Jeong, W, Cho, YH, Lee, SC, Chung, YJ, Rhee, SG & Ryu, SE (2004) Structural basis of cellular redox regulation by human TRP14, *J Biol Chem.* **279**, 48120-48125.
22. Holmgren, A (1979) Thioredoxin catalyzes the reduction of insulin disulfides by dithiothreitol and dihydrolipoamide, *J Biol Chem.* **254**, 9627-9632.
23. Krause, G & Holmgren, A (1991) Substitution of the conserved tryptophan-31 in *Escherichia coli* thioredoxin by site-directed mutagenesis and structure-function analysis, *J Biol Chem.* **266**, 4056-4066.
24. Prongay, AJ, Engelke, DR & Williams, CH (1989) Characterization of 2 active-site mutations of thioredoxin reductase from *Escherichia coli*, *J Biol Chem.* **264**, 2656-2664.
25. Østergaard, H, Henriksen, A, Hansen, FG & Winther, JR (2001) Shedding light on disulfide bond formation: engineering a redox switch in green fluorescent protein, *EMBO J.* **20**, 5853-5862.
26. Szajewski, RP & Whitesides, GM (1980) Rate constants and equilibrium constants for thiol-disulfide interchange reactions involving oxidized glutathione, *J Am Chem Soc.* **102**, 2011-2026.
27. Li, Y, Hugenholtz, J, Abee, T & Molenaar, D (2003) Glutathione protects *Lactococcus lactis* against oxidative stress, *Appl Environ Microbiol.* **69**, 5739-5745.
28. Tan, SX, Greetham, D, Raeth, S, Grant, CM, Dawes, IW & Perrone, GG (2010) The thioredoxin-thioredoxin reductase system can function in vivo as an alternative system to reduce oxidized glutathione in *Saccharomyces cerevisiae*, *J Biol Chem.* **285**, 6118-6126.
29. Sagemark, J, Elgan, TH, Burglin, TR, Johansson, C, Holmgren, A & Berndt, KD (2007) Redox properties and evolution of human glutaredoxins, *Proteins.* **68**, 879-892.
30. Maeda, K, Finnie, C, Østergaard, O & Svensson, B (2003) Identification, cloning and characterization of two thioredoxin h isoforms, HvTrxh1 and HvTrxh2, from the barley seed proteome, *Eur J Biochem.* **270**, 2633-2643.
31. Maeda, K, Hägglund, P, Björnberg, O, Winther, JR & Svensson, B (2010) Kinetic and thermodynamic properties of two barley thioredoxin h isozymes, HvTrxh1 and HvTrxh2, *FEBS Lett.* **584**, 3376-3380.
32. Kallis, GB & Holmgren, A (1980) Differential reactivity of the functional sulfhydryl groups of cysteine-32 and cysteine-35 present in the reduced form of thioredoxin from *Escherichia coli*, *J Biol Chem.* **255**, 10261-10265.
33. Jensen, KS, Hansen, RE & Winther, JR (2009) Kinetic and thermodynamic aspects of cellular thiol-disulfide redox regulation, *Antioxid Redox Signal.* **11**, 1047-1058.
34. Hawkins, HC & Freedman, RB (1991) The reactivities and ionization properties of the active-site dithiol groups of mammalian protein disulphide-isomerase, *Biochem J.* **275 (Pt 2)**, 335-339.
35. Nelson, JW & Creighton, TE (1994) Reactivity and ionization of the active site cysteine residues of DsbA, a protein required for disulfide bond formation in vivo, *Biochemistry.* **33**, 5974-5983.
36. Snyder, GH (1987) Intramolecular disulfide loop formation in a peptide containing two cysteines, *Biochemistry.* **26**, 688-694.
37. Crooks, GE, Hon, G, Chandonia, JM & Brenner, SE (2004) WebLogo: a sequence logo generator, *Genome research.* **14**, 1188-1190.
38. Finn, RD, Mistry, J, Tate, J, Coggill, P, Heger, A, Pollington, JE, Gavin, OL, Gunasekaran, P, Ceric, G, Forslund, K, Holm, L, Sonnhammer, EL, Eddy, SR & Bateman, A (2010) The Pfam protein families database, *Nucleic Acids Res.* **38**, D211-222.
39. Björnberg, O, Maeda, K, Svensson, B & Hägglund, P (2012) Dissecting molecular interactions involved in recognition of target disulfides by the barley thioredoxin system, *Biochemistry.* **51**, 9930-9939.

4 Conclusion and future plans

The Trx system plays crucial roles in thiol redox regulation (see 1.2). The structure and function of the canonical Trx with an WCGPC active site motif has been thoroughly investigated. However, relatively few investigations have described Trx homologs with altered active sites, such as e.g. EcTrx2, HpTrx2 and BaTrx2 in bacteria (see 1.3.1). An important outcome of this thesis is the discovery of a novel Trx with a WCGDC active site (TrxD) in the industrially important bacterium *L. lactis* , which represents a group of Trx present predominantly among Gram-positive bacteria.

TrxD was shown to significantly influence arsenate and tellurite detoxification but appears not play a major role in resistance toward reactive oxygen species (see chapter 2). A broader phenotype screen including e.g. addition of reactive nitrogen species may further the understanding of the physiological roles of TrxD. In addition, the role of Trx during respiratory growth should be investigated. Identification of Trx targets in global thiol proteome (see section 1.2.2) is likely to provide valuable insights into thiol-redox control in LAB.

The observation that Trx is important but not essential for stress resistance suggests that *L. lactis* possess alternative pathways to maintain the cellular thiol redox pool in a reduced state. It is unlikely that NrdH can substitute as a major disulfide reductant and *L. lactis* does not contain genes for glutathione synthesis. No close homologues for genes encoding components of the bacillithiol and mycothiol biosynthetic pathway are present in the annotated genome of *L. lactis* (P. Efler, unpublished observation). In order to understand the thiol redox metabolism in this bacterium it is thus of paramount important to identify alternative thiol redox pathways.

Biochemical characterization of recombinant TrxD revealed an altered reactivity compared to the classical WCGPC Trx. In particular, TrxD displayed an increased nucleophilicity of the active site cysteine and a higher redox potential. Furthermore, TrxD failed to reduce the model protein disulfide substrate insulin (Chapter 3). An attempt to determine the 3D structure of TrxD failed due to inability to obtain protein crystals. Bioinformatics predictions suggest that TrxD belongs to the Trx family and exhibits the Trx fold. However, it is difficult obtain a reliable homology model and it would be of a high value to determine the 3D structure of TrxD or a homologous protein as a model for the group of WCGDC thioredoxins in Gram positive bacteria.